A Case Study for Assessing the Hydrologic Impacts of Climate Change at the Watershed Scale

by

Martinus Hubertus Brouwers

A thesis
presented to the University of Waterloo
in fulfillment of the
thesis requirement for the degree of
Master of Applied Science
in
Civil Engineering

Waterloo, Ontario, Canada, 2007

© Martinus Hubertus Brouwers 2007

AUTHOR'S DECLARATION

I hereby declare that I am the sole author of this thesis. This is a true copy of the thesis, including any required final revisions, as accepted by my examiners.

I understand that my thesis may be made electronically available to the public.

Abstract

Since the advent of the industrial era atmospheric concentrations of greenhouse gases have been on the rise leading to increasing global mean temperatures. Through increasing temperatures and changes to distributions of precipitation, climate change will intensify the hydrologic cycle which will directly impact surface water sources while the impacts to groundwater are reflected through changes in recharge to the water table. The IPCC (2001) reports that limited investigations have been conducted regarding the impacts of climate change to groundwater resources.

The complexity of evaluating the hydrologic impacts of climate change requires the use of a numerical model. This thesis investigates the state of the science of conjunctive surface-subsurface water modeling with the aim of determining a suitable approach for conducting long-term transient simulations at the watershed scale. As a result of this investigation, a coupled modeling approach is adopted using HELP3 to simulate surface and vadose zone processes and HydroSphere to simulate saturated flow of groundwater. This approach is applied to the Alder Creek Watershed, which is a subwatershed of the Grand River Watershed and located near Kitchener-Waterloo, Ontario. The Alder Creek Watershed is a suitable case study for the evaluation of climate change scenarios as it has been well characterized from previous studies and it is relatively small in size.

Two contrasting scenarios of climate change (i.e., drier and wetter futures) are evaluated relative to a reference scenario that is based on the historical climatic record of the region. The simulation results show a strong impact upon the timing of hydrologic processes, shifting the spring snow melt to earlier in the year leading to an overall decrease in runoff and increase in infiltration for both drier and wetter future climate scenarios. Both climate change scenarios showed a marked increase to overall evapotranspiration which is most pronounced in the summer months. The impacts to groundwater are more subdued relative to surface water. This is attributed to the climate forcing perturbations being attenuated by the shift of the spring snow melt and the transient storage effects of the vadose zone, which can be significant given the hummocky terrain of the region. The simulation results show a small overall rise of groundwater elevations resulting from the simulated increase in infiltration for both climate change scenarios.

Acknowledgements

I would like to extend my sincere appreciation and gratitude to the following people, each providing support in their own:

- Jon Sykes for his patience, guidance, support, and friendship;
- Stefano Normani for his technical assistance and interesting discussions;
- Mikko Jyrkama for his assistance with the HELP3 model;
- Rob McLaren and Young-Jin Park for their assistance with the HydroSphere model;
- and finally, to all my friends and family for their love, support, and encouragement.

Table of Contents

List of Figures

List of Tables

1 Introduction

The Region of Waterloo relies on groundwater resources for 80% of its municipal water supply needs (RMOW, 2007). Recharge for these aquifers is derived primarily from precipitation and also from the underlying regional groundwater flow system. Studies have shown that the hydraulic head of unconfined groundwater systems can be strongly correlated with temperature and precipitation (e.g., Chen et al., 2004). Given the importance of protecting and managing this precious resource, it is prudent to investigate the potential impacts that different future climates may have on the surface water and groundwater resources.

Since the advent of the industrial era atmospheric concentrations of greenhouse gases have been on the rise leading to increasing global mean temperatures (IPCC, 2001). Through increasing temperatures and changes to distributions of precipitation, climate change will intensify the hydrologic cycle (Loaiciga et al. 1996) which will directly impact surface water resources while the impacts to groundwater are reflected through changes in recharge (Loaiciga, 2003). The IPCC (2001) reports that limited investigations have been conducted regarding the impacts of climate change to groundwater resources.

A small number of studies have been conducted regarding the potential impacts of climate change on surface water and groundwater resources in a Canadian setting. The impacts of climate change have been studied for aquifers located in the interior of British Columbia (Allen et al., 2004; Allen and Scibeck, 2007). A study by Jyrkama and Sykes (2007) assessed the impacts of climate change for the distribution and timing of recharge in the Grand River Watershed in Ontario. The results of these watershed scale studies and others worldwide suggest that climate change can have positive and negative impacts upon water resources and is dependant on geographic location.

Evaluating the potential effects of climate change at the watershed scale is not only important from a water resources perspective but also in terms of the design and safety of hydraulic infrastructure. Changes to the climate and corresponding hydrologic responses have implications for large scale infrastructure such as maintaining safe range of flows for operation of hydro-electric dams but also on the scale of urban infrastructure such as the design of curbs, sewers, and storm water detention ponds.

The objective of this study is to assess the potential impacts of projected climate change scenarios to surface water and groundwater at the watershed scale. The methodology is applied to a small watershed, Alder Creek Watershed, situated within the Grand River Watershed. The Alder

Creek Watershed is a suitable watershed for a case study due to its relatively small size and for the reason that it is well characterized. The complexity of the evaluating the hydrologic impacts of climate change requires the use of a numerical model. Several approaches are considered: stand alone, coupled, and fully-integrated groundwater- surface water models. Each approach has its advantages and drawbacks.

Section 2 of this thesis presents a detailed background study that investigates various levels of numerical model sophistication, the requirements of these models, and how these models relate to the physical processes they are intended to simulate. Section 3 provides the setting and conceptual framework for the numerical modeling and briefly summarizes recent and relevant regional hydrologic and hydrogeologic investigations. The development of the methodology and numerical models is outlined in Section 4. The application of the numerical model to simulate projected scenarios of future climate is presented in Section 5. This section also summarizes the results of the case study and identifies limitations of the approach with respect to simulating the effects of climate change. The limitations identified represent areas of improvement that can be incorporated into future research. Finally, conclusions and recommendations are given in Section 6.

2 Background

2.1 The Hydrologic Cycle

The hydrologic cycle describes the pathways that water takes in all its phases, as it moves between the atmosphere, land surface, subsurface, and open water. These pathways representing hydrological processes result from the interaction of the meteorological, geological, and vegetative conditions. A conceptual diagram of the hydrologic cycle is presented in Figure 2.1.

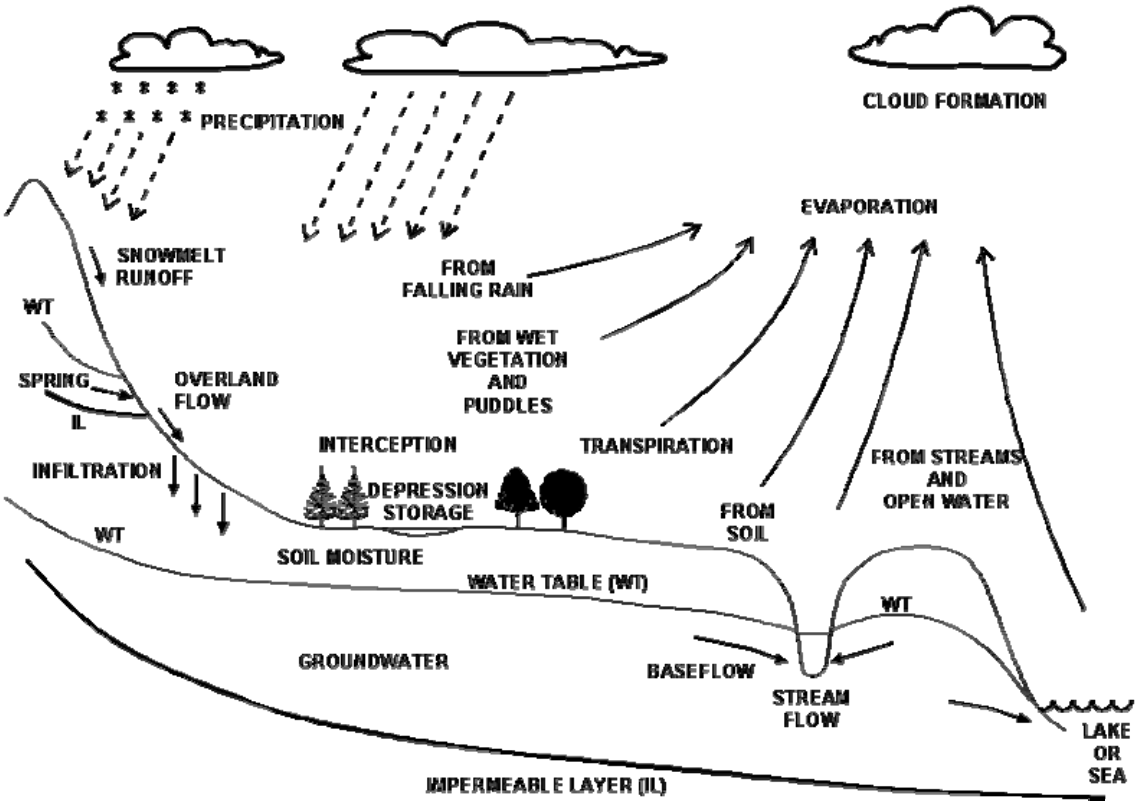

Figure 2.1 Conceptual Model of the Hydrologic Cycle (after Brutsaert, 2005)

The hydrologic cycle is comprised of several components that are all inter-connected. There is no start or end in the hydrologic cycle. It is the continuous movement of water over, on, and below the Earth's surface. To describe the hydrologic cycle we will begin with precipitation which is the driving force behind the movement of water over and through the land. The accumulation and

condensation of water vapor in the atmosphere forms precipitation which delivers fresh water (in the form of rain or snow) to the lands and oceans.

Precipitation that occurs over land will fall over the land surface or onto surface waters which will eventually return the water to the ocean through the surface water drainage network. In some cases water in the river network may infiltrate into the ground before discharging to the surface again downgradient. Precipitation that is not directly captured by the surface water network will fall onto the land surface or may be intercepted by vegetation. Some of the intercepted precipitation transfers to the ground via throughflow and stemflow while the remainder is allowed to evaporate.

The duration and intensity of precipitation event in combination with the surficial geology will determine whether precipitation that reaches the ground will infiltrate into the subsurface or flow over land. Overland flow occurs when the vadose zone becomes saturated from below (i.e., the water table rises to ground surface) or if the rate of precipitation is greater than the rate of infiltration. Overland flow may occur as run-on, whereby the water flows over land to become part of depression storage or infiltrate into the subsurface at a downgradient location, or as runoff, which is overland that reaches a surface water body.

The infiltrating water can be captured by plant uptake within and just below the root zone and is transpired through the vegetation canopy. The water that migrates beyond the zone of influence of evaporation and root uptake is referred to as percolation and will eventually reach the water table, providing recharge to the groundwater flow system. The two phase system (i.e., air and water) in the vadose zone, described in Section 2.4.1, gives rise to capillary forces that inhibit the flow of water. This results in transient storage effects as the infiltrating water migrates to the water table. Where the water table intersects the ground surface the groundwater discharges to become surface water. For large surface water bodies this is the shoreline and for tributaries the discharging groundwater provides base flow to the streams, which varies throughout the year.

Finally, water is returned from the land and oceans to the atmosphere via evaporation and sublimation. Evaporation occurs from water on the land surface (e.g. ponded water, lakes, rivers, and oceans) and from water in soil pores near the land surface. A limited amount of water can also evaporate from precipitation before reaching the land or oceans.

Historically, for simplicity, the sciences of groundwater and surface water were treated as separate entities. However, from the description of the hydrologic cycle it is apparent that they are intimately connected and in fact ought to be viewed as a single resource. When discussing the hydrologic cycle one must bear in mind the temporal and spatial scales at which hydrologic

components are being described (Winter et al., 1998). The various spatial and temporal scales that the hydrologic cycle operates on are illustrated in Figure 2.2.

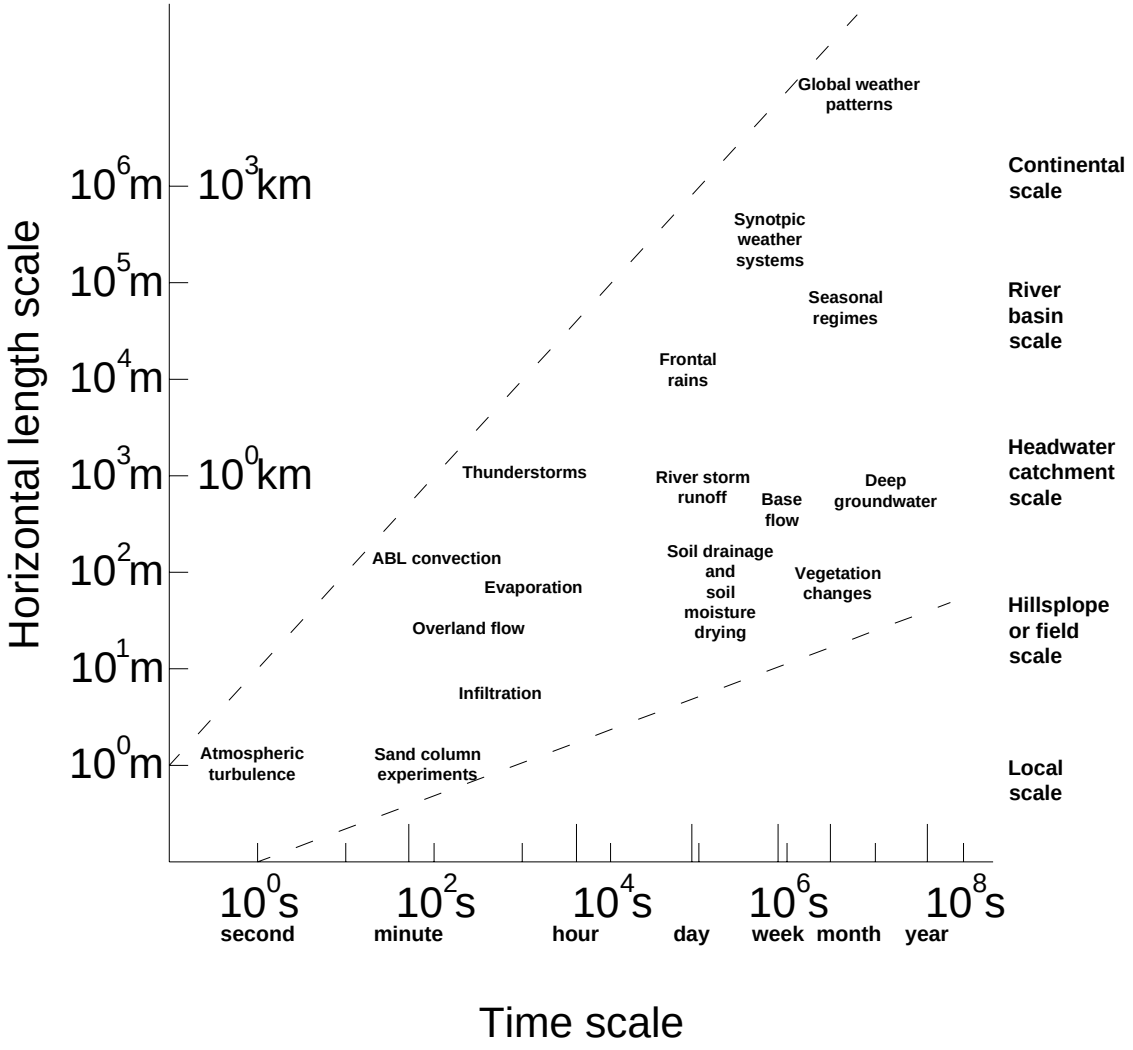

Figure 2.2 Spatial and Temporal Scales of the Hydrologic Cycle (after Brutsaert, 2005)

The geological conditions that influence the hydrologic cycle can be considered spatially variable and temporally static while the meteorological and vegetative conditions both have a high degree of spatial and temporal variability. The various scales of interaction produces considerable complexity when attempting to understand, describe, and simulate the hydrologic cycle.

2.2 Simulation of the Hydrologic Cycle

When all the components of the hydrologic cycle are accounted for as inputs, outputs, and storage mechanisms, the hydrologic cycle can be idealized as a closed system that conforms to the principal of conservation of mass (of water in all phases). Since the system is closed it can quantitatively be viewed with the concept of a water budget where the movement and storage of each component is tracked and accounted within the system.

All the hydrological processes are inter-related and dependant on each other. Whether a hydrological process is considered an input or an output is dependant on the point of view. With respect to groundwater systems the balance between the inputs and the outputs to the system can be expressed as:

$$R = P - I - ET \pm O \pm \Delta S \quad (1)$$

where: R is the recharge reaching the aquifer (percolation);
P is the precipitation;
I is the interception by the vegetation;
ET is the sum of evaporation and transpiration;
O is the lateral overland flow; and
ΔS is the change in water storage in the unsaturated and saturated zones;

The components of the hydrologic cycle must be accounted for in a deterministic, physically-based manner. To this end, Freeze and Harlan (1969) drafted a conceptual framework for the numerical modeling of the mechanisms that describes the movement and storage of water within a closed system, referred to as the "Blueprint". The major limitations of physically-based approaches include issues of scale, parameterization, capturing the spatial and temporal variability of boundary conditions, and computational intensity.

In contrast to the physically-based approach conceptualized in the Blueprint there are also "systems-based" (also referred to as empirical or "black box") approaches. In this approach the physics involved in the hydrologic processes are not considered. Rather, empirical relationships are defined between inputs (e.g., precipitation) and outputs (e.g., stream flow). This type of approach is often referred to as a "black box" approach since the mechanisms and the functional relationships of the hydrologic processes are not represented. There are two major limitations to the systems-based approach. First, parameters are often lumped and lack physical meaning implying that the conditions may need to be characterized based on the modelers experiences and biases. The second limitation is that these models cannot be used as a predictive tool for stress conditions (e.g., climate change, urban development) that are outside its calibration range (Brutsaert, 2005).

A third classification of a hydrologic response model, referred to as a "grey box" by Brutsaert (2005), is one that is an intermediate approach to the physically-based and systems-based approaches. In these types of models, a Hydrologic Response Unit (HRU) is defined based on unique combinations of areas that contain similar properties (e.g., soil, slope, vegetation characteristics). The relationship between the inputs and outputs are based on simplifications that retain some physical meaning but lack the rigorous descriptions of the relevant physical processes.

In order for the hydrologic response model to be an effective tool that can produce meaningful results it must be able to simulate all of the significant hydrologic process operating within the area of study. If the model is to be relied on in a predictive capacity it must not only be able to represent historical and current conditions but also future scenarios under new and different stress conditions.

2.3 The Physically-Based Modeling Approach

Freeze and Harlan (1969) eloquently and concisely provide a description of what physically-based modeling is:

> "In a physically-based mathematical model, the component, time-dependant hydrologic processes are represented by a set of partial differential equations, interrelated by the concepts of continuity of mass and of momentum. These equations, together with the boundary conditions that define the shape and boundary properties of the basin, comprise the composite boundary value problem that is the hydrologic response model. A boundary value problem of this complexity must, by its very nature, be solved by numerical techniques and a digital computer."

Typically, modeling the hydrologic response of a catchment is done with a surface water model or a groundwater model. Surface water models tend to oversimplify subsurface processes and groundwater models oversimplify surface water processes. This simplification is typically treated by adding a source/sink component to the model to account for hydrologic processes occurring outside the model domain of interest. For example, in surface water models infiltration into the subsurface may be simulated as a sink with no further provisions given for routing the water. Similarly, in groundwater models boundary conditions are specified to represent aquifer communication with surface water features. In either case, as water moves from one domain to another it is considered to be "lost" from the system.

In order to simulate the hydrologic response as presented by Freeze and Harlan (1969) the groundwater and surface water domains need to be 'coupled' or 'integrated' into a single framework.

The communication between the models can be done in a 'sequentially-coupled' or 'fully-coupled' approach. The sequentially-coupled approach can be implemented by either 'externally' or 'internally' coupling the hydrologic models at the water table. With externally coupled models, the simulation result from one model is applied as a boundary condition to another. Examples of this approach are Jyrkama et al. (2002) and Scibek and Allen (2006) who used HELP3 (Schroeder et al., 1994a) to simulate the processes of infiltration, evapotranspiration, and runoff to estimate the recharge reaching the water table, which is used as a boundary condition to a three-dimensional groundwater flow model, such as MODFLOW (e.g. McDonald and Harbaugh, 1996). In this case, there is no feedback from the groundwater model to the HELP3 model. The groundwater and surface water models can also be internally coupled as is done in MIKE-SHE (Abbot et al., 1986a/b). In doing so, the model iterates between the solutions provided by the groundwater model (i.e., determining the location of the water table) and the fluxes from the unsaturated and overland flow model to the water table.

A fully-coupled, or fully-integrated, groundwater-surface water modeling approach links the subsurface and surface domains at the land surface boundary through first-order flux relationships. This provides a robust and physically-based simulation approach as all the principal mechanisms for generating stream flow are accounted for, groundwater discharge providing base flow, subsurface storm flow, Dunne overland flow (saturation from below), and Horton overland flow (saturation from above). Examples of integrated models include Integrated Hydrologic Model (InHM) (VanderKwaak and Loague, 2001), MODHMS (Panday and Huyakorn, 2004), and HydroSphere (Therrien et al., 2005). In a study comparing sequential (internally-coupled) and fully-coupled models, Fairbanks et al., (2001) concluded that the fully coupled approach is robust and provides reliable solutions while sequentially-coupled models perform well when the interaction fluxes between the surface and subsurface domains are low.

2.3.1 Advantages of the Physically-Based Modeling Approach

The numerical representations of the hydrological process are based on mimicking the mechanics and properties of the processes involved whose parameters can be measured and have a physical meaning. The use of physically-based, numerical models to simulate water flow (pathways and velocities) allows for further numerical modeling to be carried out that is dependant on the water flow path such as sediment, solute, and reactive transport.

Since the simulation results are directly dependant on the distribution of parameters, such an approach is well suited to assess the potential impacts for many types of diverse water resource problems facing the environment and society today through the use of "what-if" scenarios. The parameter distributions of the numerical model can be modified to reflect the properties of future conditions and the numerical model can be re-run to simulate the outcome of such conditions. Issues that impact hydrological processes that can be evaluated using the "what-if" approach include (but are not limited to) evaluating: changes to land-use practices (e.g., urbanization, deforestation, agricultural development, etc.), sustainable water resource development, impacts to groundwater and surface water exploitation and contamination, and the impacts of climate change and salt water intrusion.

Given that the numerical model is based on the discretization of partial differential equations describing the relevant physical processes with physically meaningful parameter values, the model can be applied to different geographic locations. To further this point, Bathurst and O'Connell (1993) suggest that physically-based models can be applied with more confidence at different locations and under different conditions than those they were validated for because of the physical laws they embody.

Furthermore, these models can be used to provide the user with feed back as to the spatial distribution of the sensitivity of model input parameters. This information can be used to guide efforts to collect field information in locations where it will provide the most information and to aid in the interpretation of the simulation results (e.g., Gillham and Farvolden, 1974; Sykes, 1985).

2.3.2 Disadvantages of the Physically-Based Modeling Approach

The advantages of physically-based modeling are appealing. However, interpretation of the simulation results must be done with an appreciation for limitations of the particular physically-based model(s) employed. The limitations of models that follow the "Blueprint" stem from the assumptions made in the formulation of the mathematical expression representing the hydrological processes, the techniques employed by numerical schemes to find "well-behaved" numerical solutions to the mathematical expressions, and the issue of scale in hydrology. In addition to these, due to the complexity involved, especially when considering integrated groundwater–surface water modeling, requires the modeler to have a broad and sophisticated knowledge base.

Distributed, physically-based modeling requires that the modeler have a specialized skill set which includes understanding the hydrological response mechanisms of the basin under study, parameterization of the properties and boundary conditions, model calibration and validation, and

understanding for the relationship between the conceptual, mathematical, and numerical models (Bathurst and O'Connell, 1993). In fact, distributed, physically-based models have become so detailed and complex that the numerical model can be a problem in its own right (Bear et al., 1992).

Since the parameters have a physical meaning they can not be arbitrarily adjusted to fit the performance measure dataset but rather, may be calibrated to within an acceptable range of values. That is, the model must produce accurate results for the right reasons (Klemes, 1986). This is particularly challenging given the disparity in scales between hydrologic models, hydrologic processes, and the measurement of materials properties.

In a critical review of numerical models, Oreskes et al. (1994) contend that the verification and validation of numerical models is impossible, because in reality, natural systems are never be truly closed and model results are always non-unique. Though a model can simulate and confirm limited field observations, they must be viewed with skepticism and should not be held as absolute truth. Oreskes et al. (1994) insist that the primary value of a model is a heuristic tool and that it should be utilized as an aid in the decision making process. Essentially, one must bear in mind that though physically-based, distributed models have inherent advantages over empirical models, all models are incomplete abstractions of the natural system and increased sophistication does not guarantee more accurate results. The state of the science (and art) of hydrologic modeling requires that models be used as a tool in the decision making process (e.g., Bear et al., 1992; Bredehoft, 2003; Neuman and Wierenga, 2003).

2.3.3 Parameterization Requirements

Distributed modeling implies that the discretization of its spatial and temporal increments must be finer than the material distributions and processes being modeled (Vieux, 1993). The degree of parameterization required is directly related to the scale of discretization. As the discretization becomes more refined, the complexity of the problem increases as it necessitates that a greater number of parameter values are specified.

Specifying all necessary parameter values for each computational node/element of a spatially discretized system requires consideration to be given as to how the data is distributed over the model discetization. In the case of sparse datasets (e.g., point precipitation measurements, geologic boreholes) the information needs to be distributed in a realistic manner across the model domain. A variety of algorithms exist to interpolate and extrapolate sparse datasets, each having its own advantages and disadvantages. Ideally, sparse datasets should be distributed in a physically-based,

meaningful manner which entails giving consideration to the physical processes that give rise to the distributions that are being estimated by the algorithm. The kriging method is often used as it honors the input data, inherently considers the spatial structure of the dataset, and provides an estimate of the uncertainty. However, this method is computationally intensive and can be highly sensitive to the selection of the proper semi-variogram (e.g., spherical) and the geostatistical method employed (e.g., ordinary kriging) all of which can have a significant impact on the estimated distribution (Zimmerman et al., 1998 and Patriarche et al., 2005).

The detail and complexity of physically-based, distributed models results in extensive parameterization requirements. The effective values of all the model parameters can not be known for the entire area of study, making physically-based models vulnerable to the criticism that the model's capability exceeds data availability (Vieux, 1993). The concern of over-parameterization was recognized by Freeze (1971a) at the advent of physically-based distributed modeling. To the charge of over-parameterization Freeze (1971a) replied that if the deterministic approach can be shown to have greater value relative to the empirical approach (that requires less data) it would encourage the measurement of necessary data.

The uncertainty associated with the model structure, model parameters, and their distributions leads to the problem of *Equifinality* (Beven, 1993). The problem of equifinality is that multiple parameter sets and model structures can produce equally acceptable fits to the observed data. At its simplest, the non-uniqueness of the saturated groundwater flow problem is most readily identified by recognizing the relationship between hydraulic conductivity and recharge. As more hydrological processes are accounted for there are more parameters available for the modeler to adjust.

Concerns relating to parameterization requirements are not limited to over-parameterization but also the ability to measure effective parameter values. Beven (1993) states that physically-based models, by their nature, are designed to have parameters that are physically measurable. This is not always the case; mathematical descriptions used to simulate the hydrological processes of infiltration (e.g., Brooks-Corey, 1964) and evapotranspiration models (e.g., Kristensen and Jensen, 1980) employed by MODHMS and HydroSphere, for example, requires the specification of parameters that have little or no physical meaning. The parameters α (inverse of the air-entry pressure head), β (pore-size distribution index), and *lp* (pore-connectivity index) of the Brooks-Corey model have physical descriptors but their parameter values are assumed (i.e., *lp*) or based on fits to experimental data (i.e., α, β). In this regard, some aspects of deterministic, physically-based modeling have not improved on empirical approaches.

2.3.4 Issues of Scale

The issue of scale is one that affects all the hydrologic processes represented in groundwater and surface water models. The various hydrologic processes (identified in Figure 2.1) occur at different temporal and spatial scales (as shown in Figure 2.2). For example, precipitation events occur over large areas for short durations, overland flow occurs over short distances and is rapid, while groundwater flow occurs over large areas and is relatively slow. Even within a given hydrologic process, the effects of scale can be significant, for example, surface tension of water and the presence of macropores affect the processes of infiltration or inundation heights of roughness elements, thus affecting overland flow. In numerical models, the spatial effects of scale result from a mismatch between the size of the model elements and the heterogeneity and structure of the physical system. In an analogous manner, scale effects also occur due to a mismatch in temporal scales.

The spatial effects of scale are manifested in two ways. The first case is the ability of the model's discretization to capture the heterogeneity within the catchment and the second is in representing the variability within the model elements themselves (Bathurst and O'Connell, 1993). In addressing the first point, avoiding down-scaling could potentially be addressed by taking measurements for model parameters for every element. However, this not practical nor do measurement techniques exist to collect subsurface data at the element scale (Beven, 1993). With respect to up-scaling material and boundary condition properties on the sub-computational level to the scale of the model element, no standard methods exist. For example, in a review of the scales of processes occurring within the vadose zone (i.e., the effective representation of unsaturated hydraulic conductivity values) Harter and Hopkins (2004) find that many of the approaches taken by researchers to address the issues of scale have had some measure of success but that the assumptions that govern the use of these techniques may be exceedingly restrictive and their conclusions echo the concerns of Klemes (1986) that there is no universal solution to the problem posed by the hierarchy of significant process scales. Even in a 'relatively' homogeneous media, detailed studies have shown the effects of scale, for example, Sudicky (1986) finds that values of saturated hydraulic conductivity can vary by orders of magnitude over very short distances in the clean, homogenous sand of the Borden aquifer. The scale dependence of hydraulic conductivity with respect to the measurement technique is well known in the field of hydrogeology (e.g., Bradbury and Muldoon, 1989; Hart et al., 2006). In fact, all model parameters are subject to the effects of scale.

2.4 Challenges of Fully-Integrated Groundwater-Surface Water Models

Brustsaert (2005) summarizes the major concerns associated with distributed physically-based modeling as:

i) never being able to accurately measure the properties of natural catchments, and

ii) that the solutions to the numerical implementation of the mathematical expressions representing the hydrologic processes can only be obtained for grossly idealized conditions, which are coarse approximates of the dynamics of field processes.

The limitations of i) have already been discussed, and include the challenges of parameter value distribution and scale when implementing a distributed, physically-based approach. With respect to ii), the limitations of primary concern are in the representation of the unsaturated zone as it links the subsurface and surface domains thereby exerting controlling influence over the interaction between precipitation, recharge to groundwater, and surface runoff. The physically-based modeling of the overland flow and surface waters, as part of a fully-coupled model, also poses significant challenges in simulating event-scale hydrologic processes in a complete and rigorous manner. The issues relating to the numerical approaches to simulating variably saturated and overland flow are discussed in the following sections.

2.4.1 Flow in the Unsaturated Zone

Proper representation of the unsaturated zone is critical for conjunctive groundwater–surface water modeling. The unsaturated zone links the subsurface and surface domains and controls the partitioning of precipitation between infiltration and overland flow. Flow in the unsaturated zone is more complicated than the saturated zone because there are two fluids present, water and air. In this two-phase system, water is the wetting fluid, meaning that it preferentially coats the soil grains, and air is the non-wetting fluid. As water migrates through the unsaturated zone it displaces the air within the pore space.

Unlike the saturated zone where moisture content equals the soil porosity and hydraulic conductivity is constant for the given soil texture, in the unsaturated zone both moisture content and hydraulic conductivity are dependant on the pressure head. This gives rise to what is often referred to as characteristic curves such as those in Figure 2.3.

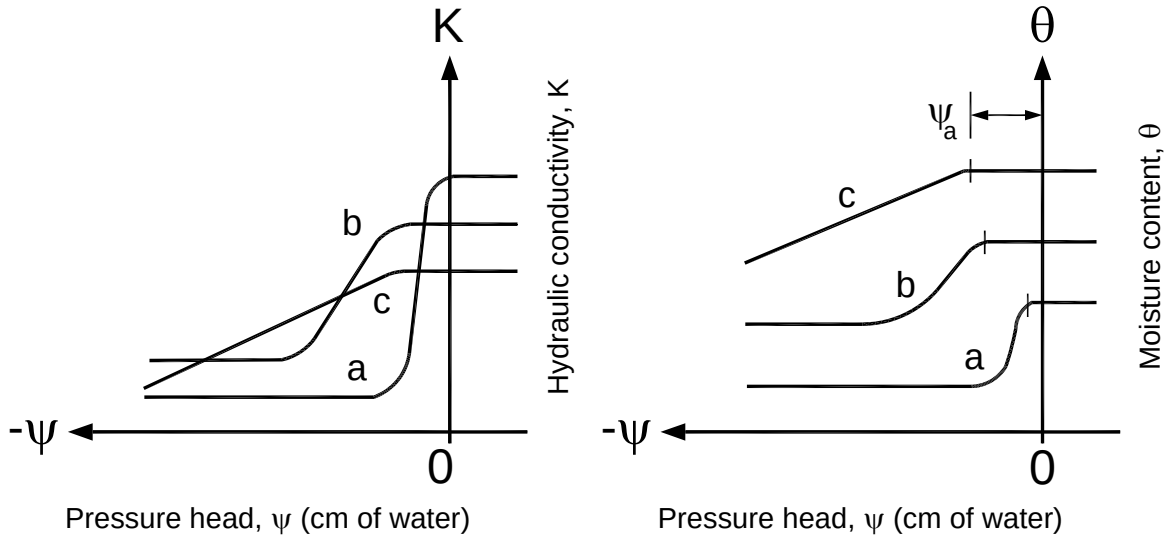

Figure 2.3 Characteristic curves illustrating the relationships between pressure head (ψ), hydraulic conductivity (K), and moisture content (θ) (after Freeze and Cherry, 1979)

Due to surface tension of water and air, the hydraulic head in the unsaturated zone is less than atmospheric (i.e., pressure head is negative), also referred to as capillary pressure. Smaller pore throats, typical of silt and clay materials, create more surface tension than larger ones, such as sand. Thus, for a given pressure head a coarse-grained material will have less moisture content than a fine-grained material. As the soil moisture increases, progressively larger pore spaces (with lower surface tensions) fill with water. This relationship between negative pressure head and soil moisture, referred to as the water-retention curve, is non-linear. Furthermore, the shape of the curve is dependant on whether the soil is wetting or drying. This occurs because drainage is controlled by the smallest pores, whereas wetting is controlled by the largest. The "scanning curves" between the main wetting and drainage curves illustrate the hysteretic effect of antecedent moisture conditions which can play a significant role in the response of a soil type to an advancing wetting front (Freeze, 1971b).

Functional relationships for soil water retention characteristics and their relation to hydraulic conductivity, as shown in Figure 2.3, have been developed by Brooks and Corey (1964), Mualem (1976), and van Genuchten (1980). The primary difference between the Brooks-Corey model and the Mualem and van Genuchten models is that the Mualem and van Genuchten models are continuous functions for the entire range of pressure heads while the Brooks-Corey model specifies a minimum displacement pressure which is the displacement pressure of air that water must overcome before infiltration can take place. The values of the parameters used in the functional relationships for various soil textures are based on fitting curves to observed data.

2.4.2 Numerical Simulation of Flow in the Unsaturated Zone

The equation describing the movement of water in the unsaturated zone is given by Richards (1931), referred to as the Richards' Equation. The Richards' Equation is derived by applying the Darcy Equation for multi-phase flow (i.e., assuming water and air are the only phases present) with the principle of conservation of mass equation, while making some simplifying assumptions.

The equation is developed for a representative elementary volume (REV) where the properties of the medium are assumed to be constant (Bear, 1972); the scale of the REV is on the order of 10^{-2} m to 100 m (Harter and Hopmans, 2004). The concept of a REV is not used to discretize the model domain for groundwater modeling on the catchment scale (or greater) and thus is subject to the effects of scale.

The Richards' Equation incorporates many assumptions that place restrictions on the appropriate use this equation, which typically include: laminar flow, that inertial forces, velocity heads, temperature gradients, osmotic gradients, and chemical concentration gradients are all negligible, that the porous medium is non-deformable, that water is incompressible, and that the air phase of infinitely mobile (Freeze, 1971a). Richards' Equation is presented as:

$$\frac{\partial}{\partial x_i}\left[\frac{k_{ij}^0 k_{rw}}{\mu_w}\left(\frac{\partial p_w}{\partial x_j}+\rho_w g\frac{\partial z}{\partial x_j}\right)\right]\pm\Gamma = n\frac{\partial S_w}{\partial t} \qquad (2)$$

where:

k_{ij}^0	are the components of the intrinsic permeability tensor;
k_{rw}	is the relative permeability;
μ_w	is the absolute viscosity;
p_w	is the fluid pressure;
ρ_w	is the density;
g	is the gravitational constant;
z	is the elevation relative to a reference datum.
Γ	is used to represent sources and sinks (e.g., evapotranspiration)
n	is porosity; and
S_w	is the storativity.

In the case of saturated groundwater flow, the k_{rw} term becomes unity and (2) becomes a linear PDE which is much less computationally intensive to solve. Generally speaking, the assumptions noted for the development of the Richards' Equation are reasonable and allow its use in a wide range of applications. However, since the effects of temperature are precluded from its development it does not allow for the simulation of the hydrologic response at freezing temperatures. This poses a restriction on its application as a tool to simulate long-term, continuous hydrologic response for

geographic locations that experience freezing temperatures that are seasonally prevalent. When the water in soil pores freeze the void space becomes increasingly restricted, causing increased tortuosity and a decrease in hydraulic conductivity, hence reducing infiltration and promoting overland flow. As the soil water freezes it expands to become ice which deforms the soil matrix, violating the premise that the medium is non-deformable. The impact of frozen soil during the winter also has implications when the soil thaws during the spring, increasing the hydraulic conductivity and allowing for the rapid infiltration of snowmelt (Jyrkama, 1999).

2.4.3 Vertical Discretization of the Unsaturated Zone

Due to the relationships captured by the characteristic curves, between pressure head – soil moisture and pressure head – hydraulic conductivity, the Richards' Equation is a highly nonlinear partial differential equation.

Both the finite difference (e.g., Panday and Huaykorn, 2004) and finite element (e.g., Therrien et al., 2005) discretization approaches are used to solve the Richards' Equation numerically. Typically, for reasons of stability, an implicit temporal discretization scheme is employed when solving the equation numerically (Paniconi and Putti, 1994). An intermediate step is required to iteratively resolve the non-linearity presented by relative hydraulic conductivity such that a numerical solution can be obtained (Paniconi et al., 1991). The intermediate iteration is necessary to solve the dependant variable (i.e., pressure head) with the nonlinear terms (i.e., moisture content and hydraulic conductivity). Various iterative and non-iterative strategies for the numerical solution to the Richards' Equation are investigated by Paniconi et al. (1991) and Paniconi and Putti (1994). Some strategies are more efficient and robust than others. However, they are all computationally burdensome relative to solving the Richards' Equation under saturated conditions (i.e., a constant hydraulic conductivity values).

Ultimately, the rate at which the wetting front infiltrates into the soil is controlled by the hydraulic conductivity of the uppermost cells. As can be seen in Figure 2.3, a small change in moisture content can result in a large change in pressure head and hence, hydraulic conductivity. The rate at which the hydraulic conductivity increases (from initially dry conditions) is dependant on the rate at which the soil moisture content increases which in turn is a function of the negative pressure head. Accordingly, if the near surface vertical discretization is too coarse then a small amount of water entering will not sufficiently increase the moisture content of the entire cell and the hydraulic conductivity will remain low. In this case, the hydraulic conductivity remains low and the other

concurrently acting hydrological process (i.e., evapotranspiration and runoff) will deplete the available water before it can infiltrate into the subsurface. Thus, for initially dry conditions, infiltration will be underestimated while evapotranspiration and runoff will be overestimated. Consequently, even if the numerical techniques employed by the chosen model can rigorously account for the initiation of both Hortonian and Dunne overland flows, if the discetization is not adequate the simulation result will not be physically correct.

The appropriate level of vertical discretization of the Richards' Equation required for simulating infiltration, evapotranspiration, and initiation of runoff can be determined through the analysis of a spatial convergence study as demonstrated by Downer and Ogden (2004). The outcome of a spatial convergence study reveals the resolution (i.e., cell size) required to achieve a solution that accurately represents the system. In order to obtain a meaningful, physically correct solution to the Richards' Equation under variably saturated conditions a very fine vertical discretization is required to capture the non-linear response of the vadose zone, as illustrated by the soil characteristic curves (Downer and Ogden, 2004). The results of their investigations show that a near surface vertical discretization coarser than 2 cm can result in significant misrepresentation of the hydrological process, (i.e., infiltration, evapotranspiration, and runoff). Downer and Ogden (2004) conclude that employing too coarse of a vertical discretization, especially at the ground surface, can result in a model that does not respond in an accurate, physically correct manner. In fact, this necessarily implies that too coarse of a discretization will result in the specification of physically unrealistic parameter values in order to achieve a solution that is consistent with observations.

El-Kadi and Ling (1993) have proposed using the Courant and Peclet numbers as criteria for estimating the necessary level of spatial and temporal discretization required to find an accurate numerical solution to the Richards' Equation. The Courant number is the ratio of travel by advection (in the vertical direction) to the cell size (i.e., Δz) and the Peclet number is the ratio of advection to dispersion. With respect to the Richards' Equation, the soil moisture diffusivity term, the product of the unsaturated hydraulic conductivity and the slope of the soil characteristic curve (Rolston, 2007), is used to represent the dispersion in the Peclet number. Numerical experiments were conducted for three soil types with a wide range of material properties (e.g., capillary height and saturated hydraulic conductivity). The results show that the Courant and Peclet numbers are highly dependant on the material type and their criteria vary by orders of magnitude for achieving an optimal solution. In general, the upper range for the Courant and Peclet numbers was found to be about 2 and 0.5, respectively. This translates to quite stringent space and time increments restrictions of 1 to 2.5 cm

and on the order of seconds to minutes, respectively. Relaxing these criteria likely leads to numerical dispersion and overshooting (El-Kadi and Ling, 1993).

The computational requirements (for both storage and processing speed) are directly proportional to the level of discretization employed in the model. This signifies that the vertical discretization required to achieve spatial convergence, which is necessary to properly represent near surface hydrological processes, may be too burdensome for the current state of available desktop computing technology when simulating the hydrologic response at the watershed scale. Indeed, Harter and Hopmans (2004) points out that the current transient modeling of the three-dimensional Richards' Equation that can be solved in a reasonable timeframe is limited to approximately 10^6 nodes while the application of the Richards' Equation at a discretization level consistent with the REV scale it is derived (i.e., 10^{-2} m and 100 m or the vertical and horizontal directions, respectively) for a watershed application (e.g., 100 km^2) with a 1 m thick root zone requires 10^{10} nodes. When further considering the discretization required for the remaining thickness of the subsurface and possible integration with surface water equations for overland flow (with even finer time-stepping requirements) this problem becomes daunting. At the discretization level of a REV, the computational effort required is impractical and the parameterization effort is impossible.

To alleviate the numerical burden imposed by the nonlinear relationships of the vadose zone, captured by the characteristic curves, an upscaling approach has been applied whereby the response of the vadose zone at the REV scale is translated to its effective response to the scale of the vertical discretization. Harter and Hopmans (2004) provide a detailed review of the various upscaling approaches that have been take by researchers. A variety of analytical and numerical models have been developed for steady-state or transient conditions, using vertically lumped soil texture or heterogeneous soil columns. Despite the research efforts to date, Harter and Hopman (2004) identify that more research still needs to be done before the upscaling approach may be utilized by the modeling practitioner.

The Richards' Equation mathematically describes the rate at which water can migrate through a variably saturated porous medium. However, when considering the process of infiltration, it is important to bear in mind that it is driven by precipitation events. Dunne et al. (1991) report that for soils that do not form seals, the infiltration rate is positively correlated with rainfall intensity. Essentially, with increasing rainfall intensity the tendency to exceed to the saturated hydraulic conductivity for larger portions of soil increases thereby increasing the average hydraulic conductivity. There is a secondary effect here as well; as soil becomes saturated and the overland

flow progressively inundates a larger portion of the downslope area where the runon can distribute the water to areas of soil moisture deficit. The portion of overland flow that does not infiltrate is captured by runoff to surface water channels.

2.4.4 The Occurrence of Overland Flow

Overland flow is controlled by the response of the vadose zone and can be triggered by two mechanisms. The first is by infiltration excess, formalized by Horton (1933), whereby overland flow occurs when the rainfall intensity exceeds the infiltration capacity of the soil, essentially saturation from above. The second mechanism is saturation from below, also referred to as saturation excess, whereby overland flow can only occur once the underlying soil is saturated (Dunne, 1970). In this case, infiltration causes the water table to rise until it reaches the ground surface. As such, as an increasing area of soil becomes saturated, a greater surface area is available to contribute to runoff; this is known as partial contributing area or variable source area. The saturation of the soils at the ground surface governs the initiation of overland flow, emphasizing the importance of antecedent moisture conditions.

The theory of overland flow initiated by infiltration excess is applicable to semi-arid environments but is a rare occurrence in vegetated, humid conditions. In the latter conditions, overland flow is most prominently generated by saturation excess and is a rare occurrence (Freeze, 1972a). Freeze (1972b) summarizes the necessary criteria for ponding to occur, as demonstrated by Rubbin (1966), as requiring a rainfall rate to be in excess of the saturated hydraulic conductivity of the surface soil and for the rainfall duration to be greater than the time required for the soil to become saturated. The rarity of overland flow can be recognized with consideration for the saturated hydraulic conductivity and typical rainfall intensities (e.g., less than the 10-yr return storm for Boston, Mass, US area as exemplified by Freeze (1972b)). The rise of the water table to generate overland flow can be rapid if the capillary fringe extends to ground surface (Gillham, 1984). As such, antecedent moisture conditions may play an important role in the generation of overland flow especially in areas of low topography (e.g., rivers).

2.4.5 Resistance to Overland Flow

In general, the pattern of flow over land is the result of gravity acting on the water in the downstream direction which is being counteracted by the internal (i.e., the viscosity of the fluid) and the external (i.e., those forces imposed by obstacles) resistance forces. All roughness elements on a

soil surface contribute to the external resistance encountered by the overland flow (Rauws, 1988). This additive nature of the resistance to overland flow has been expressed as a composite, or effective, roughness (Abrahams et al., 1995). Qualitatively, this represents the sum of the resistance presented by soil grains, microtopography, ground surface cover, and the standing vegetation. The resistance offered by each roughness element can be characterized by it is individual shape and size, as well as its spacing and pattern relative to the surrounding roughness elements (Abrahams and Parsons, 1994).

Experiments conducted in the field and laboratory generally express the effect of roughness on overland flow as the relationship between the Darcy-Weisbach friction factor and the Reynolds number. The Reynolds Number is the dimensionless ratio of inertial to viscous forces. Viscosity is dependant on temperature which can be considered constant at the event scale. As such, the viscosity of the water can also be considered constant and the Reynolds Number is effectively a measure of the overland flow velocity. There are many relationships between the friction factor and the Reynolds number (e.g., Abrahams and Parsons, 1994). The typical relationships between the friction factor and the Reynolds number are a convex upward and a negative slope (Rauws, 1988), as illustrated on Figure 2.4, though others are reported (e.g.Abrahams and Parsons, 1994). This figure highlights some of the key complexities in quantifying resistance to overland flow. It illustrates the additive nature of the forces opposing flow, in this case the contributions to simulated soil roughness from grain and form resistance. Grain resistance represents contributions from soil particles and micro-aggregates. Form resistance is offered by macro-roughness elements.

Figure 2.4 also clearly shows the non-linearity of roughness and its dependence on external factors, such as, in this case slope, which limits the application of a friction factor value to a narrow range of conditions. The convex upward relationship is typically observed on mild slopes. In this situation, the grain resistance has a lesser influence than the form resistance. As the depth of overland flow increases the roughness element becomes progressively inundated, increasing the wetted upstream-projected area, resulting in increased resistance. When the roughness element is submerged its resistance decreases (Rauws, 1988; Abrahams and Parsons, 1994; Lawerence, 1997). At steeper gradients a negative sloping relationship has been observed. This is attributed to the form friction no longer having an over-riding influence over grain friction and hence resistance continually decreases with increasing depth (Rauws, 1988).

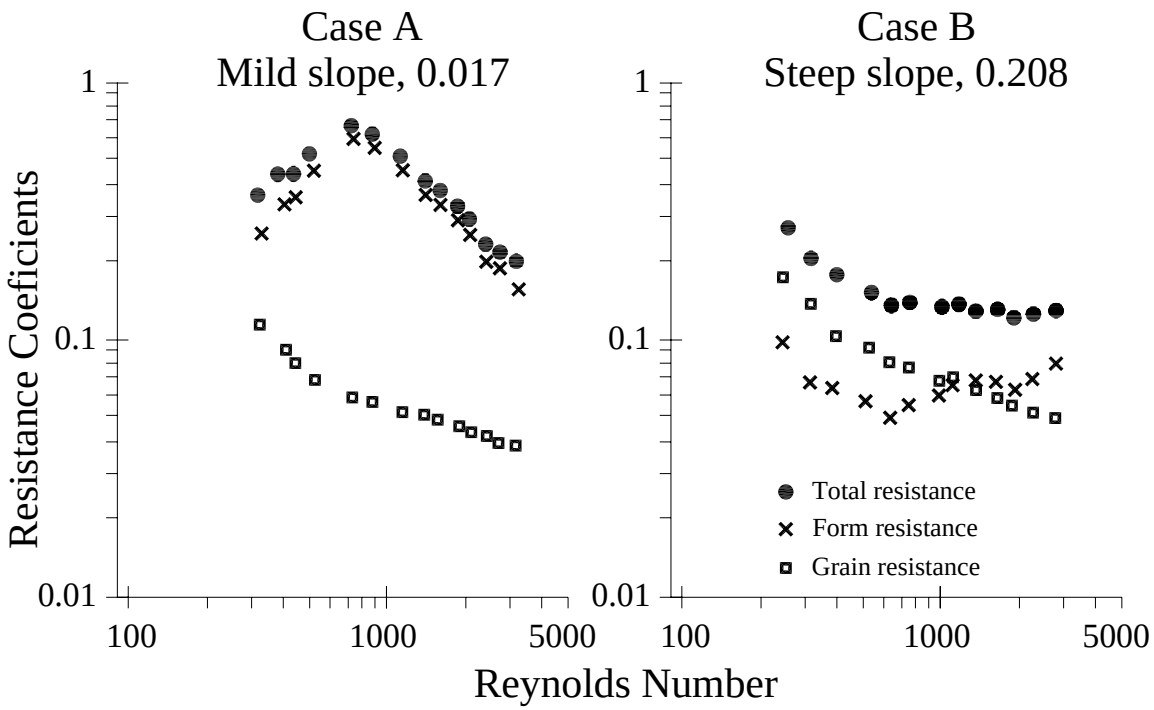

Figure 2.4 Contribution of form and grain resistance to total resistance as a function of the Reyonlds Number for mild and steep slopes (after Rauws, 1988)

The effect of vegetation on the resistance to overland flow requires due consideration. Vegetation plays an important role through retarding the overland flow velocity, thereby providing greater detention time, and allowing for greater infiltration (Dunne et al., 1991). Vegetation is also one of several mechanisms by which marcopores are generated (Walker et al., 2002) which provide preferential pathways for infiltration and in so doing decreases overland flow. The seasonality of vegetation produces a temporally varying resistance to overland flow which can significantly alter the relationship between runoff and infiltration. The greatest impacts are in areas of intense vegetation (e.g., agriculture) and in shallow channels (e.g., headwaters of the surface drainage network).

Another characteristic that is particular to vegetative resistance is that it is subject to deformation with increasing depth of flow, signifying that resistance to overland flow also varies at the event scale. This is studied in detail by Fathi-Moghadam and Kouwen (1997) who utilized physically-based parameters for the calculation of resistance (expressed as Manning's n) presented by vegetation. Their experiments show that the calculated roughness values are within the acceptable ranges, as reported by Chow (1953) and Arcement and Schneider (1984), but show that the Manning's n roughness value increases proportionally to the square root of depth and is inversely proportional to the mean velocity under marginally inundated conditions. On a similar note, overland

flow concentrated in rills gives rise to sediment mobilization and erosion. As such, the land surface is continually being deformed, creating ever-changing preferential pathways, and altering the roughness characteristics of the land surface.

2.4.6 Impact of Human Activity on Surface Water Flow Pathways

In rural and urban areas, along agricultural plots and roadways, surface water routing features have been constructed to channel overland flow. In an urban setting this is typically accomplished with curbs and storm sewers. In an agricultural setting runoff is channeled by furrows to the edges of plots where it is diverted to ditches which may also be receiving flow from tile drains. Alongside roadways, road runoff is channeled to ditches and through culverts which ultimately carry the water to streams or surface water detention ponds. In other cases roads are raised creating barriers to overland flow, creating depressions that are disconnected from the catchment outlet, reducing the effective drainage area.

The preferential pathways of human development on the land surface are typically at a finer resolution than the information (e.g., Ontario Base Maps (OBM) or a Digital Elevation Model (DEM) derived from remote sensing technology used to parameterize regional scale models. Agricultural plots, roadways, and their associated drainage networks are not necessarily oriented coincident with the slope or aspect of the land surface limiting the application of the DEM to define the drainage on scales of the stream catchment or greater.

Duke et al. (2003, 2006) present a methodology for downscaling DEM data with the ancillary information. The secondary information, road elevation, ditch depth, irrigation channels, and culvert location, are indirectly incorporated with the DEM when it is processed to derive the drainage pattern. A Road Enforcement Algorithm (REA) and a Channel Enforcement Algorithm (CEA) were developed to reroute overland flow paths from the well known D8, steepest decent, algorithm (O'Callaghan and Mark, 1984). The REA and CEA use the ancillary information to enforce drainage barriers and preferential surface water pathways. The effect on overland flow paths can be quite pronounced and shown in Figure 2.5 (Duke et al., 2006).

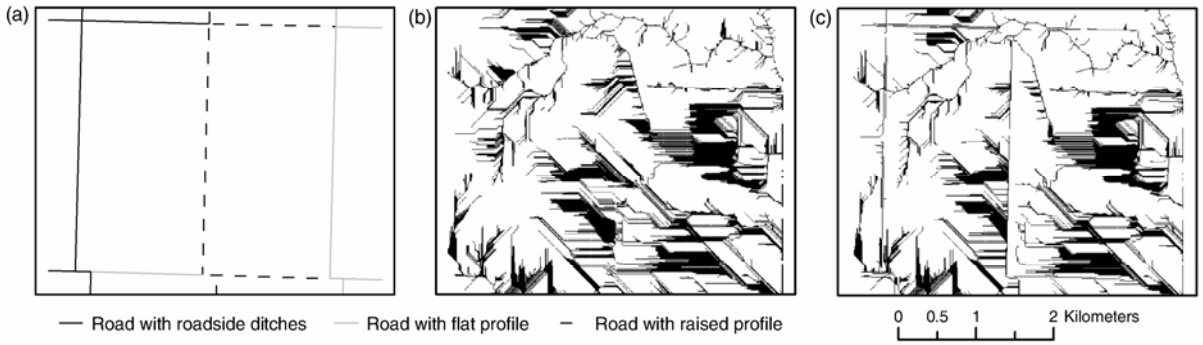

Figure 2.5 Overland flow-path patterns resulting from the REA (after Duke et al. (2003)): (a) a typical road network; (b) D8-derived drainage pattern showing the grid cells with a runoff contributing area greater than 5000 m^2, in black; (c) REA-derived drainage.

The application of this methodology to the Piyami Drain watershed, Alberta indicated that up to 49% of the watershed area is disconnected from the surface water drainage outlet (after Duke et al., 2006). This can have a significant impact on the dynamics of groundwater-surface water interaction; the distribution of increased surface water drainage by preferential pathways of ditches and culverts and the increased localized infiltration resulting from drainage barriers.

2.4.7 Numerical Simulation of Overland Flow

Shallow overland flow is expressed in a mathematical framework by the set of Saint Venant equations which couple the continuity equation with the conservation of momentum equations in the x- and y-directions. This formulation of overland flow is referred to as the fully dynamic wave model. Two common simplifications to this model are the diffusion wave equation (DWE) and the kinematic wave equation models (KWE). The DWE form of the Saint Venant equations neglects the inertial terms of the fully dynamic wave model, the resulting relationship states equivalence between the gradient in hydraulic head and the difference between the friction and gravity slopes (Singh, 2002). The KWE further simplifies the DWE approximation by neglecting the gradient in hydraulic head, essentially stating equality between friction and gravity forces (Singh, 2002). All three levels of representation of overland flow are non-linear with the DWE and KWE being less intensive to solve numerically.

The conditions under which the KWE is a valid approximation of the fully dynamic wave model for shallow overland flow is quantified by the *kinematic number* (Woolhiser and Ligget, 1967). It is found that the KWE is suitable approximation of the fully dynamic wave model under many natural conditions but may be a crude approximation under smooth urban conditions. There is a general consensus that the kinematic wave theory is reasonably accurate for modeling overland flow as the

kinematic wave is the dominant wave in surface runoff, especially during the rising and much of the recession parts of the hydrograph with recognition that the diffusion or dynamic wave models may be dominant in some cases (e.g., backwater effects) (Singh, 2002).

The KWE approximation assumes the flow to be parallel to the land surface and to be in the direction of maximum slope and limits shallow overland flow to wave translation and not being able to incorporate the subsidence of waves. For this reason, the DWE approximation is applicable over a wider range of conditions and is employed to simulate shallow overland flow in physically-based models such as InHM, MODMHS, and HS. The underlying and limiting assumption for the DWE level of simplification is that the downstream boundary conditions do not affect the overland flow. In other words, waves can only be propagated in the downstream direction and as a result, this precludes the simulation of backwater effects. For further information regarding the approximations of the Saint Venant equations the reader is referred to Vieira (1983).

The two-dimensional diffusion wave approximation for shallow overland flow is presented as (after Gottardi and Venutelli 1993):

$$\frac{\partial h}{\partial t} + \frac{\partial}{\partial x}\left(K_x H \frac{\partial h}{\partial x} \right) + \frac{\partial}{\partial y}\left(K_y H \frac{\partial h}{\partial y} \right) = Q_e \qquad (3)$$

where: K_x, K_y are the surface conductance terms in the x- and y-directions which, are dependant on the choice of relationship used to approximate the friction (e.g., Maning's n)
h is the hydraulic head (i.e., water depth plus elevation);
H is the water depth; and
Q_e is a source term (positive if entering the system)

The assumptions associated with the DWE is that the surface water flow is gradually varying with depth averaged velocities and a hydrostatic pressure distribution in the vertical direction. Furthermore, (3) assumes mild surface slope, dominant bottom shear stresses and that the Manning's equation can be used to approximate a valid frictional resistance.

When combining the groundwater and surface water interactions in a fully integrated framework, the horizontal discretization for the groundwater and surface water models is necessarily coincident. This brings to mind the question of what size control volume is appropriate for modeling overland flow. For groundwater flow the concept of a REV is well known and is the basis for deriving the flow and transport equations for a porous medium. In an analogous manner, the concept of a Representative Elementary Area (REA) is investigated by Wood et al. (1988) and is defined as: "A critical area at which implicit continuum assumptions can be used without knowledge of the patterns

of parameter values, although some knowledge of the underlying distributions may still be necessary."

The study concluded that the notion of a REA does not exist and is strongly influenced by the catchment's topography and to a lesser extent the variability of the soil and rainfall parameters. The non-existence of a REA raises the question of what is a suitable level of discretization for simulating overland flow.

2.4.8 Issues Relating to Simulating Resistance to Overland Flow

The resistance to overland flow is non-linear and strongly dependant on slope, as shown in Figure 2.4, limiting the applicability of a single "effective" friction value; Freeze (1972b) notes that it is the "weakest link in the deterministic chain" of coupled groundwater – surface water modeling. When using a term such as Manning's *n* to quantify roughness the constituents of the composite roughness are lumped into a single term. Due to scale discrepancy between roughness elements in a natural setting and the scale of the model discretization MODHMS and HydroSphere employee additional parameters to help capture the dynamics of overland flow that are neglected by using constant, composite roughness. These parameters include surface flow domain porosity, and obstruction and rill storage, for details, see Therrien et al. (2005). Though these terms better characterize the effects of the environment's geometry, defining appropriate values for these parameters remains a challenge.

As a direct result of the scale discrepancy, sheet flow is simulated over model element faces resulting from the gradient in surface water depth between surface water elevations at model (i.e., computational) nodes; in reality, this mode of overland flow is a rare occurrence as observed by Emmett (1970). The simulation of overland flow occurring only as sheet flow necessitates an overestimation of the roughness parameter. In the numerical model the elemental area is contributing to overland flow where in reality the occurrence of overland flow is highly variable, ranging from concentrated threads to sheet flow. This results in an underestimation of the local surface water velocities (having implications for transport of contaminants) even though the timing and peak of the stream hydrograph may be reproduced by the simulation.

Though it may be possible to simulate the correct stream flow hydrograph by calibration of parameters (e.g., Vieux, 1993; VanderKwaak and Loague, 2001) the parameter values themselves may not be characteristic of the natural properties they are representing but are rather applied as fitting parameters. This is due, in large part, to the scale discrepancy between the model

discretization, the scale the hydrological processes operate on, and the heterogeneity of natural systems. The effects of scale are carried forward when the flow solution is used to drive advection-dispersion models to simulate the transport of contaminants, for example, impacting estimates of first arrival times of contaminants and pathogens.

2.4.9 Temporal Discretization Requirements

When considering groundwater–surface water modeling, the modeler must take into consideration that the velocity of groundwater and surface water are orders of magnitude apart and hence, the temporal discretization becomes a critical component in deterministic, physically-based groundwater–surface water modeling.

In relation to groundwater, the velocities of overland and channel surface water flows are much greater. Dunne and Black (1970) estimate overland flow, velocities to be on the order of 100 to 500 times that of groundwater velocities. When considering channel flow the difference in flow velocities is even greater. Dunne and Black (1970) report that field measurements in small watersheds show that channel velocities are on the order of 1000 to 2500 ft/hr while overland velocities from banks areas is on the order of 20 to 200 ft/hr and that subsurface velocities are on the order of 1 ft/hr or less. The surface water velocities necessitate very small timesteps that are orders of magnitude smaller than those typically encountered in groundwater modeling.

Timesteps for routing of overland flows must be very fine during precipitation events, for example, Downer and Ogden (2004) used a maximum time-step of approximately 1 min which was relaxed to a maximum time-step of 1 hour once overland flow was completed. When consideration is given to channel flows, even finer timesteps are required to produce stable and accurate numerical solutions to the DWE. With current computing power, this limits the length of time that can be simulated to event-based or steady-state applications. The combination of highly refined spatial and temporal discretization effectively precludes rigorous, fully-integrated models from being able to simulate the possible effects of climate change as the simulation length required to make an assessment of the potential impacts is on the order of years to decades to centuries.

VanderKwaak and Loague (2001) report optimistic results using InHM to simulate the groundwater-surface water dynamics of the small, approximately 0.1 km^2, R-5 catchment near Chickasha, Oklahoma, at the event scale. The small cathcment area allowed for a fine spatial discretization to capture the dynamics of the groundwater–surface water interaction. Despite their success, VanderKwaak and Loague (2001) identified that numerical modeling of groundwater-surface

water interactions on the event-based scale requires much more detailed information, for example initial soil moisture conditions and the position of the water table, than traditional groundwater modeling.

With the sophisticated, fully-integrated groundwater-surface water models discussed herein, detailed meteorological inputs are required in order to properly simulate the timing and routing of surface water, especially when considering event-based modeling. In studies conducted by Singh (1997, 2005) it was found that storm direction and velocity and rainfall duration and intensity had significant impacts of storm runoff, infiltration, and the discharge hydrograph. Thus, unless the dynamics of storm events are captured, the overall calibration of the model will suffer as other parameter values will be adjusted (in err to compensate for unrepresented storm dynamics) to calibrate the model output to observations. This level of detailed information is not typically available.

These models show that the equations used to describe the movement of water within a closed system can be solved numerically and are based on a deterministic, physically-based approach. However, this does not necessarily imply that the simulated result is an adequate representation of reality. Singh (2002) makes the following point, referring to physically based modeling of overland flow, which is quite relevant with respect to the state of the science (and art) of hydrologic modeling:

> "Our knowledge about the validity of these descriptions and the physical meaning and measurability of the parameters contained in them is woefully inadequate. A close examination of these descriptions suggests that the so-called physical descriptions are not really physical after all, for we cannot determine their parameters beforehand and therefore a lot of fitting is to be undertaken."

2.5 A Coupled Modeling Approach

The coupled modeling approach is not as computationally intensive and shares many of the advantages of a fully-integrated approach. However, it is not as rigorous in its accounting of the dynamics of groundwater-surface water interaction. There is a variety of groundwater and surface water codes that can be coupled to investigate the interactions of groundwater and surface water. In this investigation, HELP3 is linked with HydroSphere by providing the transient recharge boundary condition.

HELP3 uses a water balance approach to abstract the surface (runoff, surface storage, snowmelt), near-surface (interception, evapotranspiration), and vadose zone (soil moisture storage) hydrological

process from daily precipitation to simulate the movement of water in a quasi-two-dimensional soil column. A benefit of HELP3 is that it uses empirically derived relationships to reflect the effects of temperature (e.g., reduced infiltration and increased runoff under freezing conditions) and vegetative growth (e.g., increased evapotranspiration, and preferential drainage by roots). The ability of HELP3 to simulate hydrologicial processes under freezing is particularly powerful as it allows for continuous simulation in geographic areas where freezing temperatures may be seasonally prevalent. A more complete and detailed description of the HELP3 model is proved by Schroeder et al. (1994b).

The HELP3 code has been extensively tested by its developers (Schroeder et al., 1994b). HELP3 has been used to simulate percolation through a clay liner overlaying mine tailings and was found to be in good agreement with field observation (e.g., Woyshnet and Yanful, 1995). The HELP3 model also compares well to other more rigorous methods (i.e., application of Richards' Equation) for simulating flow in unsaturated porous media. A study by Fleenor and King (1995) found that the two models were in good agreement under humid conditions but that HELP3 tended to estimate greater downward fluxes in arid environments. Gogolev (2002) compared recharge estimates generated by HELP3 and VS2DT (Lappala et al., 1987) for the Waterloo Moraine. VS2DT is a code used to calculate flow and transport in the unsaturated zone using the Richards' Equation. Their study showed that there is no significant gain in determining recharge estimates between the two codes. In all cases the differences between the two estimates was less than 8% except for one case for which the difference was 12.4%. It is also worth nothing that HELP3 performed the 100 year simulation period in less than 15 minutes while for the VS2DT required 2.5-7 hours. In comparing the HELP3 estimate to field estimates (made using the tritium profile method) the HELP3 estimates were within 4% of measured values. Gogolev (2002) concludes the study with the following comment that is worth reiterating, "It is considered that the HELP technology has all necessary qualities to become a core for computational technology for assessing groundwater recharge rates."

The applicability of the HELP3 technology as a tool to assess recharge to large-scale groundwater models has been shown by Jyrkama et al. (2002). In this application HELP3 was used to estimate a detailed transient, spatially distributed estimate of percolation to be used as the recharge boundary condition for a large (approximately 138 km^2) groundwater flow model. The application of the detailed boundary condition improved model calibration; at observation points the simulated heads were within 0.5 m of observed values, while the best agreement achieved using a uniform recharge boundary condition was 2 m. This study also highlights the importance of the combination that precipitation and temperature play in the distribution, quantity, and timing of recharge.

2.5.1 Overland Flow and Runoff Considerations

The rarity of overland flow in humid vegetative conditions is an additional consideration for simplifying the surface water routing component of the numerical model, thereby reducing the computation burden and making the numerical integration of groundwater and surface water systems a manageable problem. In HELP3, runoff is accounted for using the SCS method (NRCS, 1986) for the following reasons: it is widely accepted, it is computationally efficient, the required input is generally available, and it can conveniently handle a variety of soil types, land uses and management practices (Schroeder et al., 1994b). The user chooses the most appropriate Curve Number (CN) that is reflective of soil drainage characteristics, land use classification, and vegetative cover. The CN is applied and updated by HELP3 internally to account for soil moisture conditions.

HELP3 allows for the CN to be adjusted based on physical factors such as specified slope and length. Hundreds of runoff estimates were generated for combinations of slope, length, soil type, level of vegetation, and rainfall characteristics using the KINEROS model (Woolhiser et al., 1990), which uses a kinematic wave model for the evaluation of erosion and sediment transport. Relationships between the KINEROS simulation results were established by regressing CNs to reflect slope, length, and CN based on soil type and vegetation characteristics. Despite these efforts to modify the CN to have a better physical basis, the HELP3 daily runoff estimates cannot be expected to yield accurate runoff for individual storm events. However, since the SCS rainfall-runoff relationship is based on considerable daily field data, it is expected that long-term runoff estimates are reasonable and consistent with respect to the daily temporal scale (Schroeder et al., 1994b).

2.5.2 Limitations of the Coupled Approach

Major weakness in this coupled approach is that there is no feedback from the water table to the soil column. This results in an over-estimation of recharge when the depth to the water table is greater than the length of the soil column and vice-versa. There are no internal checks to ensure agreement with the flux output from HELP3 and the rising and falling of the water table from the groundwater code. This results in a less rigorous accounting of the interaction of the groundwater and surface water dynamics as would be simulated in an internally coupled (e.g., MIKE-SHE) and fully-integrated (e.g., HydroSphere) models.

In groundwater models, surface water features are typically represented by prescribed Head (Type 1) or Cauchy (Type 3) boundary conditions, which oversimplify the surface water systems. A coupled approach could be used to provide a greater degree of realism between the tributaries and the

groundwater system (e..g, Scibek and Allen, 2007). However, the approach may require simulation results to be scaled between the two models.

Each of the processes simulated in HELP3 has its own assumptions and limitations which may not be reasonable under all circumstances depending on the application of the model (Schroeder et al., 1994b). Most of the limitations in HELP3 are from the empirical relationships used to describe processes. Considerations for the effects of these processes generally enhance the model as more processes are accounted for even though their incorporation into the modeling approach employed is best described by the "grey box" characterization of Brutsaert (2005). These are viewed as short comings that do not necessarily limit the application of the model. The major assumptions used in the HELP3 model are summarized as follows:

Freezing Conditions

- precipitation on days for freezing temperatures is assumed to occur as snow
- prediction of frozen soil conditions, snowmelt, and snow accumulation are based on empirical relationships and antecedent air temperatures

Infiltration

- it is assumed that all flow in the soil column is vertical, thus not allowing for interflow or lateral flow on clay lenses
- effect of macropores from rooting channels is incorporated by using empirical relationships to modify the hydraulic conductivity

Evapotranspiration

- based on average annual wind speeds and quarterly humidity values
- humidity is assumed to be 100% on days with precipitation
- the start and end dates of the growing season and maximum rooting depths are constant for the duration of the simulation
- leaf area index is limited to a range from 0 (bare ground) to 5 (excellent stand of grass)

Runoff

- since the SCS rainfall-runoff relationship is based on considerable daily field data it is expected that long-term runoff estimates are reasonable and consistent with respect to the daily temporal scale
- runoff is most strongly dependant on the selection of appropriate CN, introducing bias
- SCS method does not explicitly consider surface topography and vegetative effects that can both enhance or retard overland flow velocities

- temporal distribution of a storm event (i.e., duration and intensity) is lumped to daily timestep thus impacting infiltration and runoff rates. It is expected that runoff is underestimated for individual high intensity, short duration storm events
- the timestep is limited to 1 day, which precludes the model to be used as a tool to evaluate the hydrologic processes occurring at the event-scale (i.e., storm)

Though the coupled approach has its limitations, it offers much flexibility and advantages to the computationally intensive fully-integrated approach. The savings for a computationally less intensive approach can be well spent on constructing detailed, continuous, long-term simulations to be used as a tool to asses the potential effects of climate change, deforestation, and urban sprawl. Another key advantage is the ability to incorporate empirical relationships to estimate the effects of vegetative growth, freezing temperatures, snow accumulation, and snow melt.

2.6 Summary

The major limitations of the fully integrated approach are that it requires a fine discretization and detailed parameter distributions, both spatially and temporally, to capture the appropriate response of their governing equations. A fine horizontal discretization of the model domain is required to explicitly represent the drainage network which includes natural systems (e.g., rivers and tributaries) and man-made infrastructure that creates preferential pathways for routing surface runoff (e.g., drainage ditches). Furthermore, it has been illustrated that roads can have a significant influence on the drainage within a catchment. Roads are typically elevated with respect to the ground surface which dissects the natural drainage pathways thereby isolating potentially large portions of the catchment from the drainage network.

Use of the Richards' Equation to simulate variably saturated groundwater flows requires that the vertical discretization of the model domain be very fine, especially at the ground surface, to properly simulate the moisture content of the soil at ground surface. The moisture content influences the relative hydraulic conductivity, expressed through the non-linear characteristic curves, which is the linchpin for determining whether or not overland flow is triggered (by saturation from above or below).

Considerations for the timing of the initiation of overland flow and peak channel flows, and given the fact that channel and overland flow velocities are several orders of magnitude greater than the velocities of groundwater necessitates that the time-stepping of the numerical solution must be

very fine. This precludes the fully coupled approach from performing long term simulations (e.g., assessing the transient effects of changing climate over100 years).

The spatial resolution for the distribution of parameter values needs to reflect the required detail of the spatial discretization. For example, to explicitly incorporate roads, drainage ditches, and tributaries requires a very fine DEM (i.e., resolution at the 1-metre or sub-metre scale) which is much finer than the resolution that is typically available for civilian use (e.g., 10 m or 25 m resolution). Furthermore, parameter values should also be reflective of the dynamic system. That is, the seasonality of vegetation needs to be incorporated as it can have considerable impacts on both the characterization of evapotranspiration and the surface roughness. It has been recognized that defining effective roughness parameter values is the weakest link in conjunctive surface-subsurface hydrologic modeling. The characterization of surface roughness is strongly dependant on surface slope and it nonlinear with respect to depth of flow (for deforming and non-deforming roughness elements). This level of detailed information is not available and directly impacts the quantity and timing of hydrologic processes.

Given the challenges of defining appropriate parameter values and the computational burden imposed by the fine temporal and spatial discretization requirements to numerically solve the Richards' and (approximations of the) Saint Venant Equations the fully integrated approach is limited to simulating small catchments over limited periods of time.

The coupled approach can be employed to achieve significant gains with respect to the computational effort, making it an appealing alternative to the fully integrated approach. A coupled modeling approach that does not use the Richards' Equation to simulate variably saturated groundwater flows alleviates the fine vertical discretization requirements that burden the fully integrated approach. Another key advantage of the coupled approach that utilizes the HELP3 model is the ability to simulate surface and vadose zone hydrologic processes under freezing conditions. In general, the parameterization requirements of the coupled approach can be equally exhaustive though the simplification of hydrologic processes in the HELP3 model eases this burden. For example, HELP3 utilizes the SCS method to approximate surface runoff thereby not requiring spatial and temporal distribution of roughness properties with the tradeoff being a less rigorous accounting of the overland flow processes.

Though the coupled approach is criticized for being less robust with respect to the fully integrated approach it allows for surface-subsurface simulations to be performed over larger areas for

longer periods of time. Ultimately, all models are an abstraction from reality and thus, the modeling approach taken needs to reflect the scope and scale of the problem that it is addressing.

3 Case Study: Alder Creek Watershed

3.1 Setting

The area of study, the Alder Creek Watershed, is part of the Grand River Watershed drainage system which is the largest in southern Ontario. The Alder Creek Watershed is drained by a network of rivers whose outlet is Alder Creek which feeds into the river Nith. The Nith empties into the Grand River which eventually drains the Grand River Watershed into Lake Erie.

The Alder Creek Watershed is approximately 17.5 km in length, 6 km in width, and drains an area of 79.5 km^2. Consideration for the boundary conditions of the numerical model necessitates encompassing a larger area termed the Study Area (discusses in Section 4.3.1), which buffers the watershed. The size and location of the approximately 203.7 km^2 Study Area relative to the Grand River Watershed and southern Ontario is shown in Figure 3.1.

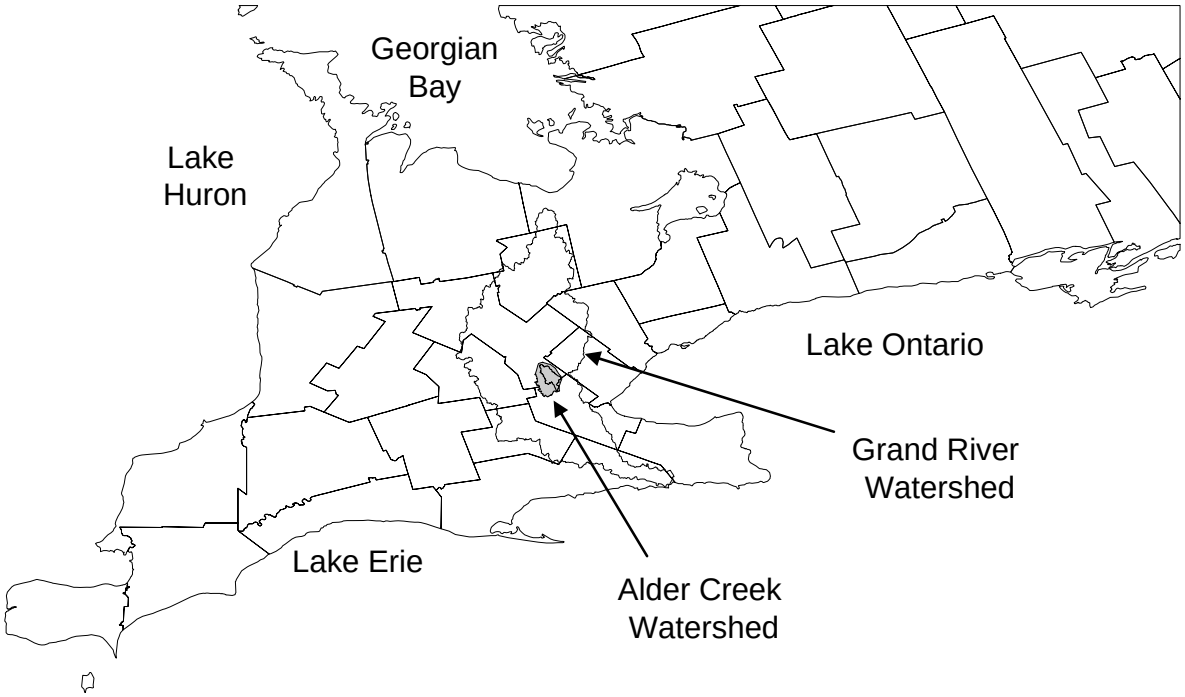

Figure 3.1 Location and scale of the Study Area (modified after Jyrkama and Sykes, 2007)

The land use (land use/land classification, LULC) for the Study Area is based on 1990 mapping by the Grand River Conservation Authority (GRCA) which is compiled into a single electronic resource by Jrykama (2003). The LULC mapping helps to characterize the Study Area and provides a

basis for deriving functional relationships between LULC and hydrologic modeling parameters. Though the mapping is outdated by nearly two decades it is believed to be reasonably accurate as little development has been undertaken in the Study Area relative to the nearby urban centers of Waterloo, Kitchener, and Cambridge. Furthermore, this is the only, and most current, source of data available. Based on the LULC map, agricultural practices dominate the Study Area comprising more than 58% by area. The classifications of pasture and forage combine to give an area of approximately 21%, followed by dense forest types and urban area comprising approximately 8% and 5%, respectively. The remaining classifications encompass less and 6% of the area of study. A detailed breakdown of contributing areas to LULC is presented in the following table.

Table 3.1 Summary of Land Use within Study Area

LULC Description	**Area (km^2)**	**Percentage**
builtup (commercial/industrial)	1.47	0.72%
builtup (residential)	9.25	4.54%
dense forest (deciduous)	12.41	6.09%
dense forest (conifer)	1.65	0.81%
dense forest (mixed)	3.68	1.81%
pasture/sparse forest	11.71	5.75%
forage	32.28	15.84%
extraction/bedrock/roads	4.06	2.00%
golf courses	0.46	0.23%
marsh	5.86	2.88%
open water	1.75	0.86%
bare agricultural fields	35.98	17.66%
row crops	52.71	25.87%
small grains	30.44	14.94%
Sum	203.72	100.00%

The Alder Creek watershed is located in the south-central portion of the Waterloo Moraine which is relied upon by the Regional Municipality of Waterloo (RMOW) to produce approximately 80% of the water supply for the region (RMOW, 2007). Several of these municipal well fields are within the Study Area and have been identified by CH2M-Hill (2003) to include, Mannheim East and West, Aquifer Storage Recovery (ASR) system, Peaking, Erb Street, St. Agatha, and New Dundee well fields. For the period of 1990 to 2000 these well fields produced, on average, at a rate of approximately 49,300 m^3/d (CH2M-Hill, 2003).

Numerous studies have been conducted to evaluate the complex hydrogeologic conditions of the Waterloo Moraine. This thesis will make use of two recent studies which utilize numerical models to estimate the water budgets for the entire Grand River Watershed (AquaResource, 2007) and for the

regional Alder Creek Watershed (CH2M-Hill, 2003) respectively prepared for the GRCA and the RMOW.

Modeling of the Grand River Watershed is facilitated using the Guelph All Weather Sequential Event Runoff model (GAWSER, Schroeter et al., 2000) and FEFLOW (WASY, 2005) to quantify the hydrologic processes occurring at the ground surface and to simulate the groundwater flow, respectively. The models are run, and parameter adjustments are made, independent of one another. Calibration is performed in an iterative manner between the two models; the infiltration output from GAWSER is checked against the recharge input specified for FEFLOW. There is no exchange of information between these models. The area of the Grand River Watershed is approximately 6,800 km^2 and groundwater flow is simulated using a 14 layer model, 6 layers for the overburden and 8 layers for the bedrock. The model is used as a tool to quantify the water resources budget within the watershed. The model achieved a reasonable global match with a mean error and a mean absolute error of 1.95 m and 5.68 m, respectively (AquaResource, 2007). The mean absolute error differs from the mean error in that the over- and under-estimated performance measures do not negate each other. Locally though, in the region of the Study Area the calibration targets were over- and under-estimated by as much 20 m.

The Alder Creek Watershed model (CH2M-Hill, 2003) is developed in a similar approach, using GAWSER and Visual MODFLOW (WHI, 2002) to respectively simulate the surface and subsurface flow systems. The groundwater flow model is comprised of 4 layers (simulated as *confined* layers in MODFLOW) representing the overburden. The first objective of the model is to improve the conceptual understanding of the regional groundwater flow system of the current conditions, 1990-2000. The model will also act as a basis for establishing a regional model to fulfill the groundwater component to the Alder Creek Groundwater Management Plan. Secondly, the model is used to conduct investigations into the impacts of potential future development on recharge and surface water flow in the Alder Creek Watershed (CH2M-Hill, 2003). Due to the smaller regional scale of the model, an improved calibration relative to Grand River Watershed model is achieved. All calibration targets were simulated within in envelope of +/- 5 m, the mean error is -0.04 m, and the absolute mean error is 1.6 m.

3.2 Regional Geology

On the scale of the Alder Creek Watershed the characterization of the regional geology is derived from The Soils of Waterloo County (Presant and Wicklund, 1971) and The Soil Survey of

Oxford County (Wicklund and Richards, 1961). On a larger scale, that reflects the geologic setting that the Alder Creek Watershed lays within, the characterization relies on The Hydrogeology of Southern Ontario (Singer et al., 1997).

3.2.1 Bedrock Geology and Topography

The sequence of bedrock formations underlying the regions of Waterloo and Oxford County belong to the Paleozoic era and are generally flat lying or dip gently towards the west (Singer et al., 1997). The bedrock was deposited approximately 400 million years ago as mud which corresponds to the late Silurian and early Devonian time (Presant and Wicklund, 1971). The majority of the region is underlain by the Guelph Formation which dips beneath the younger Salina Formation at the western edge of Waterloo County. Singer et al. (1997) report that based on previous investigations, the top of this formation is believed to have substantial fracturing and is believed to be highly permeable.

Beneath these uppermost formations lie, in order of increasing age, the Lockport/Amabel (of Middle Silurian age) Formation, followed by the Clinton-Cataract Group (of Lower Silurian age), and Queenston Formation (of Upper Ordovician age) (Singer et al., 1997).

3.2.2 Bedrock Hydrogeology

In the study of the groundwater resources in the Grand River basin, Sibul et al. (1980) described the Salina Formation as a high-capacity, water-supply source north of Kitchener-Waterloo. The authors also reported on substantial fracturing within the formation with this being encountered in two test holes located south of Kitchener. The supporting line of evidence is that mud circulation drilling could not be maintained in both test holes after approximately 1 m of penetrating into the bedrock. According to Sibul et a1 (1980), the fracturing at both test holes is indicative of the high permeability of the Salina Formation (Singer et al., 1997). From a water resources perspective, most of the bedrock formations serve as a limited source of groundwater due to either their finite spatial extent or because they are overlain by thick sequences of younger rocks (Singer et al., 1997).

3.2.3 Overburden Geology and Thickness

The overburden for the southwestern peninsula of Ontario was deposited during the Holocene and Pleistocene epochs, informally referred to as the Recent and Great Ice Age, respectively of the Quaternary Period (Singer et al., 1997). This period is characterized by the advance and retreat of major ice lobes which have left behind massive deposits of glacial till, an unsorted arrangement of clay, silt, sand, and boulders. The moraines that distinguish the Study Area are remnants of the

forward advance of the ice lobes believed to have displaced sedimentary materials parallel to the direction of their advance thus producing lateral moraines on its flanks and end moraines at the point of its furthest advance. As the glaciers melted the landscape was reworked giving rise to a complex stratification of sand and gravel interlaid with terraces of silt and clay, which were deposited in areas where melt water lakes existed (Presant and Wicklund, 1971).

The present topography remains largely unchanged since the most recent Wisconsian ice-age. The relief of the study area is characterized by a hummocky terrain with elevations ranging from approximately 415 to 285 m amsl with an overburden thickness range of approximate 35 to 145 m.

3.2.4 Overburden Hydrogeology

The general stratigraphic sequence for the Study Area are, progressing downward from ground surface, weathered surface soils, upper aquifer (Mannheim Aquifer), aquitard, lower aquifer (Greenbrook Aquifer), followed by another aquitard. The weathered surface soils can act as an aquifer or aquitard depending on its thickness, the material present, and the degree of weathering. The Mannheim Aquifer is heavily relied upon as a municipal water supply resource to the Region of Waterloo and can sustain perennial yields ranging form 3,185 to 8,190 m^3/day (CH2M-Hill, 2003). Likewise, the Greenbrook Aquifer is also used to supply the Region of Waterloo for which the municipal extraction wells are located within the City of Kitchener, located at the northeast to the Study Area.

3.3 The Hydrologic Cycle at Alder Creek

The timing of the hydrologic cycle is highly variable and closely related to climatic conditions. Singer et al. (1997) summarizes the general hydrologic trends in southern Ontario. During spring, typically mid March to early May, increasing temperatures causes the frozen ground to thaw allowing the melting snow to infiltrate into the ground. The growing season normally extends from late spring to the end of summer, thus soil water abstraction from the evapotranspiration process are also generally lower in the spring and autumn. Precipitation during autumn, typically October to early December, also provides recharge to groundwater as the void space in the soil has not been constricted by frozen pore water. Properly accounting for movement, timing, and quantity of these hydrologic processes is the basis for estimating water resources budgets and predicating hydrologic impacts from future stress conditions.

3.3.1 Watershed Delineation

The surface watershed is delineated topographically based on drainage by gravity. It can be easily and accurately mapped from topographic maps. The surface watershed is delineated in a study by Dorken (2003) by implementing the D8 method (e.g., Martz and Garbrecht, 1992) to determine the drainage structure of the watershed.

Groundwatersheds can not be delineated as easily as surface watersheds because they are not visible from the land surface, local groundwater flow systems are under the influence of regional groundwater flow systems, and groundwater divides are dynamic, responding to recharge and discharge boundary conditions (Winter et al., 2003). As such, and based on boundary condition considerations discussed in Section 4.3.3, the Study Area buffers the Alder Creek surface watershed delineation allowing for the groundwatershed to fluctuate beyond the extent of the surface watershed.

3.3.2 Recharge Boundaries

Direct recharge to the aquifer system is derived from the fraction of precipitation that percolates to the groundwater table. Thus, it is highly dependant on the response of the vadose zone which is largely controlled by the soil moisture content, as discussed in Section 2.4.1, and is under the influence of runoff and evapotranspiration processes. Influent portions of streams within the watershed can also act to recharge the aquifer in localized areas. Over the footprint of urban environments, leaky infrastructure can also provide recharge to underlying aquifers though actual quantities may be difficult to estimate (Lerner, 2002). Depending on the structure of the regional setting recharge can also be derived from the influx of regional groundwater inflow. This is not expected to be a major source of recharge as it is recognized that the regional groundwater flow system, both up- and down-gradient, generally provides the supporting hydraulic head to maintain the local aquifer system (Winter et al., 2003).

Recharge occurs everywhere except in river valleys which constitute the main zones of groundwater discharge. Though recharge occurs over large areas the rate at which it reaches the water table is highly variable and uncertain as it is dependant on a variety of factors (e.g., topography, soil type, antecedent moisture conditions, vegetation, etc.).

3.3.3 Discharge Boundaries

The Alder Creek Watershed is drained by a network of tributaries whose outlet is Alder Creek. Base flows are maintained by groundwater discharge. Generally speaking, due to the tempered

climate and high water table, the rivers in the watershed are referred to as gaining, meaning their base flows are maintained by groundwater discharging and becoming surface water. Even though, on the whole, the streams are gaining, some portions of the river network may experience losing conditions. The vertical hydraulic gradient between the stream and the aquifer is highly variable, due to the nature of the glacial depositional environment, and ongoing erosion and sediment transport processes in river dynamics.

Several wetlands have been identified in the Study Area by CH2M-Hill (2003) including, Petersburg Bog, Hofstetter Lake Wetland Complex, Upper Alder Wetland Complex, Alder Lake Marsh Wetland, and Lower Alder Wetland Complex. These are regarded as primarily being an area of groundwater discharge as the majority of these wetlands occur in the low-lying areas along the main tributary of the watershed.

4 Numerical Model

A coupled modeling approach is adopted to perform long-term simulations of the surface water and groundwater resources of the Alder Creek Watershed. Each scenario evaluated will consist of a HELP3 model to simulate the surface and vadose zone processes which is externally coupled to a HydroSphere model to simulate the saturated flow of groundwater, as conceptually illustrated in Figure 4.1. Visual Basic for Applications (VBA) is used within a Geographic Information System (GIS) framework to parameterize both models.

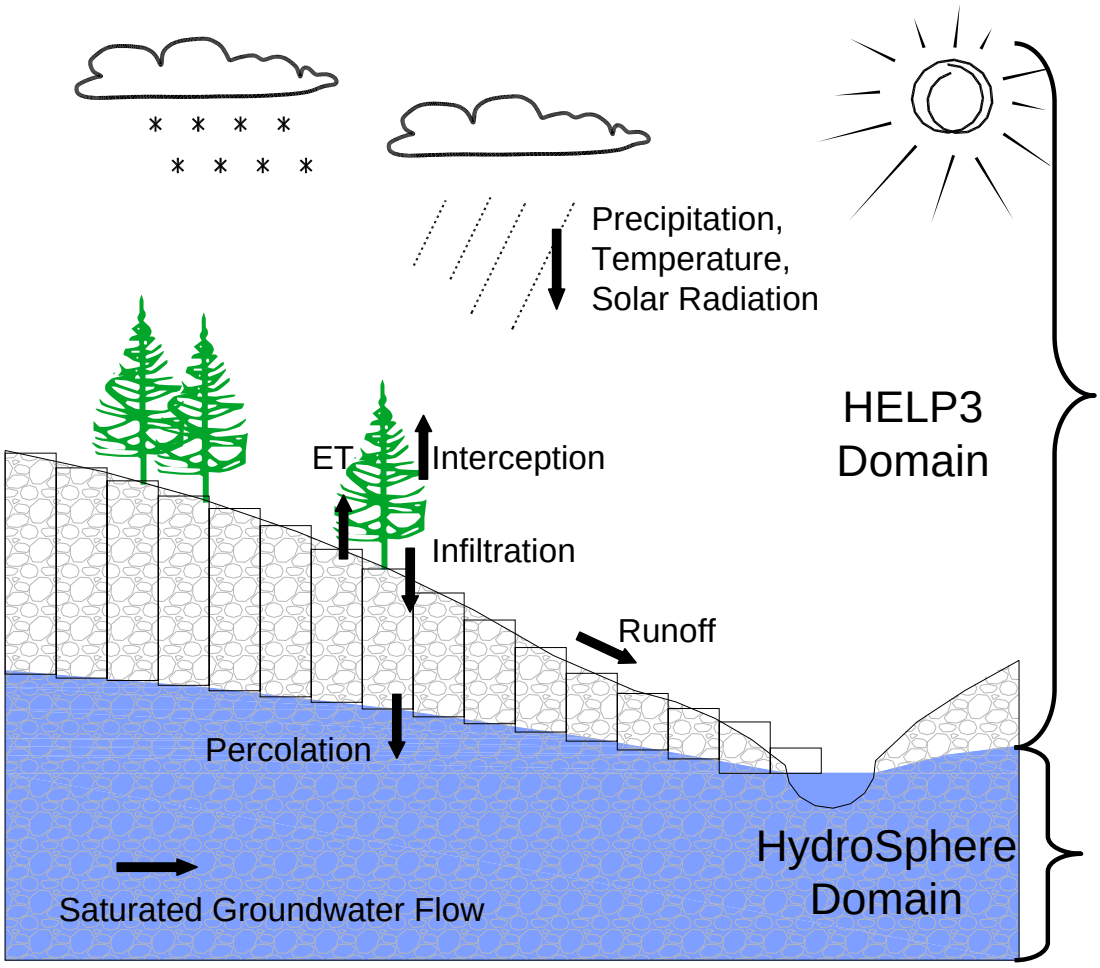

Figure 4.1 Conceptual Diagram of Model Coupling

The approach used to model the Study Area is to create a calibrated, steady-state groundwater flow model, which is reflective of average historical conditions and then, use that as the initial condition to conduct long-term transient simulations. A HELP3 simulation is performed for the

period 1990 to 2000 and temporally averaged to construct a representative, historical average, recharge boundary condition for the steady-state groundwater model. The length of the soil columns for the HELP3 models remains constant over the length of the simulation. As such, for the transient simulations the soil column length for each HELP3 model is updated to reflect the full unsaturated zone distance, as simulated by a steady-state model. With this update, the HELP3 models are re-run to simulate long-term future scenarios, 1990-2080, under baseline and climate change scenarios. The HELP3 results are then applied to the groundwater flow model (via the recharge boundary condition) which is used to simulate transient groundwater flows for the same time period.

An outline of the approach taken to simulate each scenario is to: first, generate HELP3 input files; second, run the HELP3 simulation; third, post-process the HELP3 results (aggregate to the scale of the groundwater model elements); fourth, generate groundwater model input files; fifth, run the groundwater model; and finally, sixth, post-process the simulation results of the groundwater flow model. Due to the scale and scope of the Study Area and modeling effort, and the level of detail involved, VBA is used within a GIS framework to manage and automate aspects of the modeling process.

4.1 Data Integration and Management

This study integrates into a single framework the methodologies and datasets from several previous studies including: that of Jyrkama and Sykes (2007) to simulate effects of climate change to the surface and vadose zone hydrological processes, that of Dorken (2003) to delineate the surface watershed, and to discretize and parameterize the river network for a groundwater flow model, and the subsurface property datasets of regional groundwater modeling investigations (CH2M-Hill, 2003; AquaResource 2007).

To facilitate integrating and managing this information into a single framework, a GIS and a relational database management system (RDBMS) are required to accurately and efficiently store the spatial and non-spatial data. In this application, ArcMap (by ESRI®) and MS-Access (by Microsoft®) are used, respectively. A GIS is a tool that can be used to manage, organize, query, and visualize spatial information (e.g., topography, soils distributions, land use). Spatial information in a GIS can be stored in vector (discrete points, lines, and polygons that are precisely positioned) or raster (a 2D grid of cells where each cell contains a value representing the attribute being mapped) data formats, both of which have their strengths. The strengths of vector datasets is that each feature contains topological information, defining spatial relationships to neighbors, and an attribute table for

storing additional data of various types (e.g., double, string). Raster datasets are well suited to efficiently store attributes that continuously vary in space (e.g., ground surface elevations). The key features that make GIS a powerful tool to aid hydrogeologic modeling include data management (e.g., store spatial and non-spatial data in RDBMS), data integration (e.g., combining data derived from various geographic co-ordinate systems and formats into a single framework), data visualization, and the ability to query spatial data and non-spatial data. The main weaknesses of GIS in this application are in its limited abilities to handle three-dimensional and transient datasets (Ogden et al., 2001).

Custom tools are created using VBA to access ArcObjects (by ESRI®), which are a set of platform-independent software components that provide services to support GIS applications on the desktop. To facilitate data integration and management, VBA forms are employed to create a small user interface to translate spatial and non-spatial data into model input and output files. ArcObjects allows the user to access functionality that is not available through the ArcMap user interface and custom application of those that are. Essentially, the combination of ArcMap and VBA forms provides the user interface while VBA and ArcObjects is used to process all model input and output datasets.

Processors are created to carry-out and manage all aspects of using HELP3. These processors are used to create the HELP3 input files, automate running the model, and finally to process the simulation results so that they may be integrated with the groundwater model. The HydroSphere processors translate the finite element mesh geometry, material properties, and boundary condition information into a data files for *grok* input. The grok is a pre-processor that generates the input files for HydroSphere and acts as a data integrity check (Therrien et al., 2005). HydroSphere can then be run with the inputs generated by grok.

4.1.1 HELP3 Processors

VBA in the ArcMap framework is used to manage and automate the application of the HELP3 model so that it can be used to generate a spatially distributed, detailed transient recharge boundary condition for the groundwater flow model. The inputs required by HELP3 include, meterological data, soil stratigraphy, and specification of evapotranspiration and runoff parameters. This section will outline the functionality of the HELP3 processors; the details of the input data are presented in Section 4.2.

In this application, HELP3 is used to estimate the leakage (i.e., percolation) exiting from the bottom of a one-dimensional soil column. The first step is to define all the HELP3 models that need

to be simulated. A HELP3 model is defined for each unique combination of surface (e.g., vegetative cover, percent impervious cover, etc.) and subsurface (i.e., soil layering) properties whose spatial distributions are stored in a Land Use Land Classification (LULC) and a surface soils map, respectively. Parameter information associated with each classification of LULC and surface soils are queried from the database. The intersection of these two maps produces a combination map of polygons that have the properties of both input maps. These steps are conceptually shown in Figure 4.2. The combination map produces a limited number of unique HELP3 models. However, when the meteorological forcing data is distributed to each combination polygon at the daily time step, they are all unique. The 7722 LULC polygons combined with 8362 soils polygons results in 48974 unique HELP3 models that need to be simulated. The Inverse Distance Weighted (IDW) technique is applied to distribute the meteorological input data to each HELP3 column. This produces a continuous distribution of climate forcing variables over the Study Area. Finally a d1 file is created, that specifies the locations of the input and output files, and the basic simulation parameters. With the d1 file, the HELP3 model for each polygon is run. A flow chart summarizing this methodology is illustrated in Figure 4.3.

The simulation results for the HELP3 models are aggregated to the scale of the groundwater flow model discretization as shown in Figure 4.4. The partial contributions of each HELP3 model (i.e., combination polygon) that overlaps a groundwater flow model element are weighted by contributing area to provide a recharge boundary condition to the saturated groundwater flow model. Due to a mismatch in spatial discretization, the spatially detailed HELP3 outputs are integrated over the coarser finite element mesh to obtain an average recharge rate to be used as a boundary condition for the groundwater model. Inherent in the averaging process, some information is lost as can be seen in Figure 4.4.

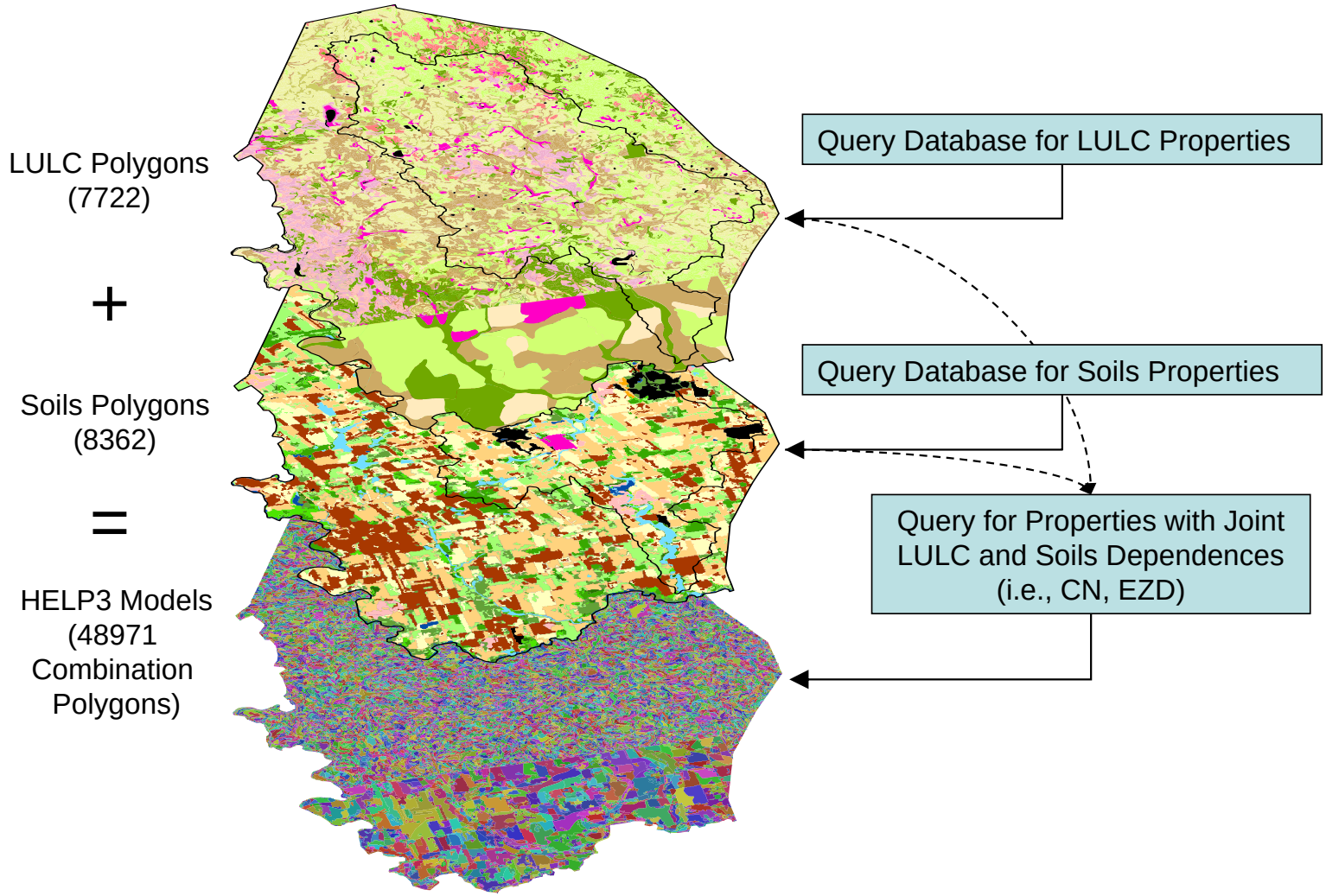

Figure 4.2 Create HELP3 combination map

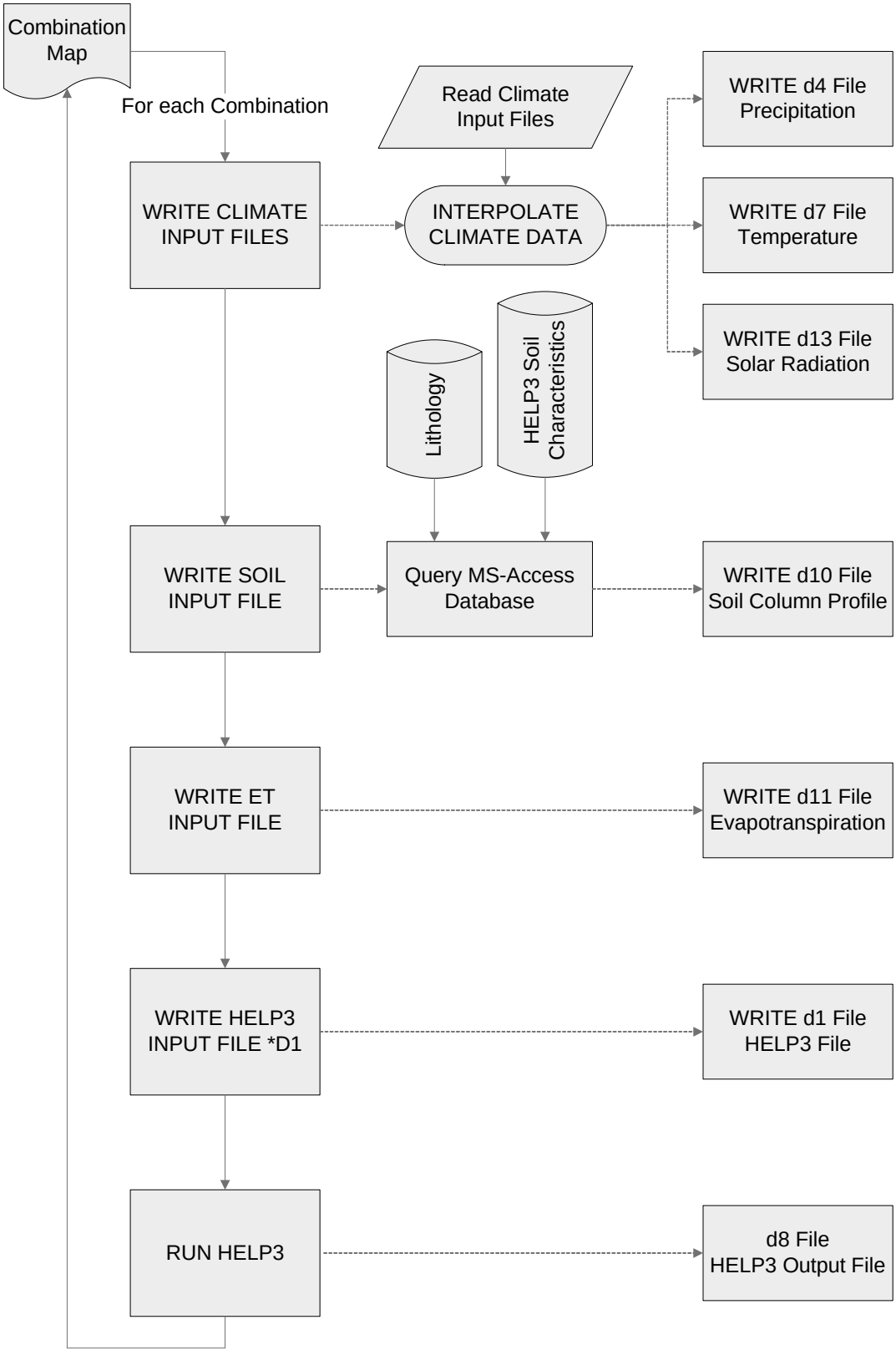

Figure 4.3 Processor to create HELP3 input files (modified after Jyrkama, 2003)

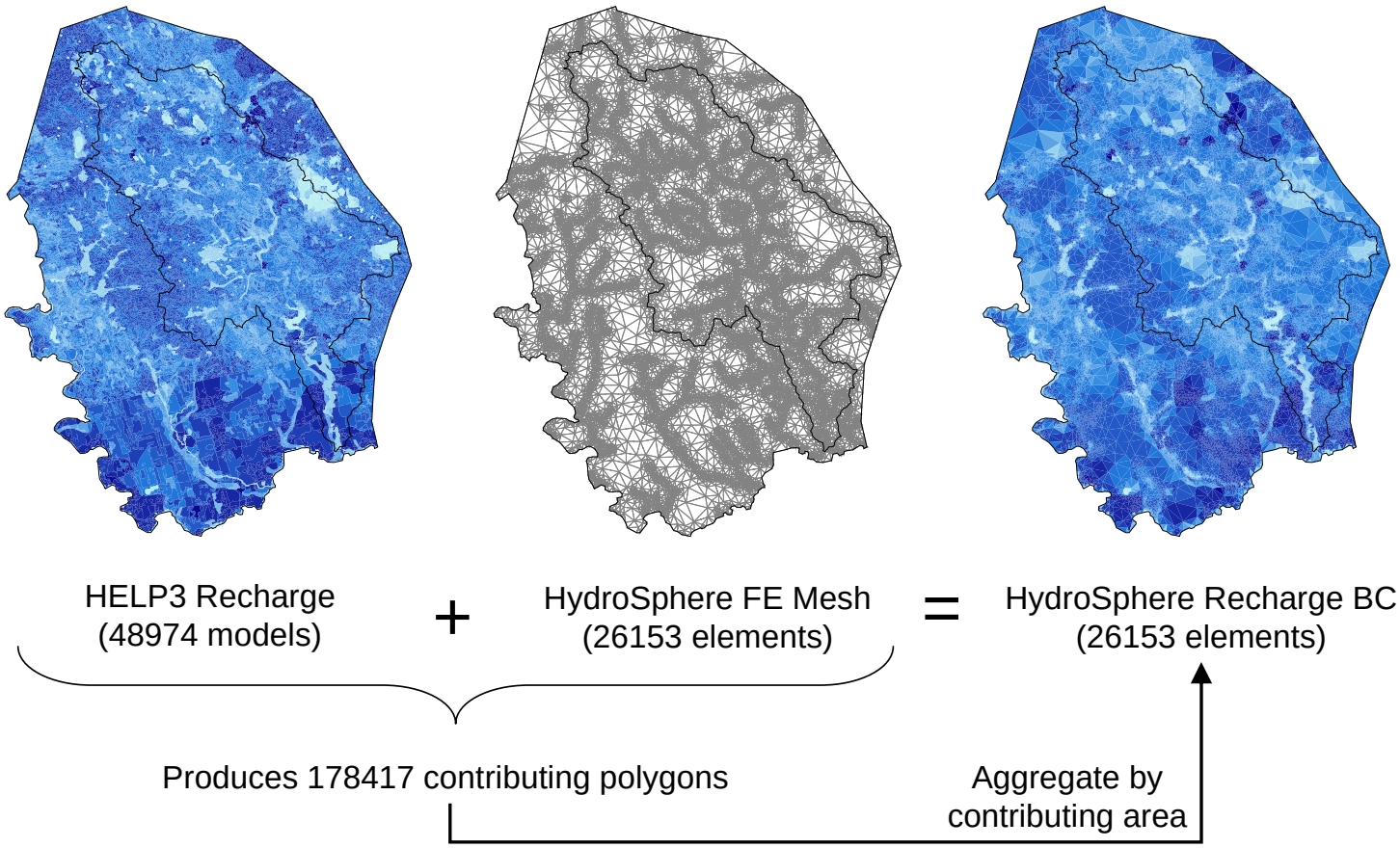

Figure 4.4 Aggregate HELP3 output to scale of groundwater model elements

4.1.2 HydroSphere Processors

Several processors were created to distribute model parameters and visualize model inputs and outputs. The primary function of the processors for HydroSphere is to create input files in the format expected by grok, a pre-processor for HydroSphere that translates the user specified information into binary input files for HydroSphere. The first step is to translate the finite element groundwater flow model discretization into vector GIS *shapefile* format for ArcMap. This allows the information regarding vertical layering, material properties, and boundary conditions to be mapped to the nodes, faces, and elements of the finite element discretization.

Vector and raster data formats are used to store material property distributions for the overburden and bedrock. Using VBA, processors are created that draw on the strengths of both formats to assign material properties. When making use of vector-based datasets, polygons defining material properties are applied to the finite elements by contributing area, similar to aggregating HELP3 combination polygons to the scale of the finite elements as shown in Figure 4.4. Raster-based datasets, typically interpolated surfaces of hydraulic conductivity, are applied at the centroid of model elements. Both data formats are linked to a database containing values of material properties for each classification. In the case of the raster datasets, i.e., continuous surfaces of hydraulic conductivity, a reclass operation is first performed to lump the distribution into 5 soil type classifications (coarse sand, sand, loam, silty loam, and clay). This establishes a link to the database so that other material property parameters (e.g., porosity) can be assigned that is complimentary to the values of hydraulic conductivity. The default soil properties of HELP3 (Schroeder et al., 1994a), see Table 4.5, are adopted as soil property values for the 5 classifications.

The use of VBA to access ArcObjects allows for detailed boundary conditions to be specified for the recharge, already summarized in Figure 4.4, and river boundary conditions. The initial discretization of the river network and parameter specifications were adopted from Dorken (2003) and updated as necessary. A processor is developed to define the river boundary conditions. This allows for a detailed, physically-based specification of all parameters used to define the elevation and river conductance terms of the river boundary condition. These terms constrain the behavior of the surface water body with the underlying aquifer. The river elevation is derived from the ground surface digital elevation model (DEM) and mapping of surface water bodies. The river bed hydraulic conductivity is calculated based on the harmonic mean on the underlying soils, read from the surface soils distribution map and queries from the soil stratigraphy database. The river geometry (e.g., width, depth) are estimated based on *power laws* that scale geometry parameters based on to the

observed river flows and drainage area. The drainage area dataset is created by performing spatial analysis routines (e.g., Martz and Garbrcht, 1992), to determine pathways of drainage by gravity and flow accumulation, with respect to the DEM. Further details for the river boundary condition parameter specification are provided in Section 4.3.3. Less involved processors were developed to handle head and well boundary conditions, specify locations for monitoring model outputs of head and flux at nodes of interest, and to specifying simulation and solver parameters.

All of these processors translate the spatial and non-spatial inputs into files for grok and are summarized in Figure 4.5. The grok translates this information into HydroSphere inputs files, the groundwater flow model can then be run.

Once the simulation has been executed the model output files are post-processed into vector and raster datasets so that they can be utilized in the GIS environment. The visualization capabilities of ArcMap allows for detailed visualization of performance measures which can then be viewed and analyzed with respect to the input data. Additionally, processors are also created to quantify the fit of the model using a set of residual statistics, see Section 4.4.

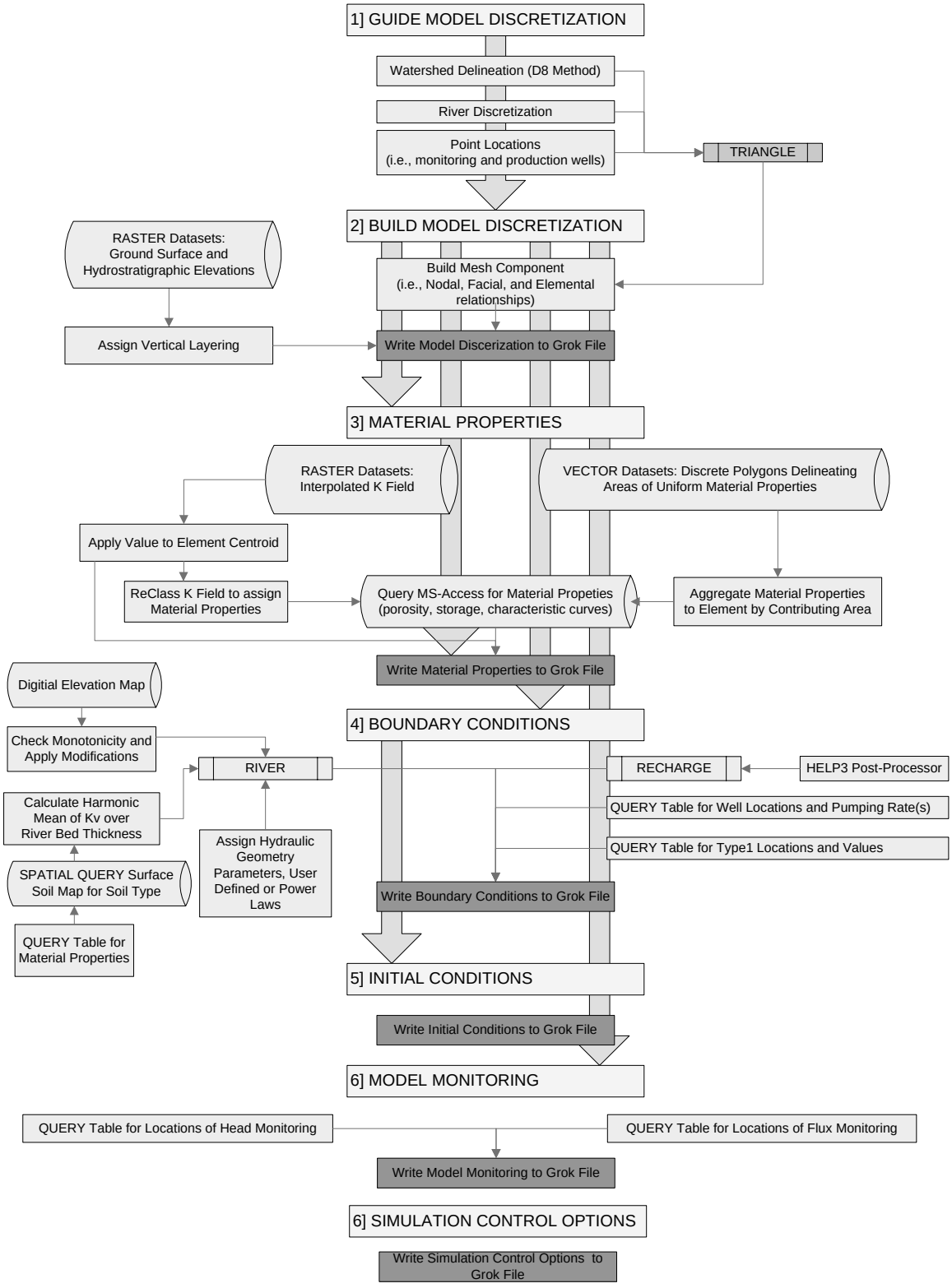

Figure 4.5 Processor to write HydroSphere input files for grok

4.2 HELP3 Model

4.2.1 Meteorological Data

The primary meteorological inputs are daily averages of precipitation, temperature, and solar radiation. Other climatic inputs include average annual wind speeds and quarterly humidity values. HELP3 inputs and outputs are on a daily time step, thus precluding it from the analysis of event-scale simulations. The daily temporal increment does not capture the intensity and duration of individual storms and imposes severe limitations for routing surface water runoff. Lumping wind and humidity values to quarterly averages takes away from the physical basis of estimating evaporation. However, these values are not necessarily typically available for a time step of a day or finer.

Daily average values of precipitation and temperature were obtained from the GRCA through a study by Jyrkama (2003) for the period 1960-2000. Geographically, these data are assimilated into 13 zones of uniform meteorology (ZUM). This assumes, for example, that the entire area of a given ZUM receives the same daily distribution of rain. The distribution and scale of the ZUMs with respect to the Alder Creek study area is shown in Figure 4.6. The ZUM methodology of grouping regions with similar climatic trends simplifies the collection of data over the large area of the Grand River watershed but results in the lumping of parameters over large spatial areas. As can be seen in Figure 4.6 the Study Area intersects ZUMs 6, 9, and 10. To create a continuous distribution of precipitation and temperature data across ZUM boundaries the IDW algorithm, with a power of 2, is used to distribute the data to the HELP3 columns. Following the methodology developed by Jyrkama (2003), the IDW technique is chosen as the interpolation algorithm as it has the advantages of being simple to implement and is computationally efficient. The precipitation and temperature values are interpolated based on the distances between the centroid of the ZUMs and the centroid of the combination map polygons.

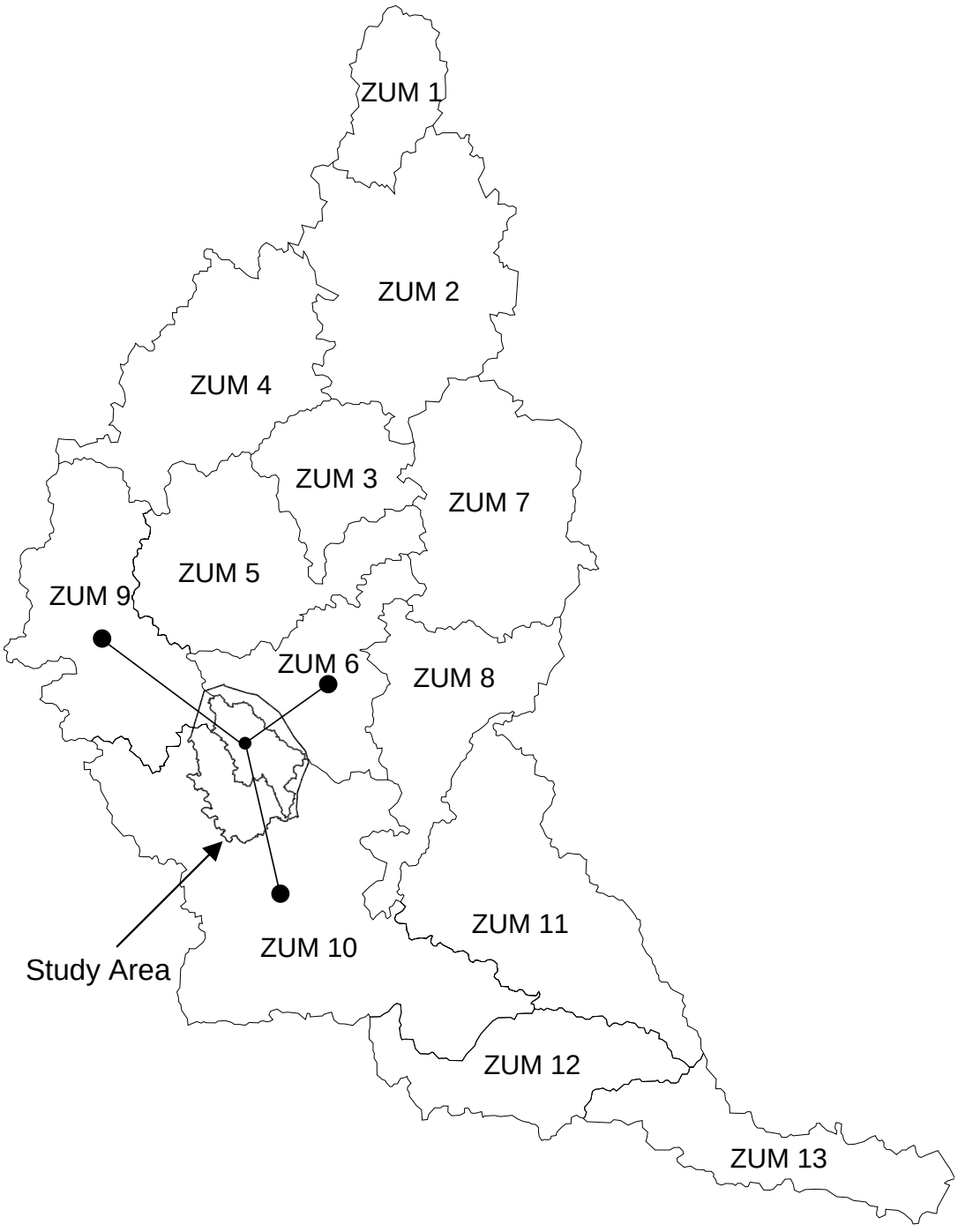

Figure 4.6 Scale of ZUMs for Grand River Watershed and Study Area

Values of daily solar radiation were adopted from Jyrkama (2003) which were generated stochastically using the WGEN (Richardson and Wright, 1984) algorithm in HELP3. Values of solar radiation were generated for ZUMs 6, 9, and 10 and distributed to the HELP3 soil columns using the IDW method as done for values of precipitation and temperature.

The 1960 to 2000 record of average precipitation, temperature, and solar radiation input values of ZUMs 6, 9, and 10 are shown in Figure 4.7 a through c, respectively. Precipitation on days of sub-freezing temperatures is assumed to be 10% water equivalence.

The remaining climatic inputs required by HELP3 include the average annual wind speed, the start and end of the growing season, and average quarterly relative humidity values. These parameter values were adopted from Jyrkama (2003) and are summarized Table 4.1.

Table 4.1 Additional Meteorological Parameters

Parameter	***Value***
Average annual wind speed	14.5 km/hr
Growing season start day	May 1st (day 123)
Growing season end day	October 7th (day 283)
1st quarter relative humidity	82.0%
2nd quarter relative humidity	73.3%
3rd quarter relative humidity	79.5%
4th quarter relative humidity	86.3%

4.2.2 Evapotranspiration Parameters

The leaf area index can be spatially distributed through its functional relationship with LULC. As such, the parameterization can only be interpreted in a relative sense with respect to the level of resolution of the LULC dataset (e.g, leaf area index value for urban vs forest classification). Establishing these indirect relationships is a practical approach where direct measurement of these parameters is not possible. A drawback to using functional relationships is that it contributes to the non-uniqueness of the model.

The evaporative zone depth (EZD) is controlled by the rooting depth which also has a functional relationship to LULC as well as soil type. The EZD is assigned based on the dominant soil type in the column. Once the soil water has migrated beyond the EZD, it is no longer available for evaporation or plant uptake on its way to the water table and is referred to as percolation. The applied values of leaf area index and evaporative zone depth (for selected soils) relative to LULC description are presented in Table 4.2. Distribution maps of LULC (Jyrkama, 2003) and surface soils (Jyrkama, 2003) are shown in Figure 4.8.

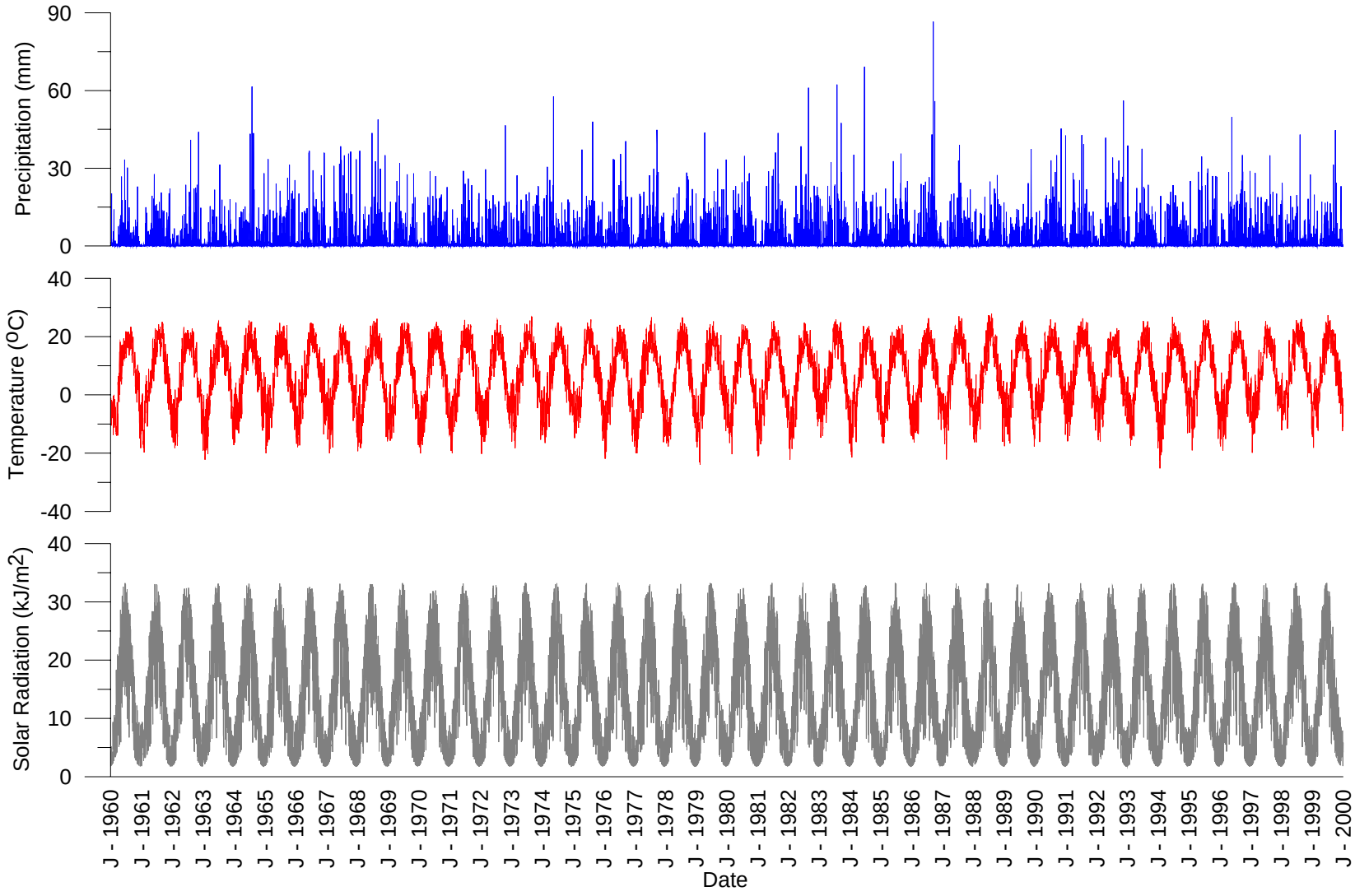

Figure 4.7 Historical Record of Precipitation, Temperature, and Incoming Solar Radiation

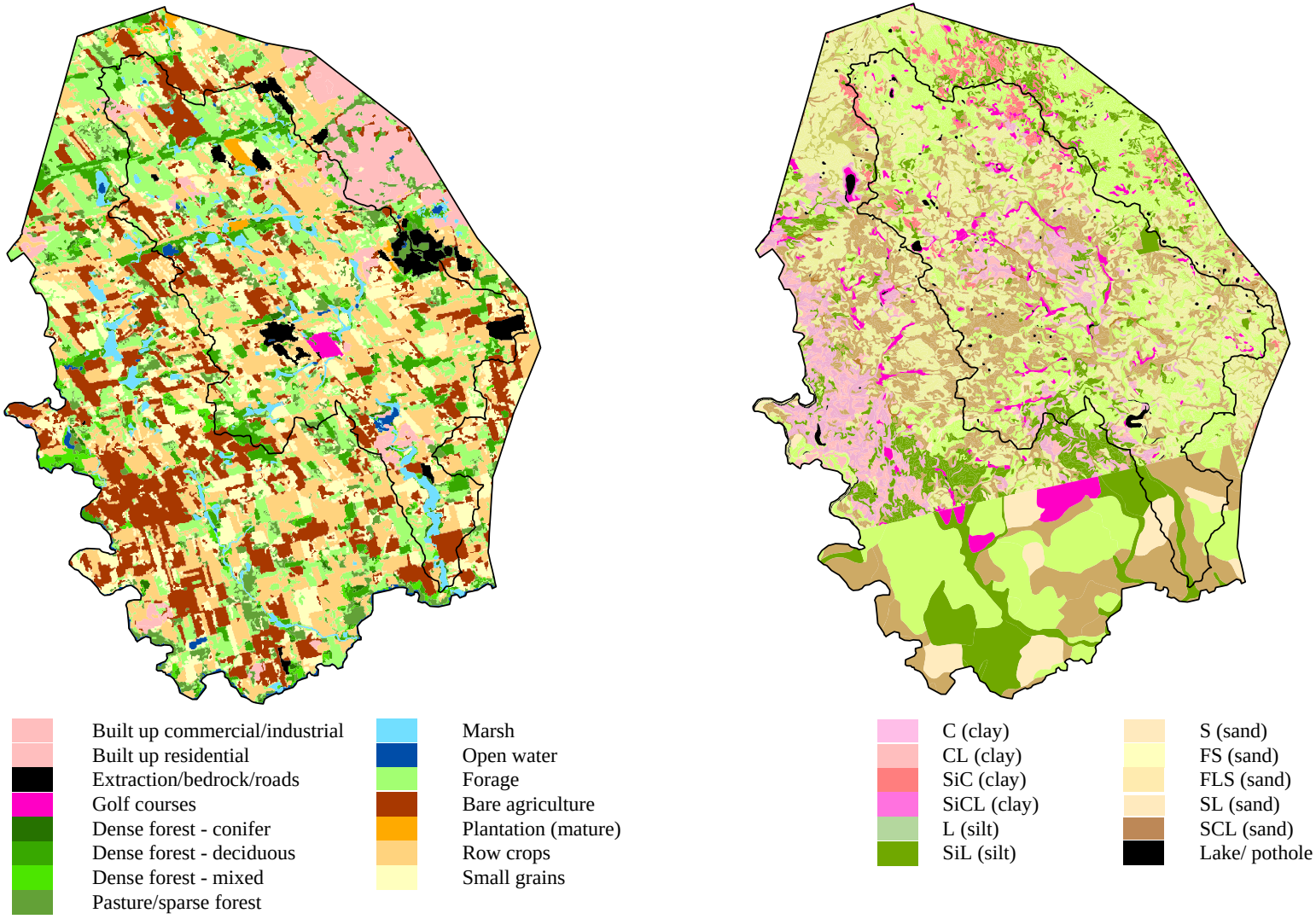

Figure 4.8 Distribution maps of LULC and surface soils

Table 4.2 Values of Leaf Area Index and Evaporative Zone Depth

LULC Description	***LAI***	***EZD (cm)***			
		Sand	***Loam***	***Clay Loam***	***Clay***
Built-up (residential)	0.5	38	43	30	19
Built-up (commercial/industrial)	0.0	10	10	10	10
Row crops	1.0	38	43	30	19
Small grains	1.5	57	76	61	38
Forage	2.0	57	76	61	38
Pasture/sparse forest	2.5	76	86	76	51
Dense forest (deciduous)	4.0	190	152	122	89
Dense forest (conifer)	4.5	190	152	122	89
Dense forest (mixed)	4.5	190	152	122	89
Plantation (mature)	2.0	114	121	76	51
Open water	N/A	N/A	N/A	N/A	N/A
Marsh	1.0	10	10	10	10
Extraction/bedrock/roads	0.0	10	10	10	10
Golf courses	2.0	57	76	61	38
Bare agricultural fields	0.0	38	43	30	19

4.2.3 Curve Numbers

The LULC distribution is again used to establish a functional relationship between land use and curve numbers. Due to the intimate relationship between surface runoff and infiltration, the curve number is highly dependant on the drainage characteristics of the surface soil. In the curve number approach, the drainage characteristics of soils are lumped into Hydrologic Soil Groups (HSGs) as shown in Table 4.3. The curve numbers for each combination of LULC classification and HSG is presented in Table 4.4. Curve numbers are adjusted during simulation based on the moisture content of the soil column (Schroeder et al., 1994a). The percent impervious values for each LULC are adopted from Jyrkama (2003) and are applied to reflect the available surface area contributing to surface runoff with the values being given in Table 4.4.

Table 4.3 Hydrologic Soil Groups (after NRCS, 1986)

Group	***Drainage Potential***	***Approximate Drainage Rate***	***Description***
A	High	> 0.76 cm/hr	Deep, well to excessively drained sand or gravel.
B	Moderate	0.38 – 0.76 cm/hr	Moderately deep to deep, moderately well to well drained soils with moderately fine to moderately coarse textures.
C	Low	0.13 – 0.38 cm/hr	Soils with a layer that impedes downward movement of water and soils with moderately fine to fine texture.
D	Very low	< 0.13 cm/hr	Clay soils with a high swelling potential, soils with a permanent high water table, soils with a clay pan or clay layer at or near the surface, and shallow soils over nearly impervious material.

Table 4.4 Curve Number and Percent Impervious Values (after NRCS, 1986)

LULC Description	***Percent Impervious***	***Hydrologic Soil Group***			
		A	***B***	***C***	***D***
Built-up (residential)	30	77	85	90	92
Built-up (commercial/industrial)	85	90	90	93	94
Row Crops	0	67	78	85	89
Small Grains	0	63	75	83	87
Forage	0	49	69	79	84
Pasture/Sparse Forest	0	43	65	76	82
Dense Forest (deciduous)	0	36	60	73	79
Dense Forest (conifer)	0	30	55	70	77
Dense Forest (mixed)	0	30	55	70	77
Plantation (mature)	0	44	65	77	82
Open Water	0	N/A	N/A	N/A	N/A
Marsh	0	98	98	98	98
Extraction/Bedrock/Roads	0	98	98	98	98
Golf Courses	0	39	61	74	80
Bare Agricultural Fields	0	77	86	91	94

4.2.4 Soil Column Data

The soil column data is based on mapping surficial geology (Figure 4.8b). This map is based on two detailed studies, Soils of Waterloo County (Presant and Wicklund, 1971) and the Soil Survey of Oxford County (Wicklund and Richards, 1961), and, based on the work of Jrykama (2003), has been compiled into an electronic datafile. These reports detail the lithology as defined by the A, B, and C soil horizons for depths ranging from 10 in (25 cm) to 36 in (92 cm). The HELP3 soil profile is constructed by relating the lithologic descriptions to 14 HELP3 default soil types. These soil types and their characteristics are presented in Table 4.5. The difference in mapping scales of the Waterloo and Oxford County studies is apparent in Figure 4.8b which results in a coarser approximation of the spatial variability of the simulated hydrologic response

For the case where the EZD is greater than the depth of the reported lithology of the surface soil, the depth of the soil column is extended to the EZD and assigned the properties of the bottom most lithologic soil type. For the transient groundwater flow simulations, the column length is set to the greater of EZD or the simulated distance to the water table for a steady-state model. With this update, the soil column length is representative of the average depth of the unsaturated zone. This can be significant factor in determining recharge estimates in areas characterized by hummocky terrain, as is the case for the Alder Creek Watershed with the greatest unsaturated zone length being approximately 70 m (based on the steady-state model). Since HELP3 and HydroSphere are coupled at the water

table, this consideration enhances the recharge estimate in two ways. First, it accounts for the additional storage of water in the soil matrix. Second, the rate of water migration for the full length of the unsaturated zone is accounted for. This is important for preserving the timing of the recharge to the water table which is controlled by the relationship between soil moisture content and hydraulic conductivity. The material properties for the additional length of soil column are taken from the layer structure of the calibrated, steady-state groundwater model. ArcMap is used to map the material properties to the HELP3 soil column, relying on the reclass operation discussed in Section 4.1.2.

Table 4.5 Applied Soil Characteristics (after Shroeder et al., 1994a)

Classification	***Total Porosity***	***Field Capacity***	***Wilting Point***	***Saturated Hydraulic Conductivity***		
Description	***USDA***	***USCS***	***vol/vol***	***vol/vol***	***vol/vol***	***cm/s***
Gravel	G	G	0.40	0.03	0.01	3.0×10-1
Coarse Sand	CoS	SP	0.417	0.045	0.018	1.0×10-2
Sand	S	SW	0.437	0.062	0.024	5.8×10-3
Fine Sand	FS	SW	0.457	0.083	0.033	3.1×10-3
Sandy Loam	SL	SM	0.45	0.19	0.09	7.2×10-4
Loam Sand	LS	SM	0.437	0.105	0.047	1.7×10-3
Fine Sand Loam	FSL	SM	0.47	0.22	0.10	5.2×10-4
Loam \ Silt	L	ML	0.46	0.23	0.12	3.7×10-4
Silty Loam	SiL	ML	0.50	0.28	0.14	1.9×10-4
Sand Clay Loam	SCL	SC	0.398	0.244	0.136	1.2×10-4
Clay Loam	CL	CL	0.46	0.31	0.19	6.4×10-5
Silt Clay Loam	SiCL	CL	0.47	0.34	0.21	4.2×10-5
Silt Clay	SiC	CH	0.475	0.378	0.265	1.7×10-5
Clay	C	CH	0.48	0.38	0.25	2.5×10-5

4.2.5 HELP3 Results

It was found that the HELP3 simulations results are highly sensitive to the initial conditions of soil moisture content, especially at early times. To initialize the soil moisture distribution in a realistic manner, 10 years of historical data, 1980-1990, are added to the beginning of every HELP3 model. This 10 year period is not used when the HELP3 results are aggregated to the scale of the HydroSphere model, rather, it is used to determine representative initial moisture contents for the transient flow analysis. Given the daily timestep length, it is assumed that all surface runoff reaches the watershed outlet. The HELP3 modeling results for runoff, evapotranspiration, and recharge are averaged over 1990-2000 and presented in Figure 4.9. This figure highlights the spatial variability of recharge and dominant roles of runoff (e.g., open water, marshes) and evapotranspiration (dense forests) for contrasting LULCs.

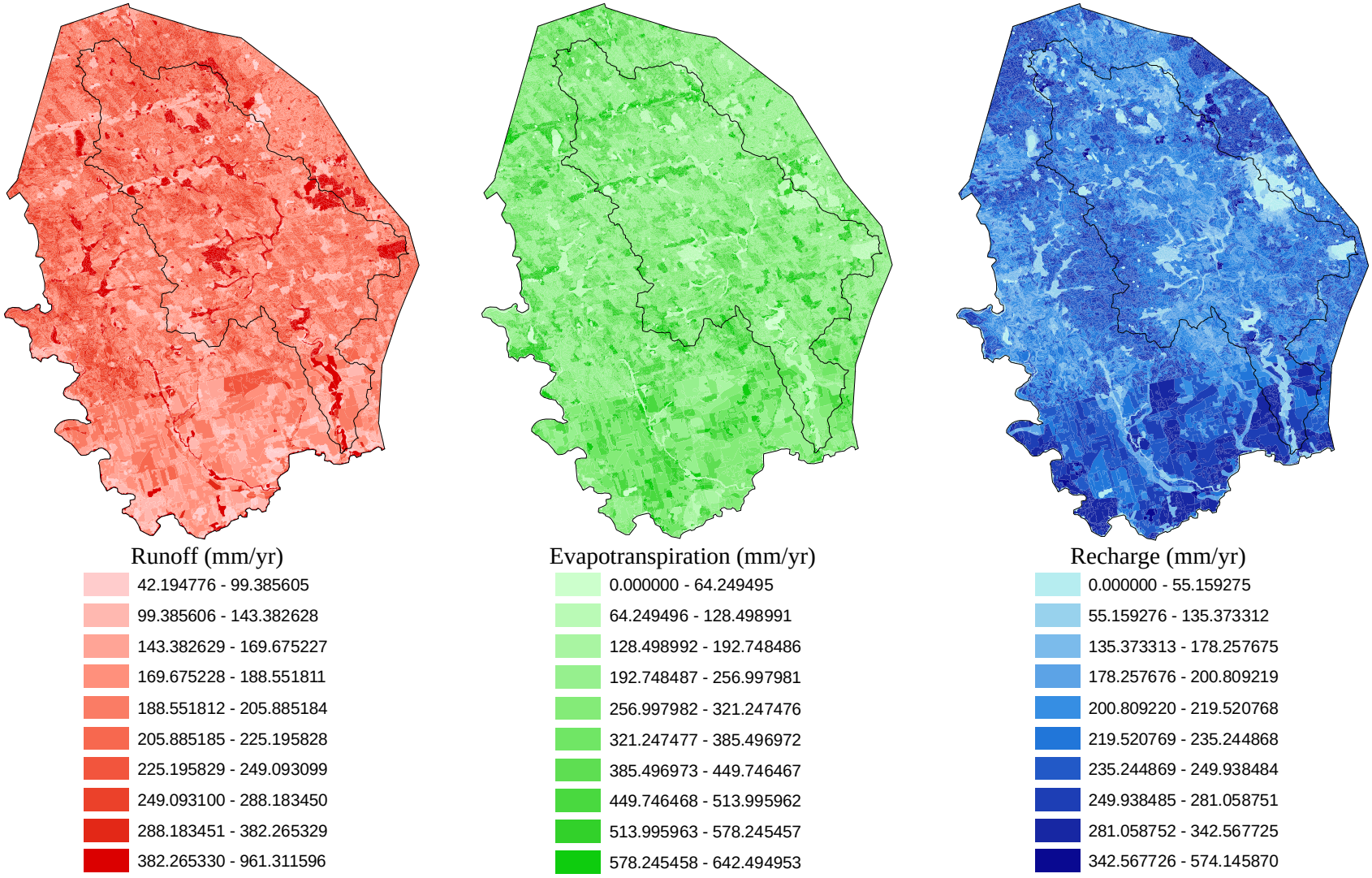

Figure 4.9 HELP3 simulation results for runoff, evapotranspiration, and recharge

4.3 HydroSphere Model

4.3.1 Discretization

The finite element approach is used to discretize the model domain using prisms because of their ability to capture the complex geometry of the watershed. Features used to explicitly guide the horizontal discretization include the Alder Creek watershed boundary and river network (modified after Dorken, 2003), the groundwater model domain boundary (modified after CH2M-Hill, 2003), the location of groundwater extraction wells, and observation points. The groundwater model domain extends beyond the surface watershed divide of the Alder Creek Watershed giving consideration to the fact that groundwater divides are not necessarily coincident with surface water divides (Winter et al., 2003) and to ensure that the extraction wells are not influenced by the model domain. The program Triangle (Shewchuk, 1996) is used to generate an efficient finite element mesh that meets the delaunay criteria; the planar discretization is shown in Figure 4.10. The finite element mesh captures the river network in detail and is highly refined in areas of steep hydraulic gradients (e.g., extraction wells). The vertical discretization is based on a regional groundwater model of the Grand River Watershed developed for the GRCA (AquaResource, 2007). The domain is discretized into 14 layers, 6 for the overburden layers and 8 for the bedrock units. Table 4.6 presents a summary of the layers in relation to the regional hydrostratigraphy. Model layers must be continuous, thus in the case of pinch-outs (e.g., windows in aquitards), a minimum thickness of 10 cm is assigned to the layer and it is given the material properties of the underlying formation.

Table 4.6 Groundwater model layer structure (after AquaResource, 2007)

Layer	***Formation***	***General Lithology***
14	Aquitard / Aquifer	Surface Soils
13	Aquitard / Aquifer	Quaternary Geology
12	Upper Overburden Aquifer	Sand and Gravel
11	Aquitard	Middle Till Unit
10	Lower Overburden Aquifer	Sand and Gravel
9	Aquitard	Lower Till Unit
8	Aquifer	Contact Zone (3m thick weathered bedrock zone)
7	Aquifer	Onondaga-Amherstburg/Bois Blanc/Bass Islands Formations
6	Weak Aquifer*	Salina Formation
5	Aquifer	Guelph Formation
4	Aquitard	Eramosa Formation
3	Aquifer	Amabel Formation
2	Aquitard	Cabot Head Formation
1	Aquitard	Queenston Formation
* In most areas of the watershed, the Salina formation is viewed as an aquitard, however some wells use this geologic unit for a source of water. For this reason, it is listed as a weak aquifer.		

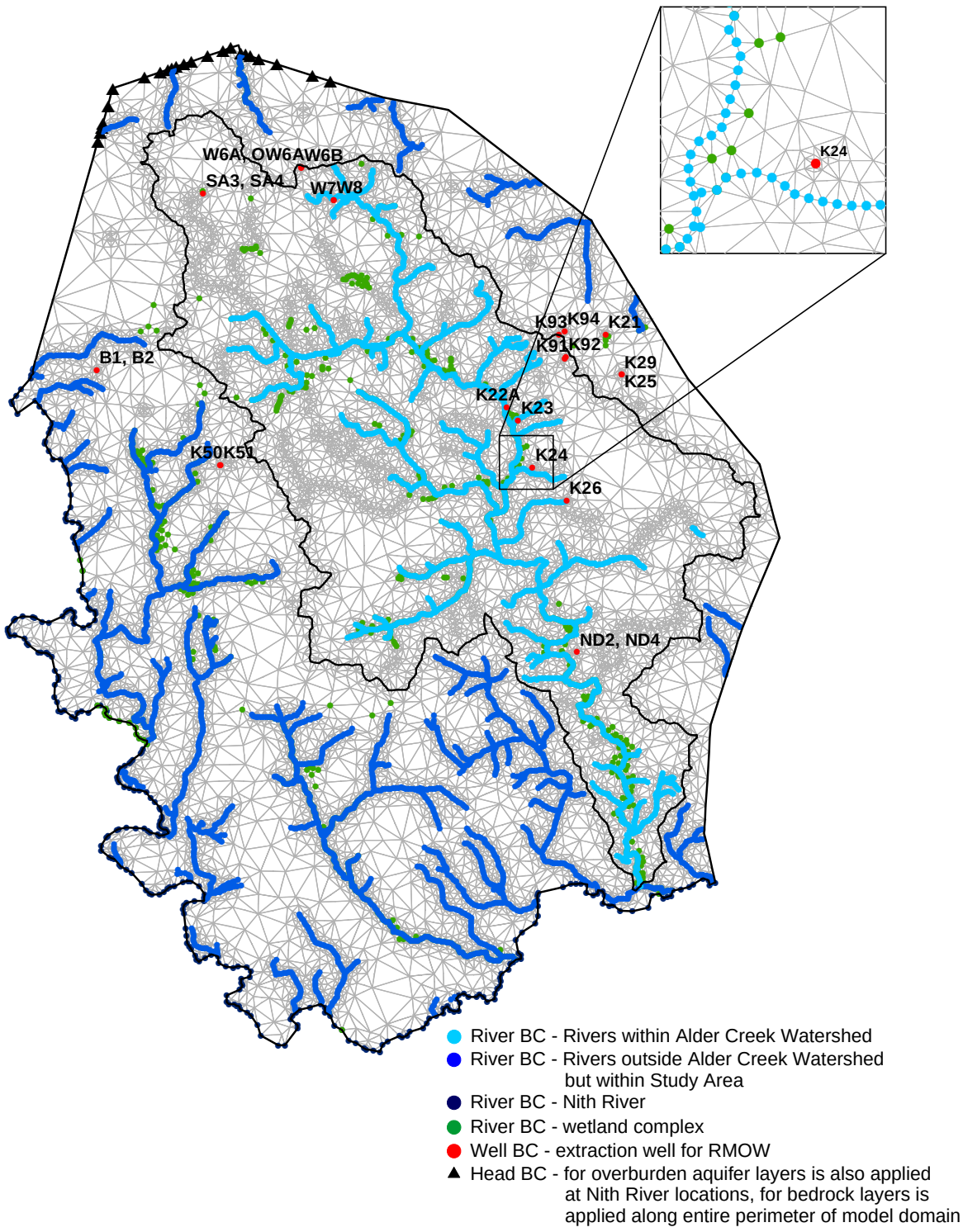

Figure 4.10 Model mesh and boundary conditions

4.3.2 External Boundary Conditions

The external boundary conditions are those that are located along the top, bottom, and sides of the three-dimensional finite element domain and communicate the external environment to the model.

The HELP3 simulation results are aggregated to the scale of the model element and are applied as recharge to the top of the model domain using a Type 2, *nonuniform rainfall*, boundary condition. In a saturated groundwater flow model, the flux from recharge boundary condition is applied directly to the simulated groundwater table, the distance to the water table from ground surface is not considered. Thus, when the simulated water table is above and below the bottom the of the HELP3 column, the time of the application of the recharge to the water table will be either under and over-estimated. However, as discussed in Section 2.4, the functional relationship between soil moisture content and hydraulic conductivity exerts a controlling influence over the rate of flow in the unsaturated zone. As a result, the timing of recharge arrival at the water table is more sensitive to preserving the relationships captured by the characteristic curves than small fluctuations of the length of the unsaturated zone.

The Nith River provides a natural flow divide for surface water and the local aquifer system. It is modeled using a Type 3, *river*, boundary condition. The river elevation is derived from the DEM, checks are made to ensure monotinicity and that it is also at or below the ground surface elevation. For the river conductance term, the length is reflective of the distance to neighboring Nith river boundary condition nodes, assigned a uniform width of 25 m, a bed thickness of 1 m, and a river bed hydraulic conductivity value is calculated using the harmonic mean of the underlying soils (from the surface soils map).

The regional groundwater flow system is represented by applying a Type 1, *specified head*, boundary condition along the perimeter of the model for the bedrock and the aquifer units. For the bedrock units, the simulated heads from the Regional Grand River Watershed Model (AquaResource, 2007) are applied along the entire perimeter. For the overburden aquifers, specified head boundary conditions are placed along the perimeter at the upgradient and downgradient locations consistent with the Alder Creek Watershed Model (CH2M-Hill, 2003). Additional specified head boundary condition nodes are placed in the overburden aquifers at locations coincident with the overlying Nith River. At these locations the specified head boundary conditions are assigned the stage elevations of the Nith River. This ensures good communication between the river and aquifer which is in accordance with the conceptual regional flow regime.

The remaining nodes along the perimeter are assigned a *no flow* boundary condition. As the name implies, there is no flux across this boundary. This is appropriate along the bottom of the groundwater flow model and along the aquitards. Application of the external boundary conditions to the model is shown in Figure 4.10.

4.3.3 Internal Boundary Conditions

The internal boundary conditions, sources and sinks, include production wells, wetlands, and rivers and are shown on Figure 4.10. There are 24 municipal extraction wells operating within the model domain that are used for the regional municipal water supply. Their production rates are reflective of the recent historical average extraction rates, 1990-2000, as presented by CH2M-Hill (2003). The aquifer from which these wells draw water is as specified by CH2M-Hill (2003).

Significant wetlands within the model domain were identified by CH2M-Hill (2003) and are represented with the river boundary condition. The elevation of the wetland is specified to be equal to the ground surface (i.e., DEM) and hydraulic conductivity is set to $1x10^{-8}$ m/s as estimated using field techniques (CH2M-Hill, 2003).

The river network is the primary drainage mechanism for the Alder Creek watershed. It drains the surface runoff and carries base flow, from groundwater discharge, to the watershed outlet. The river network is modeled using the river boundary condition. The work of Dorken (2003) is used as a basis for quantifying the river boundary condition parameters. Its application is summarized below; see Dorken (2003) for details.

The exchange of water between aquifer system and the river is given by:

$$Q_{RIV} = COND_{RIV}\left(h - h_{RIV}\right) \tag{4}$$

where $COND_{RIV}$ is the river conductance term;
h is the simulated aquifer head; and
h_{RIV} is head (i.e., stage) in the river.

This formulation assumes that the aquifer head, river head, and river geometry are constant over the river reach given by the discretization of the river boundary condition. The river stage controls the direction of the flow between the surface water body and the aquifer (i.e., into or out of the groundwater flow domain) and the conductance term controls the rate at which the water is exchanged.

The stage profile for all the rivers within the Study Area were derived from the DEM and mapping of the surface water bodies. Ground surface elevations were extracted at river boundary

condition nodes; checks were made to ensure monotinicity between neighboring boundary conditions, that the stage profile is flat over surface water bodies (e.g., river traversing through wetlands and lakes), and that the river elevation is always at or below ground surface, see Figure 4.11. The conductance term from (4) can be represented as:

$$COND_{RIV} = \frac{K_{bed} L_r w_r}{Th_r} \tag{5}$$

where: $COND_{RIV}$ is the conductance value of the river reach;
K_{bed} is the hydraulic conductivity of the river bed material;
L_r is the length of the river reach;
w_r is the width of the river reach; and
Th_r is the thickness of river bed thickness.

In order to be consistent with the physically-based modeling approach adopted in this study, each parameter of the river conductance term is estimated in a deterministic, physically-based manner. The reach length is set based on the half distance between up- and down-gradient river boundary condition nodes. The river bed thickness is assumed to 0.5 m for all branches of the river network and the river bed hydraulic conductivity is calculated using the harmonic mean of vertical hydraulic conductivity values of the surface soils for the first 0.5 m of depth.

The remaining parameters, pertaining to river geometry, are estimated using the empirical power relationships developed by Leopold and Miller (1956). These formulae provide relationships between contributing area, channel flow, and channel geometry.

$$A_c = C_m L_c^j \tag{6}$$

where: A_c is the contributing area;
C_m is the channel maintenance coefficient;
L_c is the contributing length, sum of all upstream lengths; and
j is a fitting exponent.

The contributing area is a related to the observed flow using:

$$Q = xA_c^y \tag{7}$$

where: Q is the channel discharge;
x is a fitting coefficient coefficient;
y is the contributing length, sum of all upstream lengths; and

This relationship is then used to estimate river geometry parameters in terms of the flow:

$$w = aQ^b \quad (8)$$

$$d = cQ^f \quad (9)$$

where: w is the channel top width;
d is the average channel;
a, c are fitting coefficients; and
b, f are fitting exponents;

The optimum values to the fitting coefficients and exponents are determined by fitting the power relationships to channel discharge measurements and are summarized in Table 4.7.

Table 4.7 Summary of fitting parameters to specify hydraulic geometry (after Dorken, 2003)

Channel Parameter	*Unit*	*Fitting Parameters*	*Parameter Value*
A_c	m^2	C_m	214.31
		j	1.113
Q_{avg}	m^3/s	x	2.738E-07
		y	0.75
w	m	a	5.973
		b	0.50
d	m	c	0.8078
		f	0.40

These relationships were used to derive a detailed, physically-based river boundary condition for all rivers within the Alder Creek Watershed. For the branches of rivers within the Study Area but outside of the Alder Creek Watershed uniform values of width and depth are applied based on rivers of similar size located within the Alder Creek Watershed.

The results of this methodology to detail the river boundary conditions can be seen in Figure 4.12 where the size of the symbol (i.e., river boundary condition node) is scaled to the magnitude of the river conductance term. It shows the river conductance term increases with stream order owing to an increase in the drainage area manifested through larger hydraulic geometry of the channel. The conductance term is also strongly dependant on the hydraulic conductivity of the bedding materials which is most pronounced as the stream meanders over highly contrasting soil types, see Figure 4.12. For clarity in illustrating this relationship, the surface soils mapped in Figure 4.12 are classified into four broad categories, sands (in light orange), silts (in green), clays (in pink), and miscellaneous (e.g., potholes in black).

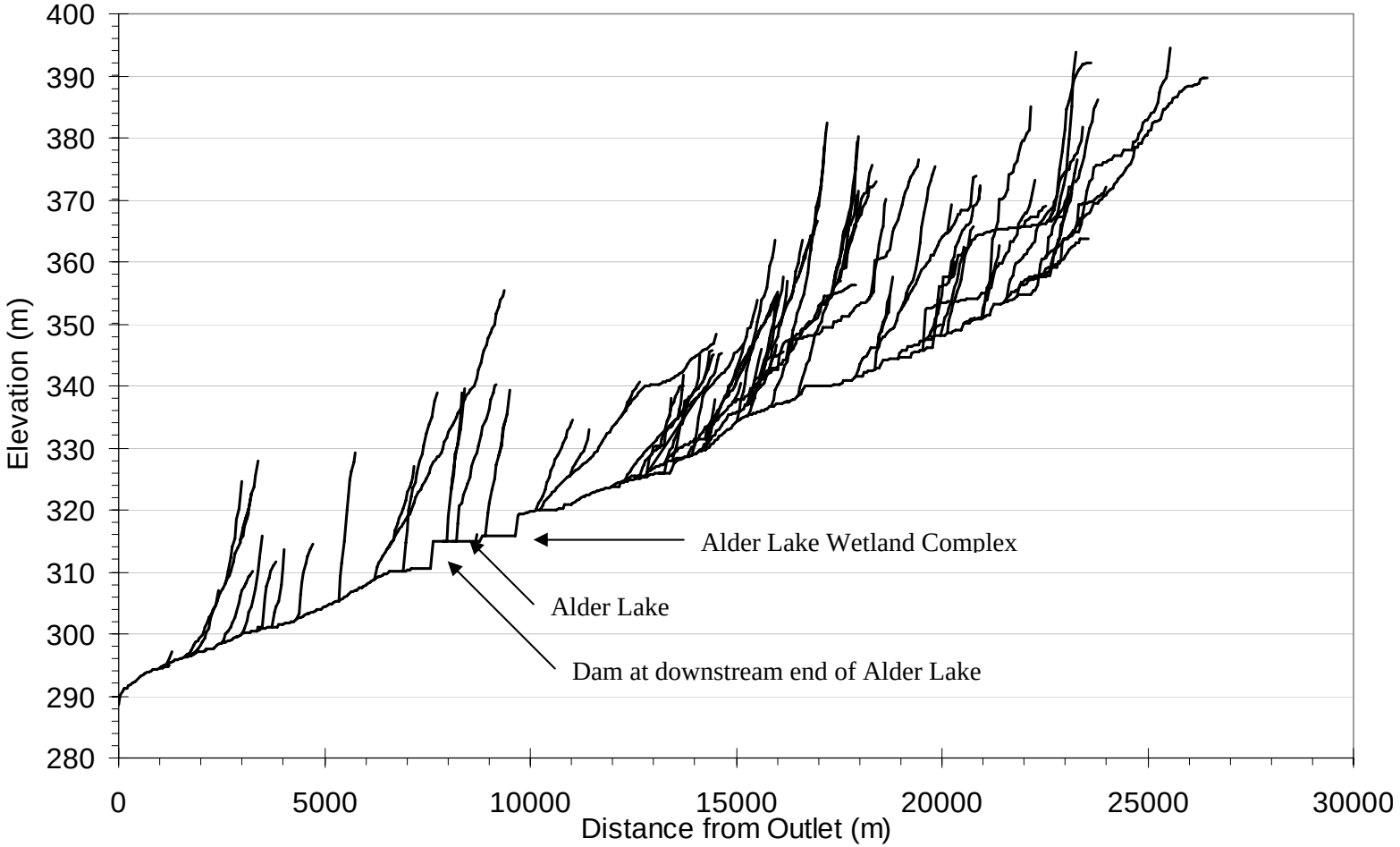

Figure 4.11 Stages of river boundary conditions for drainage network within the Alder Creek Watershed

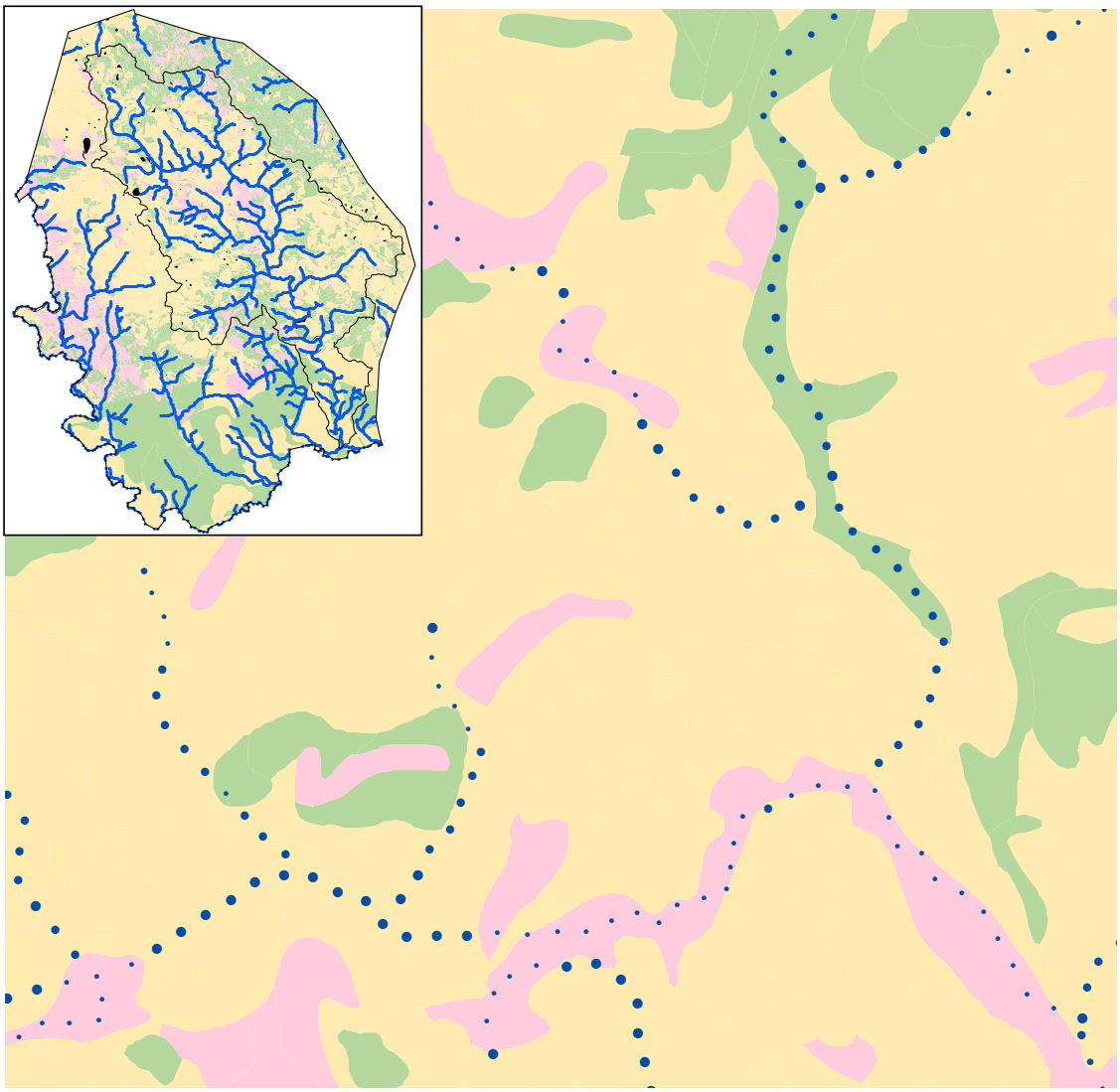

Figure 4.12 River boundary condition conductance with symbology scaled to show influence of hydraulic geometry of rivers and riverbed hydraulic conductivity

4.3.4 Initial Conditions

The initialization of heads for the steady-state model analysis is to set all nodes equal to the ground surface elevation. This is chosen as the regional-scale water table tends to be a subdued reflection of the topography (Toth, 1962). The simulated hydraulic head of the calibrated, steady-state groundwater model is used as the initial condition for all transient simulations.

4.3.5 Material Distributions

The material distributions for the groundwater model are based on the hydrostratigraphy and layer structure identified in Table 4.6. The methodology of their application is discussed in Section 4.1.2. The bedrock layers, Layers 1 through 8, have simple distributions of their material properties which are uniform, for the most part, across the model domain. The hydraulic conductivity value for the bedrock aquifer and aquitard units ranges between 2×10^{-4} to 5×10^{-5} m/s and 5×10^{-6} to 1×10^{-8} m/s, respectively (AquaResource, 2007).

The six overburden layers, also adopted from AquaResource (2007), have complex material distributions that are based on interpolated surfaces of hydraulic conductivity interpreted from borehole information. The general hydrostratigraphy from the ground surface is aquitard/aquifer, upper aquifer, aquitard, lower aquifer, and finally aquitard. The range in hydraulic conductivity values for the overburden deposits is 1×10^{-4} to 10 m/s (AquaResource, 2007). Given the extreme heterogeneity of the glacial till deposits it is difficult to clearly differentiate between aquifers from aquitards in some locations, creating a complex hydrogeologic system. The top layer, 14, is relatively thin (i.e., 1 m) and has a nearly uniform distribution of hydraulic conductivity that is approximately two orders of magnitude greater than the underlying materials giving it an effect similar to a recharge spreading layer (Therrien and Sudicky, 1996). The effect of the recharge spreading layer is to allow shallow groundwater to preferentially migrate into zones of higher hydraulic conductivity thereby alleviating groundwater mounding near the ground surface. The remaining material parameters (e.g., porosity) are applied based on the distribution of hydraulic conductivity. The range of values in hydraulic conductivity is mapped to five classes of soil types with these being coarse sand (CoS), sand (S), loam (L), silt loam (SiL), and clay (C), (Table 4.5).

4.3.6 Observation Data

The observation dataset of groundwater elevations used to calibrate the model is that used in the Alder Creek Watershed study undertaken by CH2M-Hill (2003). A total of 64 monitoring locations are within the Study Area, 6% are located within the surface aquifer/aquitard, 75% are in the upper overburden aquifer, 3% are in the lower overburden aquifer, and 16% are within the aquitard separating the upper and lower aquifers. Since most of the observation dataset is within the upper overburden aquifer, the statistical measures of model performance will be biased toward the performance of the upper overburden aquifer rather than the system as a whole. The advantage is that model feedback will be focused on the most crucial areas, the local water supply aquifer, while the

drawback is that this will provide relatively less information as to how the aquifer interacts with the system as a whole. The locations of the wells in the groundwater model observation dataset are shown in Figure 4.13. A linear trend (MS-Excel®) is used to analyze the relationship between groundwater elevations in the upper over burden aquifer, ranging from 299.95 to 361.93 m, and ground surface elevations, ranging from approximately 291.45 to 391.84. At corresponding locations these two parameters are weakly correlated (i.e., $R^2 = 0.51$) indicating that the hummocky topography may play an important role in the local recharge.

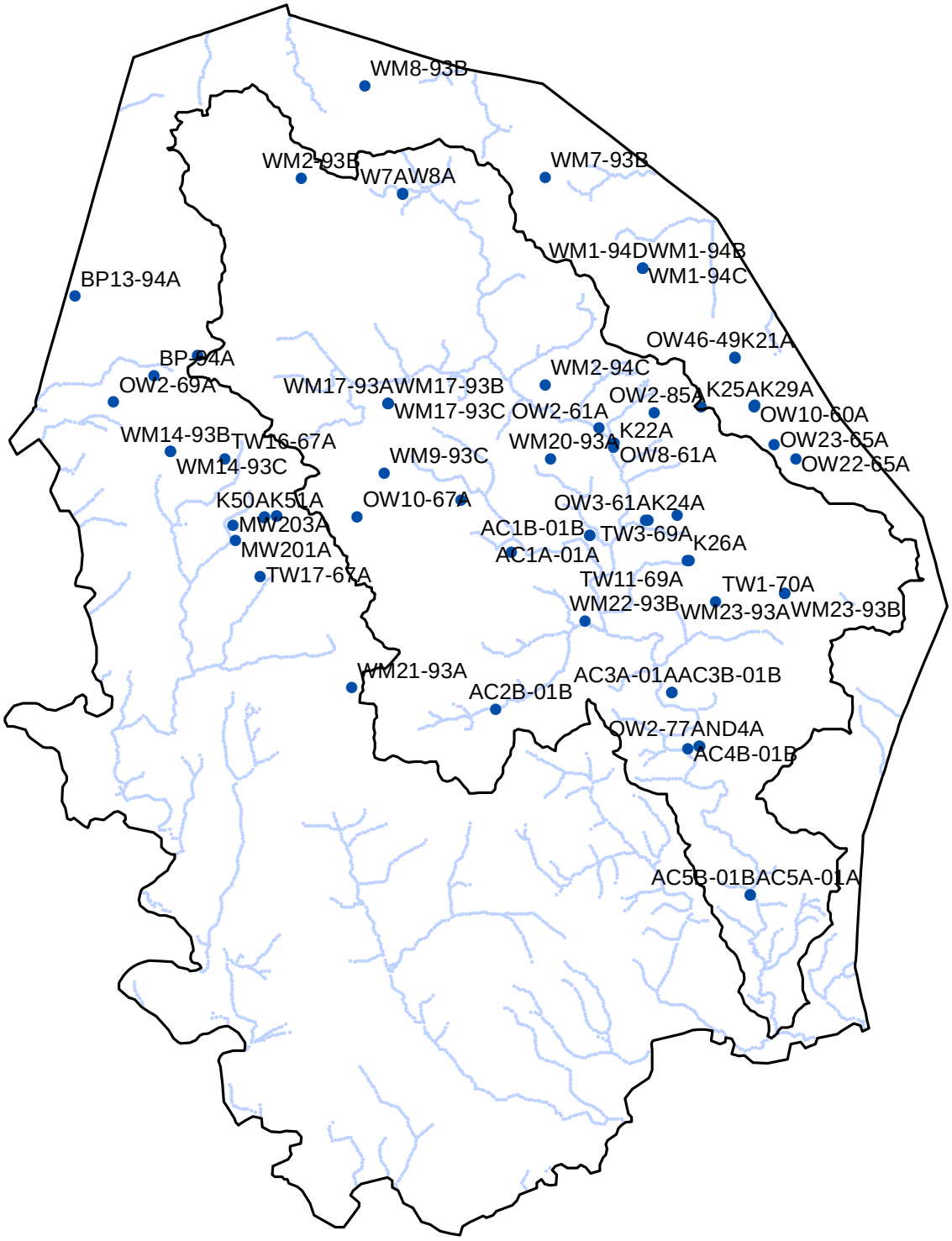

Figure 4.13 Locations of observation dataset

4.4 Parameter Calibration

Parameter calibration is an essential component of modeling since the numerical approaches are only a coarse approximation of reality and parameter values are subject to the effects of scale. The mismatch in scales comes from the discrepancy between the scale of the model elements and the scale for which the governing equations are derived and the mismatch between the scale of the model elements and the scales of measurement. Accordingly, all model parameters are subject to the effects of scale and require calibration.

Calibration of model parameters can be a large effort due to the large number of degrees of freedom of parameters. The computer resources required for solving a model of this scale and complexity precludes the calibration from adequately addressing the problem of equifinality (Beven, 1993). As such, a heuristic approach is used to calibrate the model whereby parameters are adjusted within a physically plausible range to improve the simulation results.

The calibration performance is assessed using quantitative and qualitative measures. Statistical parameters are calculated to quantify and evaluate residuals determined as the difference between simulated and observed values of hydraulic head while stream flows are qualitatively assessed. The residual statistics used to assess the model fit include minimum, maximum, mean error (ME), mean absolute error (MAE), the root mean squared (RMS) error (the standard deviation), and the normalized root mean squared error (NRMS). The mean error does not necessarily indicate a good fit to the observation dataset since a small mean error may be the result of large positive and negative residuals negating each other. The absolute mean error is not subject to this bias and is also employed to help assess the fit of the model. The RMS indicates the spread of the simulated results while the NRMS enhances this feedback by scaling the spread relative to the observed range in groundwater elevation values, resulting in a scale-independent measure. A qualitative assessment of the simulation results is also necessary to assess the overall match of the model (particularly in areas with sparse observations) and to ensure the simulated directions of groundwater flow are consistent with the conceptual model. Furthermore, the residual statistics do not provide any feed back about the spatial distribution of the error which should ideally be randomly distributed over the domain (Anderson and Woessner, 1992).

The parameters focused on in the calibration include the hydraulic conductivity of all units, the river boundary condition elevation and conductance terms, and the head boundary condition. The

recharge boundary condition is constrained by defining the distributions of the subsurface material properties extracted from the LULC and surface soils database.

The distributions of hydraulic conductivity exerted the greatest influence during the calibration procedure. The effects of scale on hydraulic conductivity, increasing in value per unit volume, are well known and are a result of the spatial averaging that occurs over model elements with respect to the measurement techniques (e.g., Bradbury and Muldoon, 1989). Studies also show that, on a regional scale, due to potential fractures and preferential pathways induced through boreholes, the vertical hydraulic conductivity of aquitards applied in groundwater flow models may be several orders of magnitude greater than core measurements of the same formation (Hart et al., 2006). The adjustment to hydraulic conductivity values also reflects compensating for the parameterization of the external Type 1 boundary conditions that communicate the regional gradient and flows to the model. This boundary condition is derived from the Grand River Watershed Model which has poor fit in the locality of the Study Area. The final distribution of hydraulic conductivity is up-scaled with respect to the initial distribution; a fence diagram showing cross-sections of the hydraulic conductivity distribution of the calibrated model is presented in Figure 4.14. The riverbed conductance is adjusted by up-scaling the vertical hydraulic conductivity of its constituent soil types thus preserving the relative differences in conductance between each river boundary condition given by the channel geometry.

The manually calibrated model produces a reasonable match to the observation dataset. The statistical measures of the model fit are given in Table 4.8. The NRMS is the most informative statistic indicating that on average the simulated heads deviate by approximately five percent of the total head loss of the system, signifying that the errors are a relatively small part of the overall model response (Anderson and Woessner, 1992).

Table 4.8 Residual statistics of calibrated model

Statistical Parameter	***Value***
Minimum	-5.99 m
Maximum	7.11 m
Mean Error	-0.52 m
Mean Absolute Error	2.32 m
Root Mean Squared Error	2.93 m
Normalized Root Mean Square Error	5.05%

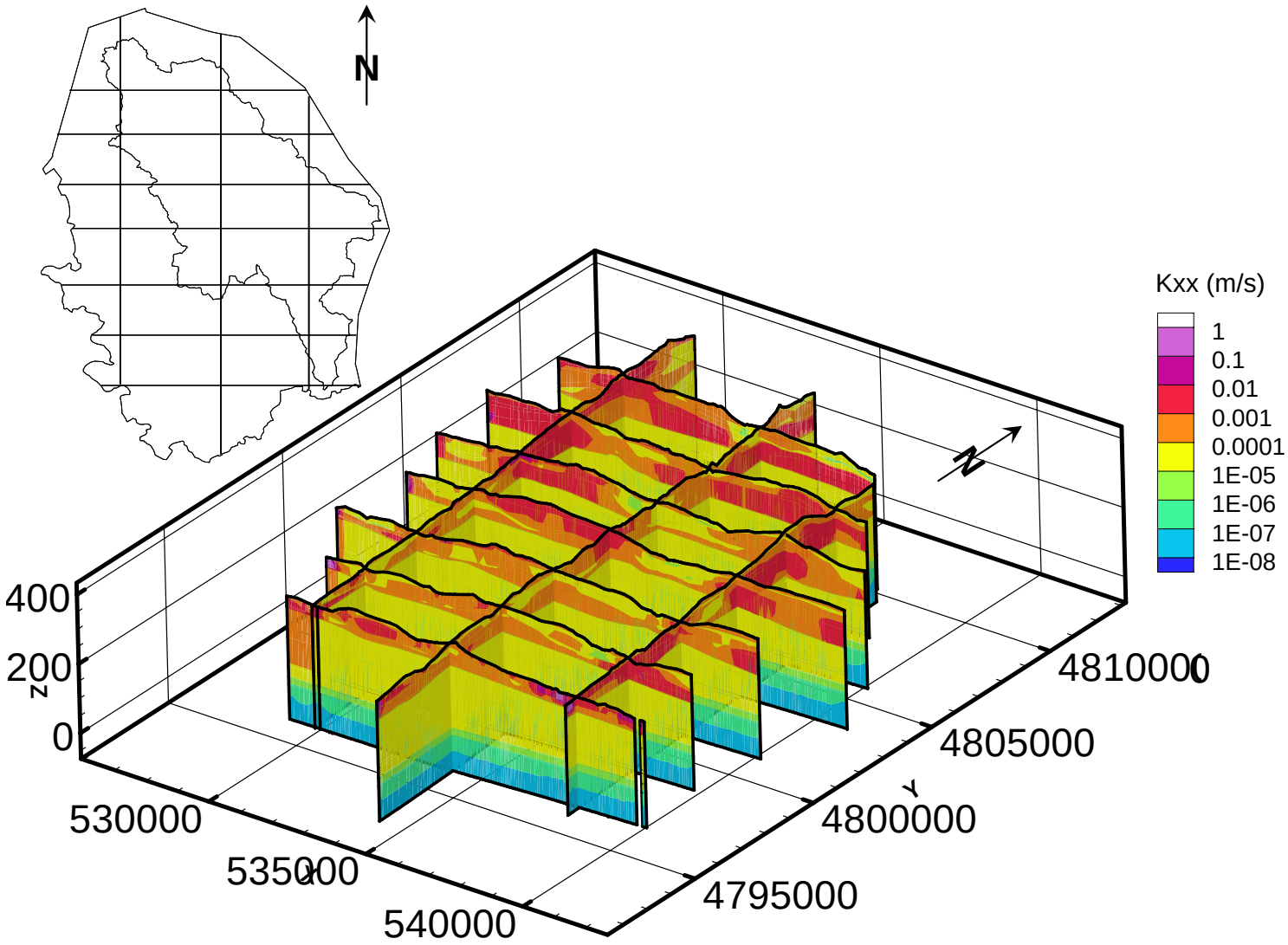

Figure 4.14 Fence diagram of hydraulic conductivity distribution for calibrated model

The calibration results are presented in Table 4.9. The total error, given as the sum of the calibration residuals, is 148.54 m. Generally, the greatest errors are located in the vicinity of well fields, particularly those under the influence of nearby river boundary conditions. Achieving a better model fit in these areas could be addressed by refining the vertical discretization allowing for greater resolution of the simulated head field and more accurate placement of well boundary conditions. The tradeoff for increased resolution however is limited by the practicality of increased computational requirements. Additionally, the eastern model boundary condition may not be well represented by a no flow boundary condition as this portion of the model domain may be under the influence of the Kitchener-Waterloo well fields in the adjacent Laurel Creek Watershed. Tile drainage of agricultural plots is not accounted for in the model. This may have an exerting influence on the relationship between infiltration, interflow, and surface runoff in localized areas as 58.5% of the Study Area is comprised of an agriculture related land class. The author is unaware of any field estimates to guide the inclusion of tile drainage in the model.

A plot of the simulated versus observed values of hydraulic head, presented in Table 4.9, is shown in Figure 4.15. With reference to the line of perfect agreement between simulated and observed values, Figure 4.15 shows the balance of over- and under-predicted simulated values, with a tendency to under-predict observed values as indicated by the mean error.

The simulated water table for the calibrated model is shown on Figure 4.16. To provide an indication of the areas of over- and under-prediction, the calibration residuals are also plotted. The symbology of the residual reflects direction and magnitude of the error by color (blue for over- and red for under-prediction) and size respectively. The locations of the largest residuals (those greater than 5 m) are labeled on Figure 4.16. The simulated water table is in agreement with the conceptual understanding of the flow system. The contours of hydraulic head show larger tributaries receiving baseflow while first and second order tributaries tend to show surface water recharging groundwater indicating some of the headwater portions of the streams may not be perennial.

Table 4.9 Calibration results

Observation ID	***Observation X***	***Observation Y***	***Observation Head (m)***	***Simulation Head (m)***	***Residual (m)***
MW201A	530420.0	4803535.0	346.02	343.40	-2.62
MW203A	530385.0	4803785.0	348.22	347.47	-0.75
OW8-99B	531093.3	4803927.0	352.08	350.56	-1.52
WM17-93C	532895.0	4805752.0	353.08	351.78	-1.30
AC1B-01B	536156.0	4803610.0	332.05	331.81	-0.24
AC2B-01B	534625.7	4800798.0	336.98	335.10	-1.88
AC3A-01A	537487.0	4801079.0	317.97	318.46	0.49
AC3B-01B	537487.0	4801079.0	317.95	318.46	0.51
AC4B-01B	537741.0	4800160.0	317.52	313.34	-4.18
AC5B-01B	538748.0	4797797.0	299.95	304.51	4.56
ASR-OW2B-96B	537950.3	4805696.0	329.61	329.83	0.22
K21A	538505.3	4806484.0	324.58	325.80	1.22
K22A	536538.2	4805046.0	325.64	332.73	7.09
K24A	537054.7	4803861.0	317.50	319.35	1.85
K25A	538815.5	4805709.0	327.45	323.82	-3.63
K26A	537733.0	4803204.0	325.41	320.67	-4.74
K29A	538818.0	4805693.0	324.25	323.95	-0.30
K50A	530898.7	4803907.0	340.58	342.19	1.61
K51A	530889.3	4803902.0	345.00	340.14	-4.86
ND4A	537938.1	4800208.0	314.10	312.77	-1.33
OW22-65A	539483.6	4804854.0	329.73	325.42	-4.31
OW23-65A	539135.7	4805081.0	328.84	326.29	-2.55
OW2-69A	528446.6	4805771.0	351.58	353.47	1.89
OW2-77A	537924.3	4800200.0	313.49	312.76	-0.73
OW3-61A	537095.5	4803858.0	325.27	328.31	3.04
OW46-49	538504.2	4806495.0	328.00	327.29	-0.71
OW8-61A	536545.3	4805108.0	328.37	335.48	7.11
OW8-99A	531093.3	4803927.0	351.41	350.56	-0.85
TW11-69A	537758.4	4803201.0	326.69	327.53	0.84
TW1-70A	538192.0	4802541.0	327.52	324.10	-3.42
TW17-67A	530823.4	4802940.0	350.74	346.38	-4.36
W7A	533126.6	4809136.0	345.19	342.50	-2.69
W8A	533130.0	4809149.0	345.50	343.04	-2.46
WM14-93C	529368.0	4804971.0	352.38	352.67	0.29
WM15-93B	529810.0	4806530.0	357.96	355.34	-2.62
WM15-93C	529810.0	4806530.0	357.96	355.34	-2.62
WM17-93A	532895.0	4805752.0	351.98	351.78	-0.20
WM17-93B	532895.0	4805752.0	352.08	351.78	-0.30
WM18-93B	534070.0	4804188.0	349.22	344.97	-4.25
WM1-94C	537006.0	4807940.0	335.60	336.31	0.71
WM1-94D	537006.0	4807940.0	335.74	336.31	0.57

Table 4.9 Cont'd

Observation ID	***Observation X***	***Observation Y***	***Observation Head (m)***	***Simulation Head (m)***	***Residual (m)***
WM20-93A	535523.0	4804855.0	334.54	339.15	4.61
WM21-93A	532300.0	4801150.0	346.00	340.01	-5.99
WM22-93B	536072.0	4802225.0	326.30	326.49	0.19
WM23-93A	539310.0	4802680.0	327.89	323.46	-4.43
WM23-93B	539310.0	4802680.0	327.78	323.46	-4.32
WM2-93B	531481.0	4809394.0	356.13	355.29	-0.84
WM2-94C	535430.0	4806050.0	338.01	338.13	0.12
WM7-93B	535436.0	4809410.0	341.93	337.00	-4.93
WM8-93B	532519.0	4810890.0	353.46	353.47	0.01
WM-OW3AC-92B	534887.1	4803341.0	341.59	340.71	-0.88
WM14-93B	529368.0	4804971.0	352.21	352.67	0.46
AC1A-01A	536156.0	4803610.0	330.10	331.72	1.62
BP13-94A	527830.0	4807490.0	355.23	356.47	1.24
BP-94A	529103.2	4806200.0	351.57	356.01	4.44
OW10-67A	532387.5	4803920.0	353.25	349.03	-4.22
OW16-60A	538823.3	4805717.0	328.54	325.89	-2.65
OW2-61A	536299.6	4805356.0	332.58	334.67	2.09
OW2-85A	537189.3	4805605.0	330.40	331.38	0.98
TW3-69A	537565.6	4803941.0	327.00	326.68	-0.32
WM1-94B	537006.0	4807940.0	330.24	333.43	3.19
WM9-93C	532830.0	4804620.0	353.48	350.56	-2.92
AC5A-01A	538749.0	4797798.0	302.20	304.82	2.62
TW16-67A	530252.5	4804855.0	351.58	355.63	4.05

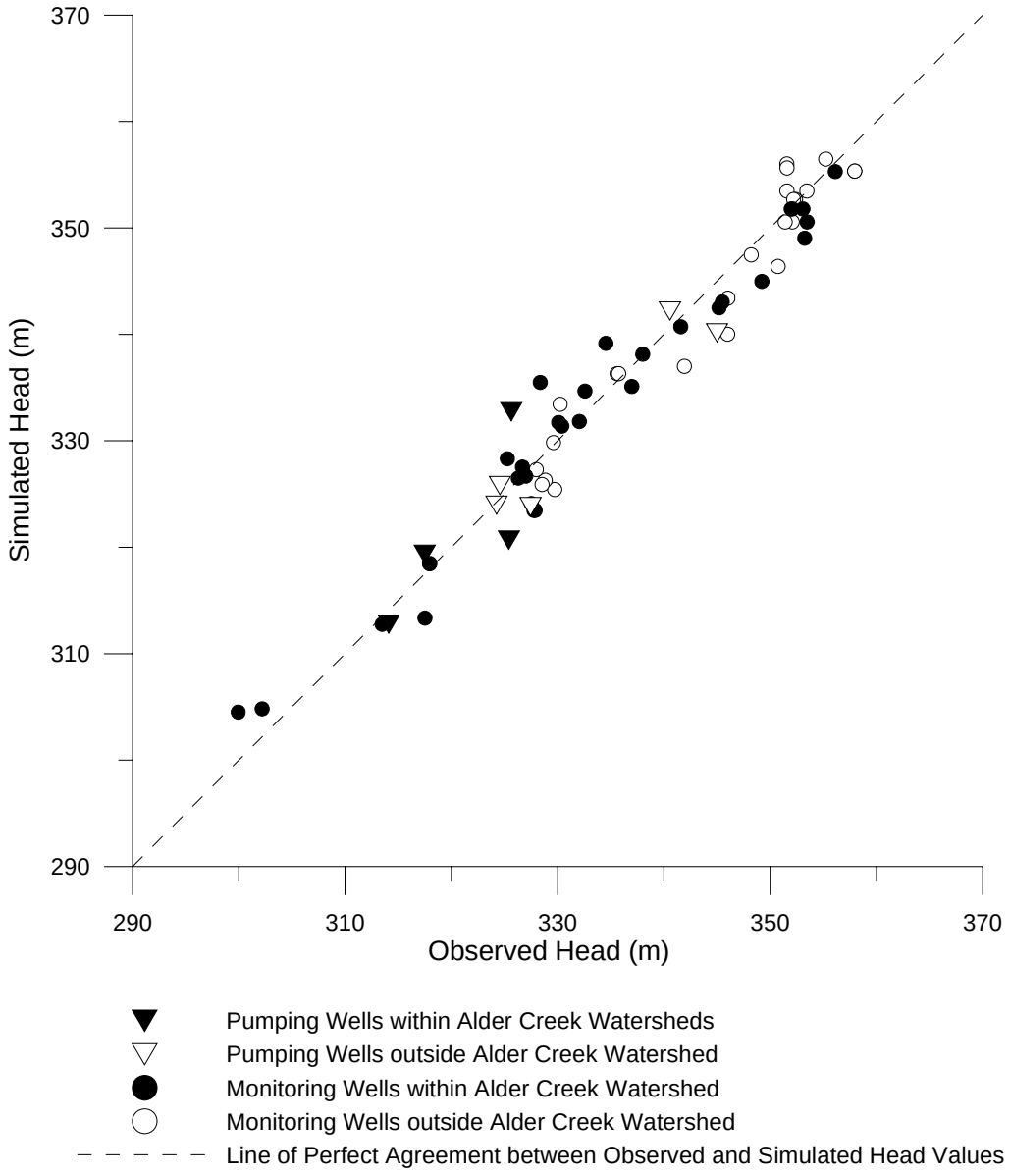

Figure 4.15 Calibration results

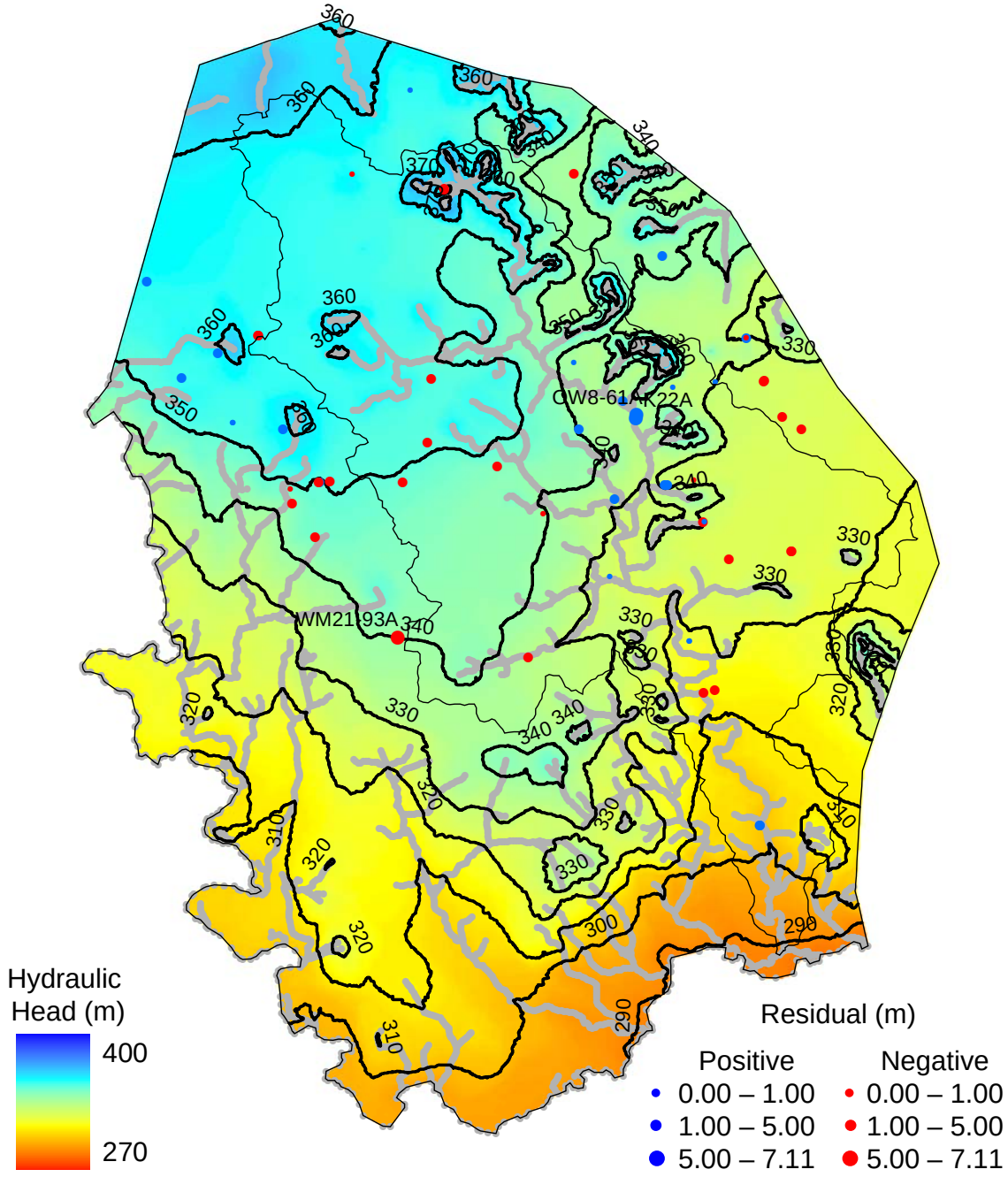

Figure 4.16 Simulated water table head (m) for calibrated model

4.5 Model Sensitivity

A sensitivity analysis was performed to quantify the uncertainty in the calibrated model caused by uncertainty in the estimates of parameter distributions and boundary conditions (Anderson and Woessner, 1992). Due to the number of degrees of freedom of parameters, a perturbation approach is used to conduct the sensitivity analysis. The calibrated parameters for the hydraulic conductivity (K) of the overburden (o/b) and bedrock (b/r) layers, and river boundary conditions (Kv) are adjusted by 10%; the reference head for river (i.e., river elevation) and Type 1 boundary conditions are adjusted by 1 m; and the flux for the recharge boundary condition is adjusted by 10%. Each of these parameter perturbations are independently applied to the calibrated model and then it is re-run. The time required for a complete and comprehensive sensitivity analysis of the problem does permit combinations of parameter adjustments to be evaluated though correlations exist between parameters (e.g., hydraulic conductivity and the recharge boundary condition).

The results are assessed by visual interpretation of hydraulic head and residual statistics with these being summarized in Table 4.10. The table presents the sum of residuals and the percent change of the sum of residuals, with respect to the calibrated model. A negative percent change signifies that the sum of the errors has improved (i.e., lessened) with respect to the calibrated model. The hydraulic head distribution for each sensitivity parameter adjustment is also checked to evaluate the result over the entire model domain. This revealed that in some cases, even though an improvement is made to the sum of the errors, the overall performance of the model was worsened (e.g., increase in number of residual outliers). The sensitivity analysis shows that the calibrated model is most sensitive to the hydraulic conductivity of the upper and lower overburden aquifers, model layers 12 and 10, respectively, and the river elevation of the river boundary conditions. This is largely due to the majority of the observation dataset being located within the upper overburden aquifer. The calibrated model is also highly sensitive to a decrease in the head specified for Type 1 boundary conditions. The boundary condition provides the head support for the Study Area as the Alder Creek Watershed is under the influence of the regional Grand River Watershed flow system. The sensitivity analysis indicates the model solution is near a local minimum and that a reasonable calibration has been achieved.

Table 4.10 Sensitivity analysis results using 10% perturbations to select model parameters

Parameter	***Perturbation***	***Sum of Residuals***	***Percent Change***
K for o/b surface (layer 14, 13)	+ 10%	148.48	-0.04%
K for o/b surface (layer 14, 13)	- 10%	148.76	0.15%
K for o/b aquifers (layer 12, 10)	+ 10%	146.73	-1.22%
K for o/b aquifers (layer 12, 10)	- 10%	150.62	1.40%
K for o/b aquitards (layer 11, 9)	+ 10%	148.34	-0.13%
K for o/b aquitards (layer 11, 9)	- 10%	149.08	0.36%
K for b/r aquifers (layer 8, 7, 6, 5, 3)	+ 10%	149.01	0.32%
K for b/r aquifers (layer 8, 7, 6, 5, 3)	- 10%	149.01	0.32%
K for b/r aquitards (layer 4, 2, 1)	+ 10%	148.50	+0.01%
K for b/r aquitards (layer 4, 2, 1)	- 10%	148.50	+0.01%
Kv for all river BCs	+ 10%	148.10	-0.30%
Kv for all river BCs	- 10%	149.07	0.36%
Reference head all River BCs	+ 1 m	146.58	-1.32%
Reference head all River BCs	- 1 m	160.98	8.37%
Head for all Type 1 BCs	+ 1 m	148.74	0.13%
Head for all Type 1 BCs	- 1 m	153.88	3.59%
Flux for all Recharge BC	+ 10%	148.88	0.23%
Flux for all Recharge BC	- 10%	148.13	-0.28%

The model sensitivity can also be extended to provide feedback as to where the model is most sensitive. This information can be used to guide future field activities to collect data where it will provide the most information (e.g., Sykes, 1985) which in turn can be used to further constrain the problem and improve the model calibration result. This effort is reserved for future work.

5 The Potential Impacts of Climate Change for the Alder Creek Watershed

5.1 Background: Global Warming, Climate Change, and Climate Trends

The term climate change refers to the ongoing climate cycle of the Earth while global warming refers to an increase in global mean surface temperatures caused by an increase in the atmospheric concentrations of greenhouse gases (GHGs) stemming from anthropogenic sources (Loaiciga, 2003). The usage of these terms climate change and global warming have become synonymous (Loaiciga, 2003) and in this report the term climate change refers to alternations to the natural variability of the climate derived from anthropogenic activities.

Given the link between emissions of GHGs and climate change, scenarios describing future emissions of GHGs are constructed as a basis for developing projections of future climate. These scenarios consider a wide range of the main driving forces (e.g., demographic, environmental, economic) that contribute to future emissions; details of these scenarios are described in a Special Report on Emissions Scenarios (SRES) (IPCC, 2000). The climate projections from two contrasting scenarios, A2 and B2, are used in this case study. The basis for the A2 scenario is projected future world with moderate growth that is relatively more heterogeneously distributed and the B2 scenario describes a world in which the emphasis is on local solutions to economic, social, and environmental sustainability, intermediate levels of economic development and a lower population growth rate than A2 (Parry, 2002). In all, a total of forty scenarios are constructed which are all considered to be equally likely and therefore, as an ensemble, represent a range of plausible to potential future outcomes (IPCC, 2000).

Analysis of precipitation and temperature records for Canada (e.g., Zhang et al., 2000; Whitfield et al., 2002) indicates the presence of trends and periodicity in climate data. Understanding the historical trends in climate variability can aid in distinguishing the effects of climate change from the natural variability of the system. A study by Zhang et al. (2000) shows that the Canadian climate has been changing over the past century, on the whole, becoming both warmer and wetter. For southern Canada, from 1900-1998, the annual mean temperature and precipitation have increased between 0.5 and 1.5°C, and 5 % to 35 %, respectively.

Analysis of the historical variability of Canadian climate can provide a reference dataset from which the potential impacts of climate change can be assessed. The occurrence of extreme events in global weather patterns, such as El Nino, can provide a microcosm of insight into how the hydrologic cycle may respond to climate change scenarios.

5.1.1 Impacts to the Hydrologic Cycle

Climatic conditions are the driving forces of the hydrologic cycle. As such, perturbations to the natural variation in climate from GHG emissions will impact all components of the hydrologic cycle, both in terms of timing and quantity. An increase in temperature and precipitation is expected to elevate evapotranspiration rates, reduce the number of freezing days leading to seasonal increases in infiltration, while an increase in the incidence of severe storms promotes increased amounts of surface runoff. In other words, climate change would intensify the global hydrologic cycle (Loaiciga et al. 1996). Though climate change has been recognized as one of the greatest influences stressing the hydrologic system, relatively little research has been undertaken regarding the potential impacts to groundwater (IPCC, 2001).

The impacts of climate change on groundwater resources are experienced through the recharge reaching the aquifer (Loaiciga, 2003). Consequently, relative to surface water resources, aquifers are buffered from the effects of a changing climate (e.g., Chen et al., 2004) and as such will become an increasingly important resource. Recharge is a complex process influenced by many variables; recharge is affected directly through changes to percolation (i.e., the net effect of infiltration from precipitation and evapotranspiration) and indirectly through the leakage from surface water resources. In essence, the groundwater flow system is linked to all hydrological process and as such, to estimate the impacts impacts of climate change to recharge requires an understanding of how the other processes in the hydrologic cycle are affected. This level of complexity requires the use of a sophisticated numerical model.

Chen et al. (2004) have analyzed historical climate data (precipitation and temperature) and groundwater levels for the upper carbonate aquifer near Winnipeg, Manitoba. The findings of this study show that groundwater levels in the upper carbonate aquifer show a strong correlation with both precipitation and temperature. The study also reveals that groundwater levels exhibit a time delay between 1 to 2 years in responding to climatic conditions. Numerical investigations by Brouyère et al. (2004) suggests that a thick unsaturated zone may smooth seasonal changes in percolation thus masking the effect of climate change. This is relevant to the Study Area as it derives its recharge

from precipitation and is situated beneath a hummocky terrain where the thickness of the saturated zone is highly variable. Based on the calibrated model the thickness of the unsaturated zone varies from 0 m near wetlands, where the water table intersects the ground surface, to as much as approximately 70 m in hilly areas with high relief. The impacts of climate change to the hydrologic cycle have direct implications for water resources decision making and infrastructure.

5.1.2 Impacts to Water Resources Decision Making and Infrastructure

Decisions regarding water resources policies and infrastructure are largely based on the assumption that past hydrologic events are a good indication of future hydrologic events, referred to as the critical period approach by Loaiciga et al., (1996). Typically, a degree of conservatism (e.g., safety factors) is employed in this approach in recognition of hydrologic (and other) uncertainties as well as the limited number of historical observations. The uncertainties of future hydrologic conditions stemming from climate change are of a different nature because the uncertainty cannot be estimated based on historical observations, but rather, are based on climate predictions of limited reliability (Loaiciga et al., 1996).

Over the past century, the overall trends of precipitation and temperature in Canada and southern Canada has been getting warmer and wetter (Zhang et al., 2000) and according to global (Chen et al., 2003) and regional climate models (Sousounis and Grover, 2002) these trends can be expected to be accompanied by an increased incidence of severe weather events (IPCC, 1995).

As such, in some cases the current state of water resources infrastructure may be inadequate to cope with future climate conditions. The implications of inadequate design of infrastructure can have a potentially large range. For instance, infrastructure for event based hydrologic events (e.g., storms) in cities such as curbs, storm sewer and detention ponds may no longer be adequate to mitigate against flooding and water quality issues. The increased incidence of severe storms has implications for infrastructure on a larger scale; the adequacy and safety of the design of roadways, bridges, and floodplains will have to be assessed. Infrastructure, relating to the production of hydropower that relies on continuous rates of flow to be within a specified range for safe and efficient operation, may be under threat (e.g., Filon, 2000).

5.2 GCMs, RCMs, and the Hydrologic Model

General Circulation Models (GCMs) are used to forecast future climate conditions under GHG emissions scenarios. GCMs, with a coarse scale of approximately 300 km, are intended to predict the

average, synoptic-scale, general-circulation patterns of the atmosphere (Loaiciga et al., 1996) and thus cannot be relied on to provide accurate prediction of future climate at regional or local scales. Regional Climate Models (RCMs) are nested within GCMs, meaning the GCM provides the boundary conditions for the RCM and internally the RCM predicts climate evolution at a refined scale.

5.2.1 Uncertainties in Climate Models

Uncertainties in the modeling of future climate arise from the limited inclusion of feedback loops (Loaiciga, 2003), sensitivity to initial conditions (Tsonis, 1991), and the issue of scale (Loaiciga et al., 1996). These uncertainties give rise to disagreements between climate models on both global and regional scales (Chen et al., 2003).

Loaiciga (2003) identifies several important climate feedback loops, the interaction between the climate forcings and the response of the environment to either accentuate or dampen those forcings, which are not well captured in GCM and RCM models. Some feedback loops are better understood than others. Some key climate feedback loops identified by Loaiciga (2003) include: water-vapor, cloudiness, surface albedo, soil moisture, and vegetation. Cloudiness is identified as a feedback loop with great uncertainty as clouds can have both positive and negative feedbacks by, respectively, trapping infrared radiation that contributes to surface warming and reflecting incoming solar radiation back to space thus reducing the energy reaching the Earth's surface, relative to clear skies (Loaiciga et al., 1996; Loaiciga, 2003). Another poorly understood feedback loop is with respect to vegetation. The vegetation feedback loop is also of concern to hydrologic models as it directly impacts the evapotranspiration water budget, a key component for estimating recharge to groundwater systems.

Feedback from vegetation can potentially be both positive and negative, having counteracting effects (Eckhardt and Ulbrich, 1998). A positive feedback is the rise in surface temperature and CO_2 which intensifies potential evapotranspiration and leaf area by stimulating plant growth and increasing the growing season, thereby also increasing interception and transpiration. Conversely, a negative feedback can result from an increase in the surface temperatures and vapor pressure that can decrease stomatal conductance, which is the rate at which water vapor can evaporate from leaf pores, thus reducing plant transpiration. Though this study is focused on the watershed scale, the conceptual implications of the feedback loop apply to models of all scales.

The implication of not accurately capturing the response of feedback loops is that feedback will modify the hydrologic response of the system, thus impacting the simulation results. Not

incorporating feedback in a physically based manner imposes limitations on the value and certainty of the modeling results. This is simply illustrated when considering how the vegetation will respond to changes in weather and how that response will in turn affect and modify the response of the hydrological processes.

In addition to the uncertainty accompanying the lack of understanding and implementation of feedback loops in GCMs and RCMs there are also concerns of divergent simulation results based on small changes to initial conditions (i.e., chaos effect). Instability and non-periodic solutions to hydrodynamic flow is shown by Lorenz (1963), concluding that unless the initial conditions are known exactly, the prediction of distant future states is impossible by any method. Indeed, using current models, Tsonis (1991) shows a divergence in climate predictions resulting from a slight perturbation of the initial conditions. Perturbations of 1% were applied to the reference case and within forty years the mean global climate diverged significantly. Given the instability of climate prediction and the great uncertainty inherent in establishing the initial conditions, the chaotic instability of climate poses severe limits to climate predictability at all scales (Sneyers, 1997).

5.2.2 Issues of Scale

GCMs were designed to predict the average, synoptic-scale, general-circulation patterns of the atmosphere for coarse discretizations, as a result the GCM is not a tool for the hydrologist (Loaiciga et al., 1996). The scope of the hydrologist is to translate how the impacts of global warming will perturb forcing variables (primarily precipitation and temperature) and how these perturbations will impact the hydrologic cycle and water resources at a spatial scale relevant to the study.

A nesting approach is typically used to relate predicted impacts of global warming at the scale GCM to the scale of the hydrologic model. In such an approach the solution to the GCM becomes the boundary and initial conditions for the RCM and in turn the output variables from the RCM become the forcing input variables (e.g., precipitation) for the hydrologic model (Loaiciga, 2003). This approach is conceptually shown Figure 5.1.

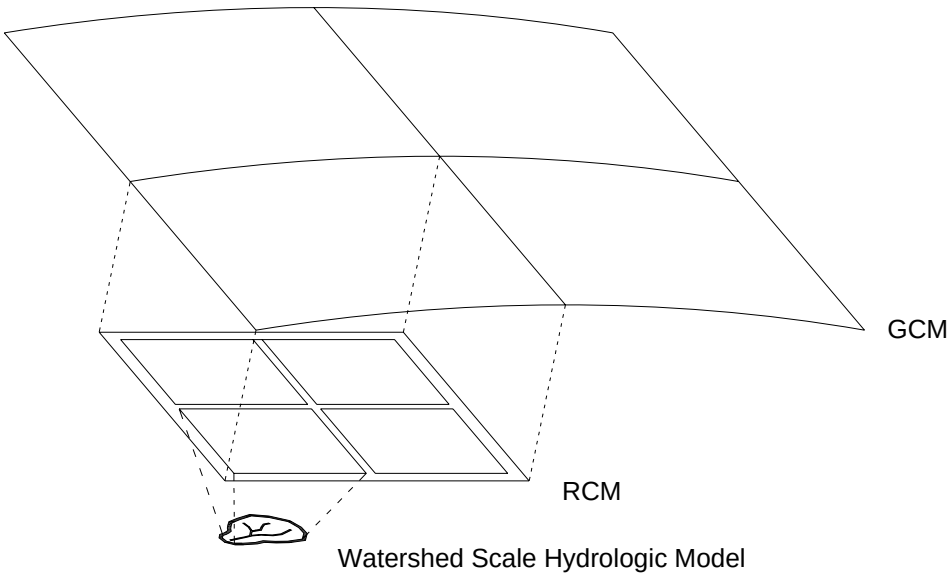

Figure 5.1 Conceptualization of nesting approach scale forcings to the hydrologic model from the GCM (after Loaiciga, 2003)

The coarse spatial discretization of GCMs (e.g., 300×300 km^2 cell size) hinders assignment of representative parameter values, boundary conditions, and the implementation of feedback loops (Loaiciga et al., 1996). Temporal scales are also an issue as atmospheric conditions vary on the order of a fraction of a day while deep ocean circulation timescales can be as large as 1000 years (Loaiciga et al., 1996). Detailed hydrologic investigations, on the other hand, require consideration for the scales of spatial heterogeneity of land use practices, surface characteristics, and soil materials that influence surface water and groundwater processes.

The importance of estimating physically-based, detailed temporally and spatially distributed rates of recharge to groundwater models, in urban and rural environments, is shown by Jyrkama et al. (2002) and Jyrkama and Sykes (2006). The value of preserving the physical basis and scales (both spatial and temporal) for recharge allows for an enhanced understanding of how climate change can affect the distribution of recharge on the regional watershed scale (e.g., Jyrkama and Sykes, 2007). Such an approach would allow for the identification of areas that are most vulnerable and sensitive to the impacts of climate change so that mitigation strategies can be more effectively implemented.

In order to effectively gauge the impacts of climate change on water resources requires consideration of agricultural, environmental, and socio-economic information and that it be incorporated into the model. Ideally, this information should be coupled with the model as feedback loops so that the simulated hydrological processes reflect the changing conditions rather than

applying prescribed scenarios. Research has been conducted that incorporates (to varying degrees) the long-term land use, vegetative response, human water demand, and other socio-economic information with the hydrologic model (e.g., Bouraoui et al., 1999; Loaiciga et al., 2000; Eckhardt and Ulbrich, 2004; Holman, 2006). In other investigations, all stresses other than climate change remain constant over the simulation period so that the impacts of climate change can be isolated and evaluated (e.g., Allen et al., 2004; Brouyère et al., 2004).

5.2.3 General Predictions of Climate Modeling

General predictions of future climate trends for the period 1990-2100 resulting from climate change include: an increase in globally averaged surface temperature of 1.4 to 5.8°C over the period, both global increases and decreases in precipitation ranging from 5 to 20 % with a greater likelihood that precipitation will increase over high-latitude regions in both summer and winter, northern hemisphere snow cover, permafrost, and sea-ice extent are projected to decrease further, and global mean sea level is projected to rise by 0.09 to 0.88 m (IPCC, 2001)

Sousounis and Grover (2001) compare potential future weather patterns predicted by two General Circulation Models, the Canadian Coupled Climate Model (CGCM1) and the Hadley Coupled Climate Model (HadCM2), over the Great Lakes region. Both models show a decrease in the number of extremely cold days and an increase in the number of extremely hot days. In terms of future precipitation, both models show increased amounts, which are primarily a result of an increase in heavy precipitation events. The temporal distribution of the increase in precipitation between these two models differs. The CGCM1 simulation results show an emphasis in increased precipitation occurring from December to July while the HadCM2 simulates the increase as being emphasized from July to December.

Chen et al. (2003) compare the projections of future climate over North America as simulated by two regional climate models, MM5 and RegCM2 that are driven by the same general circulation model forcing. The results of their comparison reveal that on the whole, temperature and precipitation will rise over North America. Depending on the model and the geographic location, monthly mean temperatures and precipitation are simulated to vary between -4 to +7°C and between -2 to +4 mm/day, respectively.

Hydrologic modeling of the Great Lakes, using the model predictions from the CGCM1 and the HadCM2 models as forcings, depicts a range of potential impacts to the Great Lakes (Lofgren et al., 2002). On one extreme, using input from the CGCM1, lake levels are projected to drop with the

maximum being 1.38 m for Lakes Michigan and Huron by the year 2090. In contrast, using inputs from HadCM2, lake levels are projected to rise up to a maximum of 0.35 m on Lakes Michigan and Huron by the year 2090. The rise or fall of the water levels in the Great Lakes has implications for modeling of groundwater-surface water impacts to the Study Area. As mentioned, the Alder Creek Watershed is a small sub-watershed of the Grand River Watershed. The head support for the groundwater within the Grand River Watershed ultimately comes from precipitation and from Lake Huron which is influenced by the other Great Lakes as they are a connected network. The Grand River Watershed drains directly into Lake Erie, providing the regional groundwater discharge boundary. Relative changes to the levels in the Great Lakes impacts the regional groundwater flow field in the Grand River Watershed and hence will impact the regional groundwater system underlying the surficial aquifers within the Alder Creek Study Area.

5.3 Modeling Approach

Climate modeling simulation results should not be taken as predictions of future climate but rather as representing a plausible range of potential future climate evolution. The usefulness of simulating future climate scenarios is to understand the plausible range of potential outcomes. On the basis of these climate projections, "what-if" scenarios can be constructed to evaluate the hydrologic impacts and the risks and opportunities associated with future climate change. Scheraga and Furlow (2002) affirm that when these evaluations are presented to policy makers in a timely manner they can be used to make informative decisions about resource allocation despite the existence of scientific uncertainties.

5.3.1 Climate Change Studies at the Watershed Scale

Several studies have evaluated the potential impacts of climate change on surface water and groundwater resources at the watershed scale. A selection of studies, with an emphasis towards groundwater related applications, is summarized below. These studies show a wide range of methodologies, numerical models employed, and results.

In Belgium, studies have been conducted as to how climate change may impact surface water flows in eight catchments with varying characteristics (Gellens and Roulin, 1998). Climate change impacts were applied by perturbing observed series, deduced from GCMs. It was found that impacts to stream flow were driven by changes to precipitation and in most cases the sign of the impact is the same. Due to the variability in catchment characteristics, it was deduced that the impacts to streams

situated in loamy catchments, with high infiltration rates, is damped by large groundwater capacities and that streams that are primarily dependant on surface runoff for sustenance are more sensitive to the climate changes.

A study of the potential impacts that climate change can have on the groundwater resources of the Chalky Aquifer, which lies in Geer Basin, Belgium, is studied by Brouyère et al. (2004). Local climate change scenarios were constructed using IPCC scenarios as a basis, calculating monthly change rates of precipitation and temperature, and applying these change rates to a baseline period of observed data. The simulation results show that the impact of climate change is dependant on the GCM used to construct the climate change scenarios. Two of the three GCMs used to construct the climate change scenarios resulted in a reduction of groundwater levels and base flows while the other predicted groundwater fluctuations that were more or less representative of the baseline levels or slightly higher.

Studying the potential impacts of climate change on the Bièvre-Valloire watershed in France, Bouraoui et al. (1999) used a disaggregation approach to scale down the forcing variables required by the hydrologic model from a GCM. The results of the study showed that climate change had little impact on precipitation while evaporation rates increased, thus reducing recharge. From the simulation results, the authors infer impacts to the agricultural as groundwater withdrawal for irrigation may not be sustainable for the cultivation of traditional crops.

The potential impacts of climate change on the Grand Forks Aquifer and its major tributaries, the Kettle and Granby Rivers, in southern British Columbia have been studied by Allen et al. (2004), Scibek and Allen (2007), and Scibek et al. (2007). In these studies, the results of GCM were downscaled using a statistical procedure to construct scenarios of potential future climate. These scenarios of potential future climate were applied to a stochastic weather generator to construct daily climate forcing values for the hydrologic models. Visual MODFLOW (WHI, 1997 and 2004) was used to develop a three-dimensional groundwater model of the regional aquifer and Visual HELP (WHI, 2000) to simulate the hydrologic processes occurring in the unsaturated zone and surface water. In all three studies, the surficial, unconfined aquifer was found to be relatively insensitive to the effects of climate change. In the study by Scibek et al. (2007), BRANCH, developed by the USGS (Schaffranek et al., 1981), is used to simulate the effects of climate change on tributary flow and these results were linked to the Visual MODFLOW groundwater model to update the RIVER (USGS, 1988) boundary condition. The results reveal that the timing of the runoff peak shifts to earlier in the year most likely caused by a warmer climate resulting in an earlier snowmelt and more

rain in the winter season. The shape of the river hydrographs and peak water levels were found to be similar to present (baseline) conditions.

More recently, using HELP3, the impacts of climate change to spatially varying recharge estimates for groundwater is done for the Grand River Watershed by Jyrkama and Sykes (2007) with respect to the general climate predictions reported by the IPCC (2001). The results show an intensification of the hydrologic cycle, increases to runoff, evapotranspiration, and recharge though the distribution is quite variable. The detailed daily simulations show that the timing of these processes has shifted with increasing temperature (e.g., increased recharge in the winter months). This study makes use of the detailed methodology for estimating physically-based, detailed, spatially-disturbed and temporally varying recharge by Jyrkama (2003), summarized in Section 4.2.

5.3.2 Methodology Applied to Study Area

As outlined in Section 4, the calibrated groundwater flow model is used as an initial condition to conduct long-term transient simulations. The surface and vadose zone hydrologic processes are simulated with HELP3 using a daily time step for the period 1990-2080. HydroSphere is then used to simulate daily saturated groundwater flow for the same period using the leakage output from HELP3 to construct a detailed, spatially-distributed recharge boundary condition. Due to computer memory limitations, the groundwater model is run in two year increments. Continuity is maintained by using the head distribution from the last day of a two year simulation as the initial condition for the first day of the following two year simulation (e.g., the head distribution for the last day of the 2020-2022 simulation is used as the initial condition for the 2022-2024 simulation).

A baseline scenario is constructed to quantitatively asses the effects of climate change. The daily record of climate data available covers the period 1960-2000. To construct a baseline climate dataset for 1990-2080, the actual parameter values for the period 1990-2000 are used and the entire record, 1960-2000, is looped twice to provide data for the periods 2000-2040 and 2040-2080.

To evaluate the effects of climate change, scaling factors are applied to the baseline values of precipitation, temperature and incoming solar radiation datasets. These scaling factors obtained from the Canadian Institute for Climate Studies (CICS, 2007) and are based on the results from using the second generation Canadian General Circulation Model (CGCM2) to simulate the A2x and B2x scenarios with respect to a reference scenario. More information regarding the CGCM2 is given by Flato and Boer (2001). There are no RCM available over the region of the Study Area to use as an intermediary to scale between the GCM and hydrologic models as idealized in Figure 5.1; thus, the

scaling factors derived form GCM simulations are applied directly to the climate dataset as done in similar studies (e.g., Allen et al., 2004). "The rationale behind the use of scaling factors is that – although GCMs may not accurately estimate the local statistics of regional climate variables – their internal consistency and strong physical basis may provide plausible estimates of their ratios and differences" (Loaiciga et al., 2000).

Scaling factors are available on a monthly basis for time slices 2020, 2050, and 2080 (CICS, 2007). Between time slices, linear interpolation is used to distribute the monthly scaling factors to the daily time step for HELP3. Scaling factors for precipitation and solar radiation are multiplied with baseline values and the scaling factors for temperature are added to baseline values. The monthly scaling factors for precipitation, temperature, and solar radiation are presented in Tables 5.1 through 5.3, respectively. Seasonal and annual averages are also reported to help characterize the trends of the projected future climate scenarios.

The precipitation scaling factors show the greatest monthly variability with both large increases and decreases which are generally emphasized over the winter and summer seasons. Increases to precipitation are shaded in grey to readily differentiate seasonal precipitation trends for scenarios A2x and B2x. On average, scenarios A2x and B2x are respectively characterized as slightly drier and wetter future climate conditions relative to the reference dataset. Considering the net adjustment to precipitation over all time slices is small, the greatest impacts will be a result of changes to the timing of the precipitation.

The temperature scaling factors for both scenarios show increased temperatures over all months for all time slices. The greatest increases in temperature occur during the winter season followed by spring, summer, and then autumn. The rise in monthly temperatures becomes more pronounced with increasing time with a projected annual average temperature increase of approximately 5.3°C by 2080 for the A2x scenario. Solar Radiation is generally projected to decrease under the A2x and B2x scenarios with increases shaded in grey (Table 5.3) for ease of identification.

Changes to individual climate forcing variables can both accentuate and dampen hydrologic processes while simultaneous perturbations to multiple climate forcing variables have the potential to compound or negate the net hydrologic response with respect to the distribution of water quantities and timing.

Table 5.1 Climate Scaling Factors for Precipitation Climate Forcing

Month	***Time Slices for A2x Scenario***			***Time Slices for B2x Scenario***		
	2020	***2050***	***2080***	***2020***	***2050***	***2080***
January	-1.013	-5.836	-3.312	-7.302	3.659	-2.599
February	-5.388	-1.892	3.622	-4.879	5.043	0.597
March	-3.989	-5.493	11.699	-6.467	2.381	6.724
April	6.432	8.279	15.001	2.458	8.308	11.799
May	-0.601	-1.205	-0.293	-0.746	-6.769	-1.077
June	-0.288	-8.274	-5.234	-1.929	-1.544	-3.872
July	-1.334	1.439	-7.724	-9.383	-1.095	-4.782
August	2.867	6.799	-12.283	8.689	9.629	-0.294
September	3.180	0.095	-8.827	8.369	11.89	-2.96
October	0.041	-4.887	5.734	5.212	1.944	4.628
November	-3.407	-7.574	-2.341	-0.235	-3.214	-4.244
December	1.059	-0.247	-2.257	-0.379	0.083	-6.704
Winter	-3.463	-4.407	4.003	-6.216	3.694	1.574
Spring	1.848	-0.400	3.158	-0.072	-0.002	2.283
Summer	1.571	2.778	-9.611	2.558	6.808	-2.679
Autumn	-0.769	-4.236	0.379	1.533	-0.396	-2.107
Annual	-0.203	-1.566	-0.518	-0.549	2.526	-0.232

Table 5.2 Climate Change Scaling Factors for Temperature Climate Forcing

Month	***Time Slices for A2x Scenario***			***Time Slices for B2x Scenario***		
	2020	***2050***	***2080***	***2020***	***2050***	***2080***
January	2.454	4.438	6.105	2.357	3.698	4.733
February	2.450	5.571	9.232	2.867	4.340	6.569
March	2.608	4.417	7.874	2.859	3.785	5.701
April	2.871	4.743	8.07	2.639	4.089	5.758
May	2.049	3.456	5.58	2.266	3.473	3.859
June	1.300	2.752	4.555	1.394	2.211	3.050
July	1.718	2.757	4.533	1.608	2.314	3.142
August	1.262	2.605	4.191	1.265	2.261	2.838
September	1.479	2.762	4.437	1.527	2.496	3.237
October	0.748	2.358	3.476	1.200	1.565	2.651
November	1.113	1.816	3.131	1.188	1.597	2.287
December	1.123	1.494	2.103	0.676	1.249	1.637
Winter	2.073	4.809	7.737	2.694	3.941	5.668
Spring	2.073	3.650	6.068	2.100	3.258	4.222
Summer	2.073	2.708	4.387	1.467	2.357	3.072
Autumn	2.073	1.889	2.903	1.021	1.470	2.192
Annual	2.073	3.264	5.274	1.821	2.757	3.789

Table 5.3 Climate Change Scaling Factors for Solar Radiation Climate Forcing

Month	***Time Slices for A2x Scenario***			***Time Slices for B2x Scenario***		
	2020	***2050***	***2080***	***2020***	***2050***	***2080***
January	-1.824	-3.648	-5.804	-2.29	-3.467	-4.404
February	-3.856	-8.363	-13.044	-3.564	-7.268	-10.737
March	-7.814	-14.191	-22.557	-8.644	-12.011	-19.733
April	-11.022	-16.363	-19.258	-9.863	-15.977	-15.735
May	-2.863	-0.644	-1.343	-2.096	2.971	1.757
June	1.880	-0.273	-2.886	0.480	-0.229	0.672
July	-2.220	-7.362	-9.810	-1.844	-6.665	-7.553
August	-2.603	-7.381	-2.603	-2.778	-10.569	-7.673
September	-0.878	-4.887	-4.634	-3.319	-5.326	-2.805
October	1.605	0.136	-0.036	0.452	0.403	-1.196
November	-0.190	-0.232	-1.341	-0.716	1.133	0.187
December	-1.576	-0.286	-0.991	0.113	-0.952	-0.369
Winter	-4.498	-8.734	-13.802	-4.833	-7.582	-11.625
Spring	-4.002	-5.760	-7.829	-3.826	-4.412	-4.435
Summer	-1.900	-6.543	-5.682	-2.647	-7.520	-6.010
Autumn	-0.054	-0.127	-0.789	-0.050	0.195	-0.459
Annual	-2.613	-5.291	-7.026	-2.839	-4.830	-5.632

As already mentioned in Section 4.2.4, the length of the HELP3 model columns have been updated (i.e., increased) to incorporate the full length of the unsaturated zone for conditions where the distance to the water table, under average (steady-state) conditions, is greater than evaporative zone depth. This is an important consideration as it incorporates the transient effects of water storage in the vadose zone which can be significant as in some areas the distance to the water table is as much as approximately 70 m, owing to the hummocky topography of the region.

5.3.3 HELP3 Results

In order to present the results of the HELP3 models in a meaningful manner the volume of output data needs to be reduced to a manageable amount. This is accomplished by lumping the results for the 14 categories of LULC, given in Table 3.1, into the following three broad classes: agriculture related – bare agriculture, row crops, small grains, and plantation; forest related – dense conifer, deciduous, and mixed forest types, pasture/sparse forest, forage, and golf courses; and urban related – built-up commercial/industrial and residential, extraction/bedrock/roads, and marsh, The marsh LULC is lumped within the urban related class in recognition of its high SCS curve number. For each broad class the results of the HELP3 models are averaged according to their contributing area.

The analysis of the impacts of climate change focuses on the period 2020-2080. For the reference scenario hydrographs of monthly average precipitation, runoff, evapotranspiration, and recharge for the three broad classes are given in Figures 5.2, 5.3, and 5.4, respectively. The model output data is at the scale of the daily time step. However, for illustrative purposes, the monthly average is shown as it condenses the volume of data to a manageable amount, reduces the variability, and allows for trends to be visualized. This set of figures clearly shows the timing of the hydrologic cycle. Precipitation occurs most heavily in summer and autumn months while runoff processes are most dominant in the spring season (coinciding with the melt of winter snow). The rates of evapotranspiration are highly dependant on the length of the growing year, showing a minimal abstraction from the water budget during the winter and peaking during the summer. These figures also highlight the variability of the timing of the recharge as it is delivered to the water table. Generally, rates of recharge peak during the spring and then decay in an exponential fashion for the remainder of the year. These figures also demonstrate that the recharge received by the water table is not sensitive to individual monthly spikes of increased or decreased precipitation. This may be attributed to the transient storage effects of the unsaturated zone which are enhanced given the hummocky terrain of the Study Area.

The hydrologic response characteristics of each broad class of LULC are difficult to precisely identify on Figures 5.2 to 5.4 due to the scale of the plots. The agriculture related class shows the greatest amount of recharge with moderate amounts of runoff and evapotranspiration relative to forest and urban related classes. The forest related class shows the greatest evapotranspiration with the least amount of runoff and moderate recharge while the urban related class is characterized with the greatest runoff, and the least evapotranspiration and recharge, relative to the other broad classes.

A summary of the relative impacts of the climate change scenarios (to the reference scenario) over the period 2020-2080 is presented in Table 5.4. To summarize the data, the hydrologic processes of runoff, evaportranspiration, and recharge are spatially averaged for the agriculture, forest, and urban related classes and temporally averaged over twenty year increments (2020-2040, 2040-2060, and 2060-2080). The spatial and temporal lumping of the simulation results dampens the transient details of the hydrologic response. Detailed hydrographs summarizing the average monthly changes to the response of agricultural, forest, and urban related classes under A2x and B2x climate change scenarios are presented in Figures 5.5 to 5.7 and 5.8 to 5.10, respectively. Each broad category of LULC presents hydrographs for changes to precipitation, runoff, evapotranspiration, and recharge relative to the reference scenario.

Table 5.4 Summary of changes the HELP3 hydrologic budget for A2x and B2x scenarios

Time	***A2x***			***B2x***		
	Agriculture	***Forest***	***Urban***	***Agriculture***	***Forest***	***Urban***
Δ Average Monthly Runoff (mm)						
2020-2040	-5.99	-5.52	-4.02	-5.17	-4.81	-3.15
2040-2060	-6.89	-6.74	-4.85	-4.55	-4.50	-2.49
2060-2080	-9.97	-8.77	-7.45	-7.83	-7.05	-5.03
Δ Average Monthly ET (mm)						
2020-2040	3.22	3.20	2.78	2.82	2.75	2.50
2040-2060	3.73	3.55	3.17	3.39	3.22	2.85
2060-2080	5.78	5.28	5.14	4.50	4.13	3.99
Δ Average Monthly Recharge (mm)						
2020-2040	2.53	2.08	0.89	3.01	2.72	1.20
2040-2060	1.72	1.75	0.36	2.51	2.64	1.13
2060-2080	3.47	2.76	1.33	4.12	3.75	1.66

In both the A2x and B2x scenarios, all three broad classes of LULC show a shift in the timing of the runoff. The change in runoff hydrographs are characterized by an earlier spike followed by an abrupt decrease, owing to an earlier commencement and ending of spring time snow melt caused by increasing temperatures. The changes to the distribution of monthly precipitation appears to have less of an impact on runoff than increasing temperatures given that on average the runoff abstractions from precipitation decrease despite both increasing and decreasing fluctuations to monthly precipitation, see Table 5.1. As seen in Figures 5.5 to 5.10 and summarized in Table 5.4 the net affect is a decrease in runoff and thereby allowing more water to be available for the processes of evapotranspiration and infiltration.

The gradually increasing temperatures have intensified the simulated rates of evapotranspiration for all three broad classes of LULC. Generally, evapotranspiration has increased throughout the year with greatest increases being concentrated in the summer months. The brief decreases in evapotranspiration, shown in Figures 5.5 to 5.10, may be due to the limited availability of water from the relatively drier autumn months, see Table 5.1, under the influence of projected climate change. The increase to evapotranspiration processes are more pronounced for the agriculture and forest related classes relative to the urban related class as it is characterized with relatively lesser amounts of vegetation and greater areas of impervious surfaces.

On average the recharge to the groundwater table increases for both drier (A2x) and wetter (B2x) projections of future climate. In all cases, the greatest increases in recharge occur during the spring season after which the increase recedes to near reference amounts. The shift in the spring melt has a

pronounced effect on recharge as it increases the amount of water available to infiltrate into the subsurface before evaptranspiration demands peak in the summer season. In both the A2x and B2x scenarios, the urban related class shows a markedly lesser increase to recharge compared to the agriculture and forest related classes due in part to the greater coverage of impervious surfaces, lessening the area available for infiltration. The B2x scenario shows a greater increase to recharge relative to the A2x scenario which is attributed to the greater amounts of precipitation occurring during the winter months, see Table 5.1.

To summarize, these results highlight the importance of capturing the changes in timing of hydrological processes resulting from the projected impacts of climate change. This is most clearly demonstrated by increased amounts of recharge under average drier (A2x) and wetter (B2x) projections of future climate evaluated in this case study.

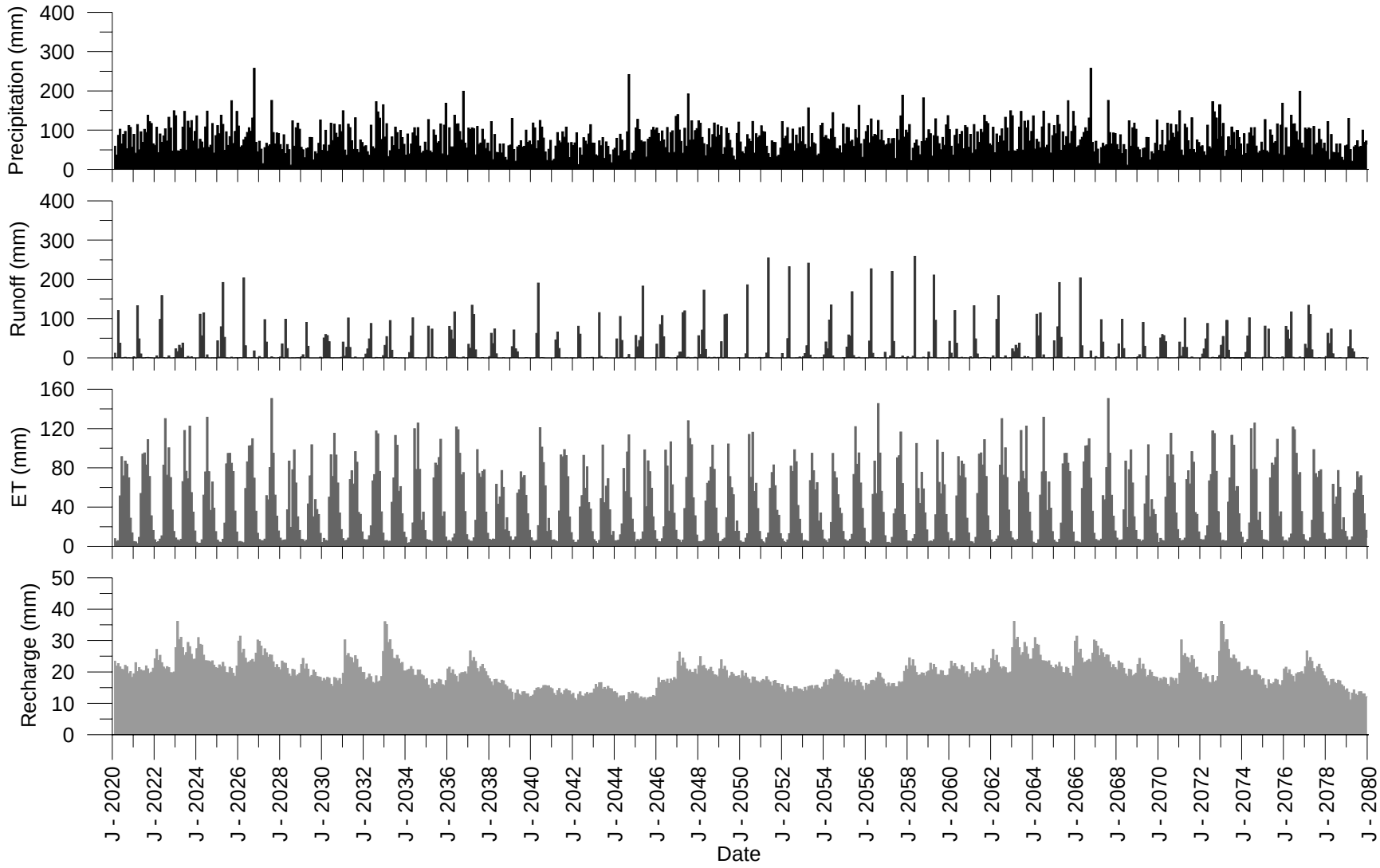

Figure 5.2 Reference scenario simulation results for the agriculture related class

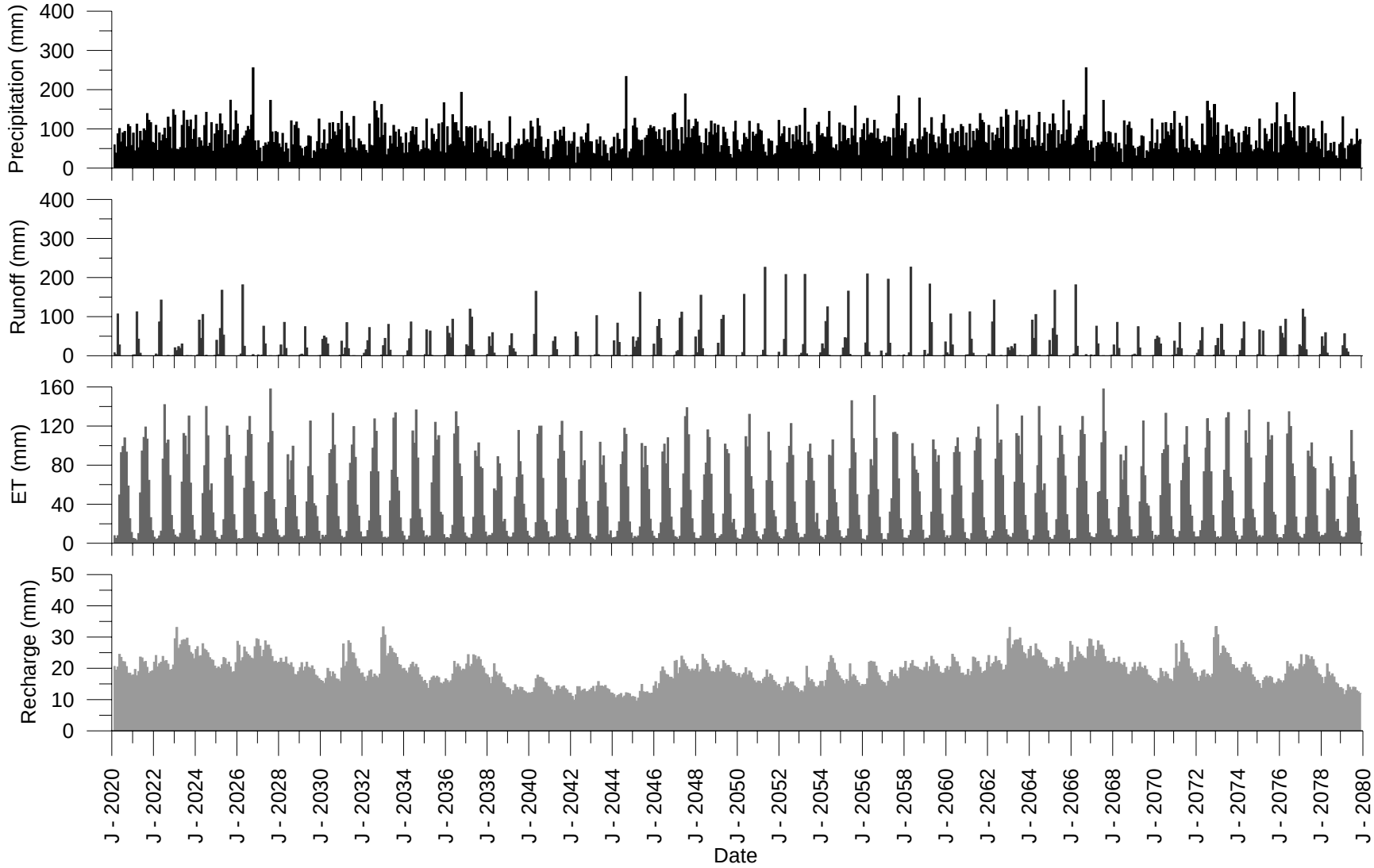

Figure 5.3: Reference scenario simulation results for the forest related class

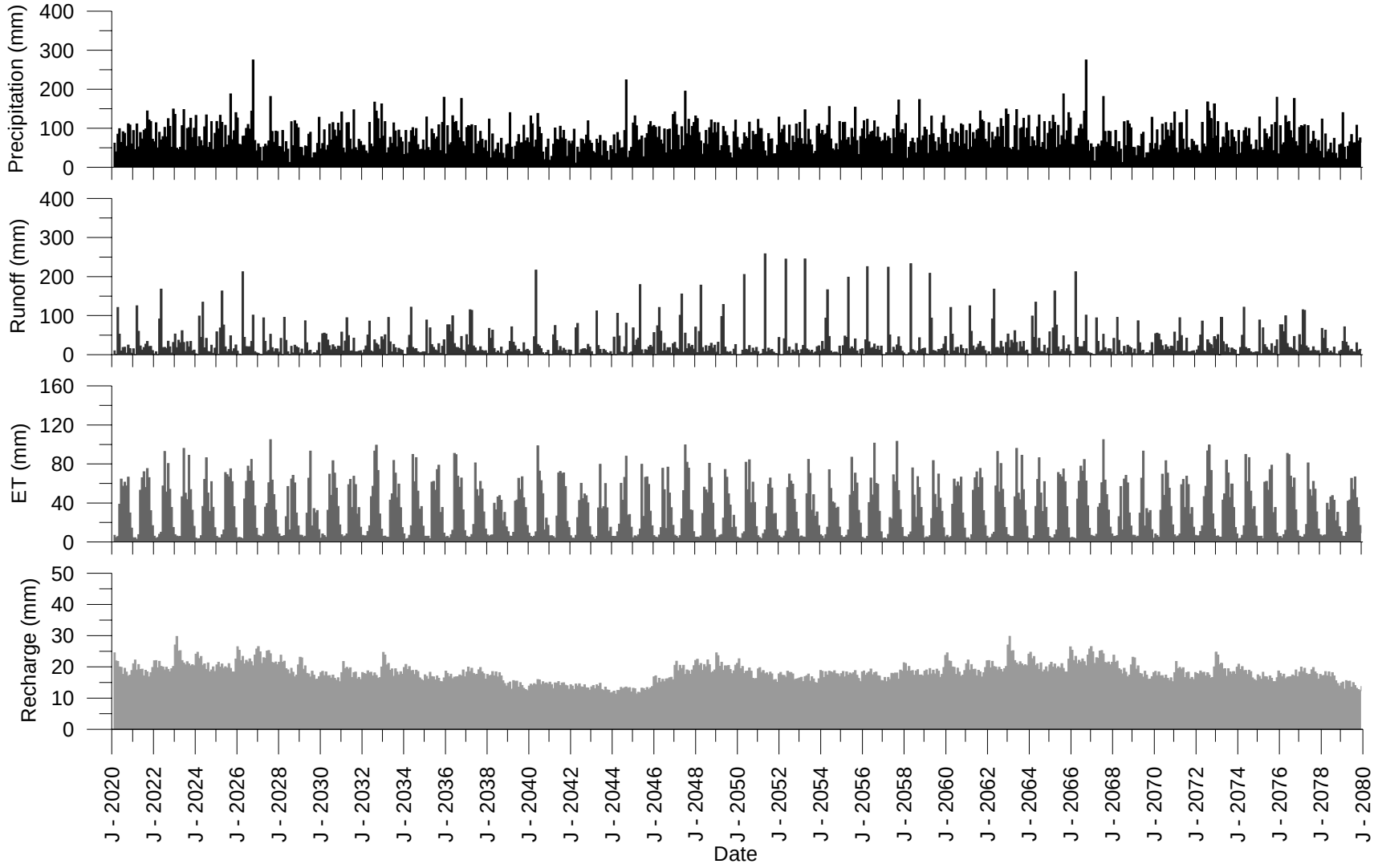

Figure 5.4 Reference scenario simulation results for the urban related class

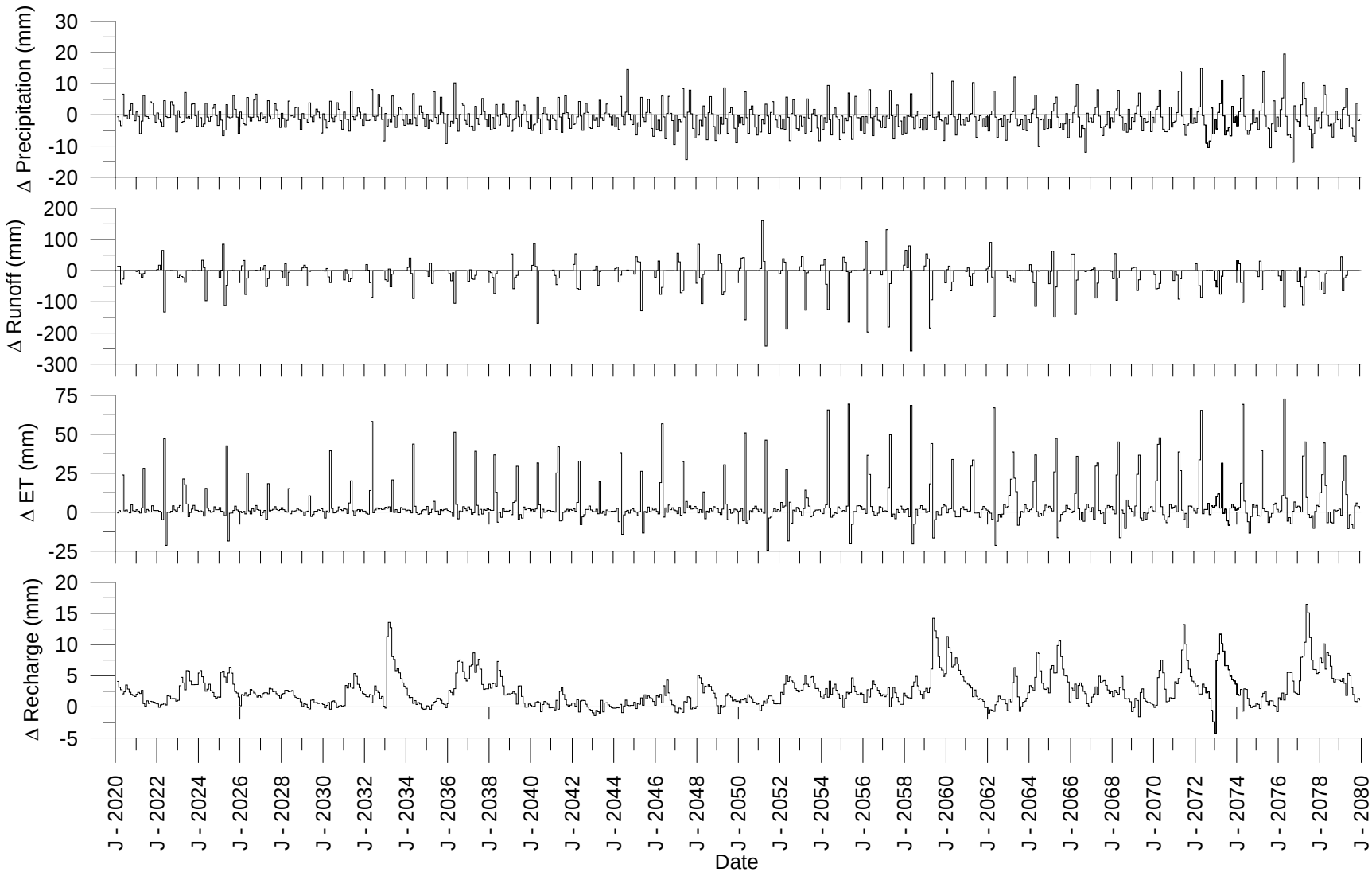

Figure 5.5 Relative impact of A2x scenario for the agriculture related class

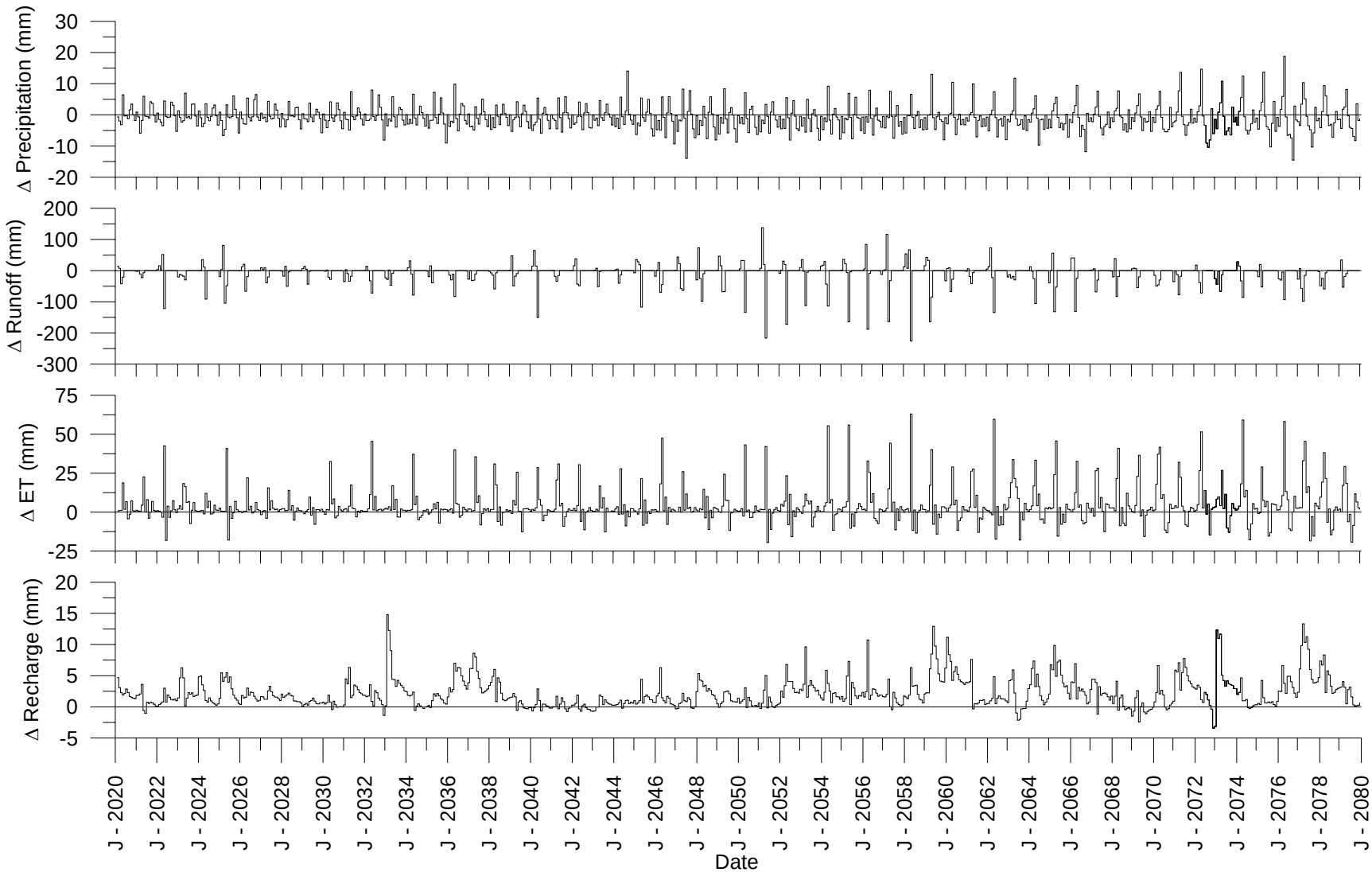

Figure 5.6 Relative impact of A2x scenario for the forest related class

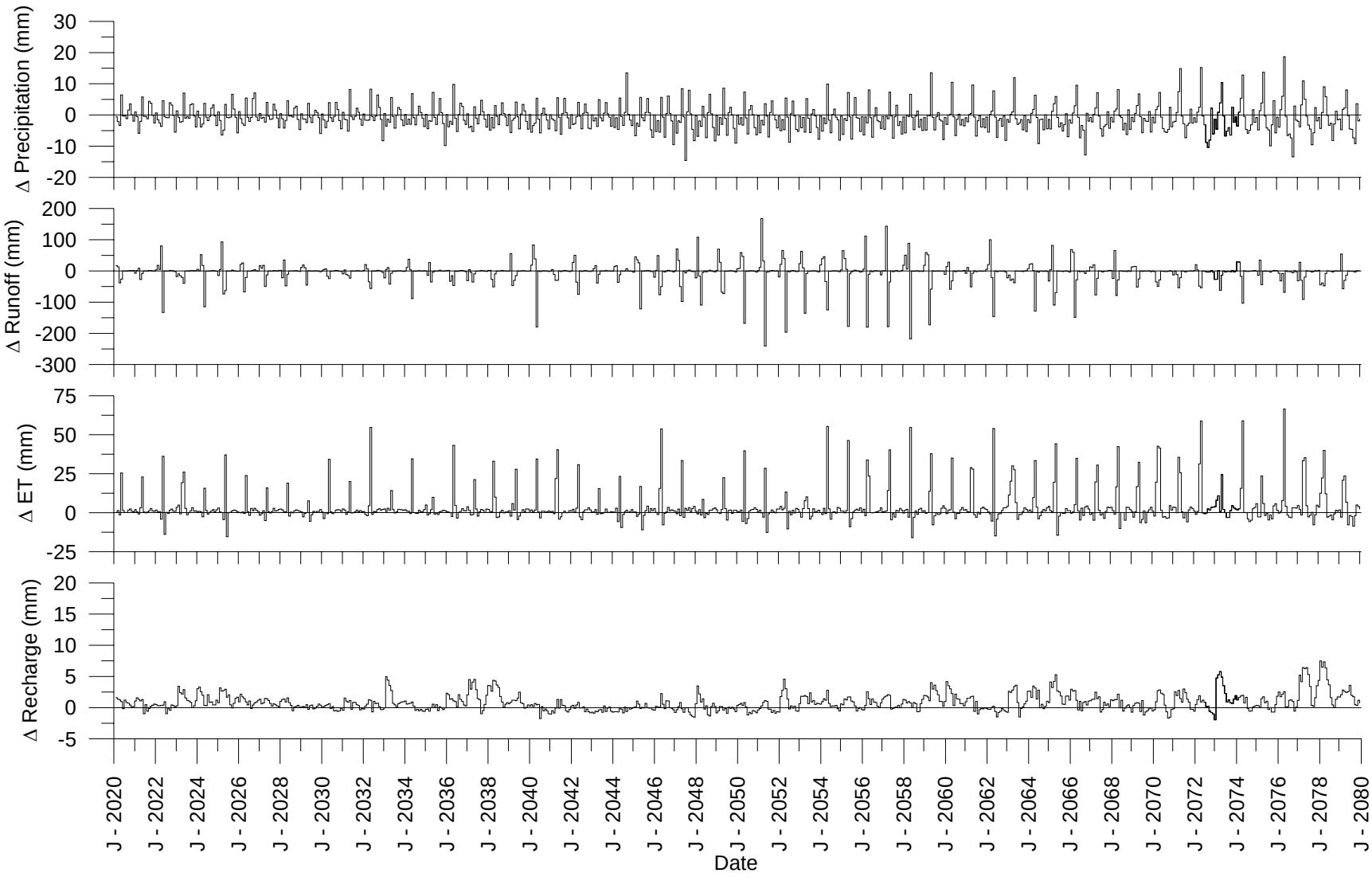

Figure 5.7 Relative impact of A2x scenario for the urban related class

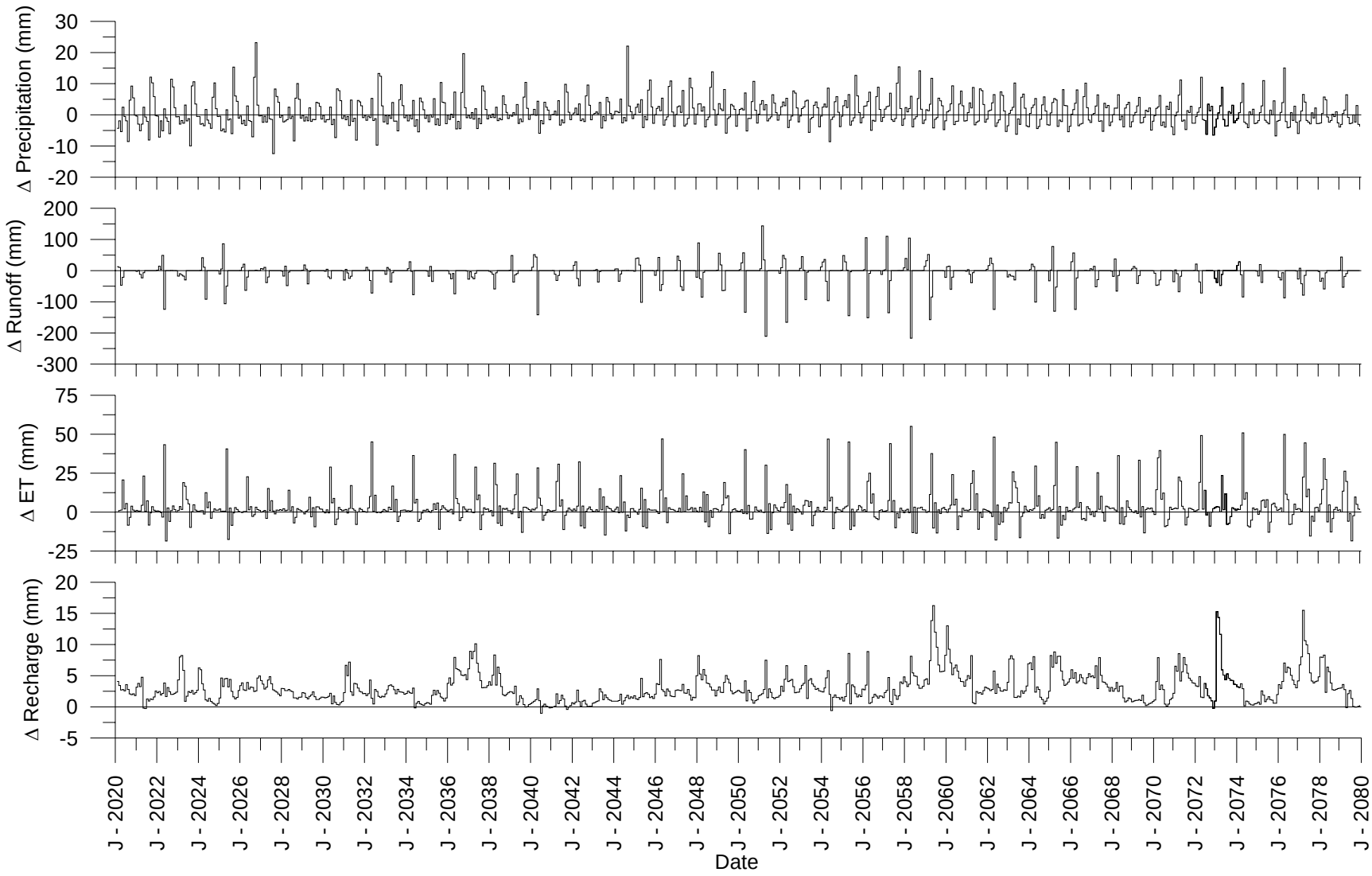

Figure 5.8 Relative impact of B2x scenario for the agriculture related class

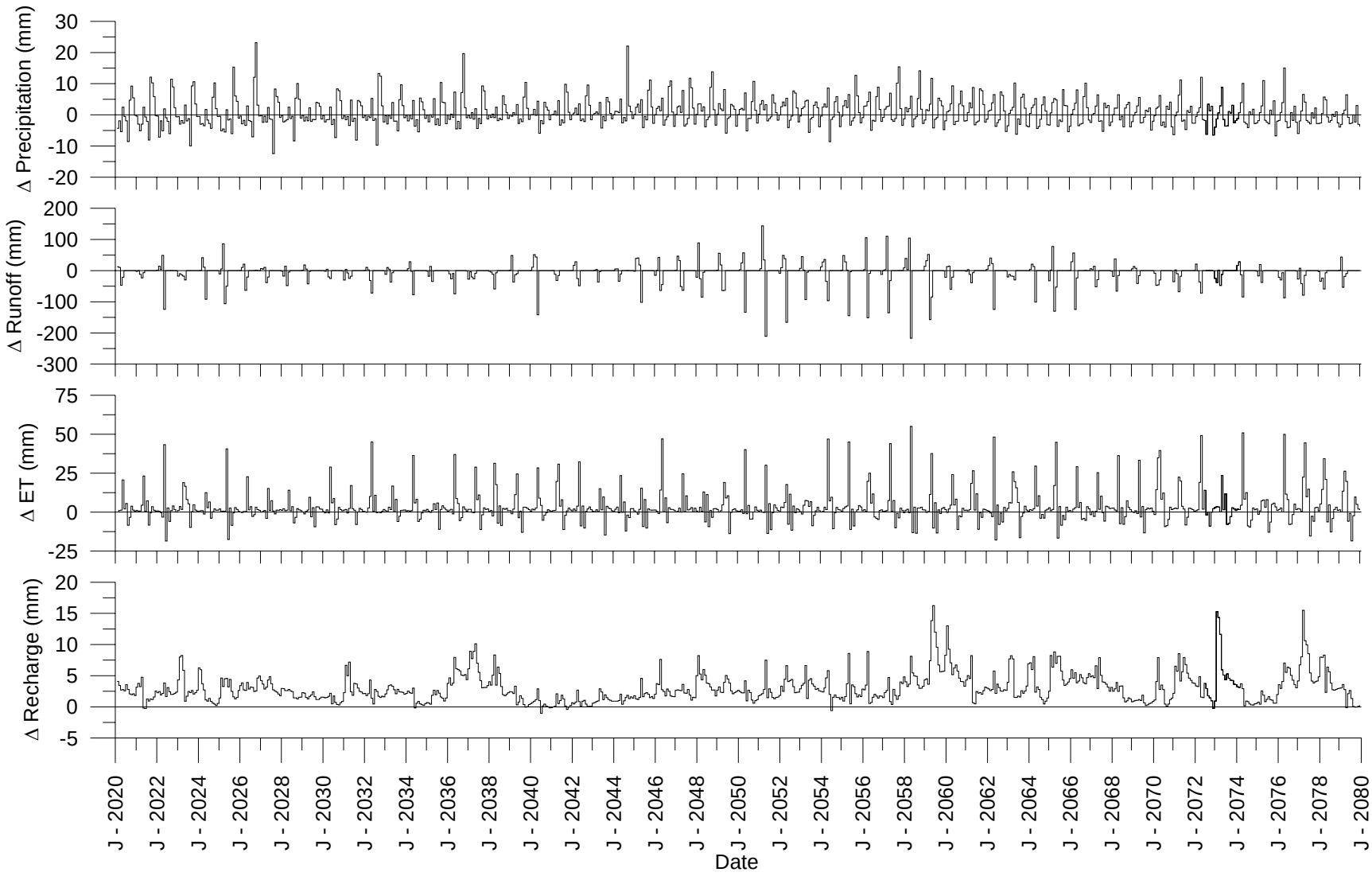

Figure 5.9 Relative impact of B2x scenario for the forest related class

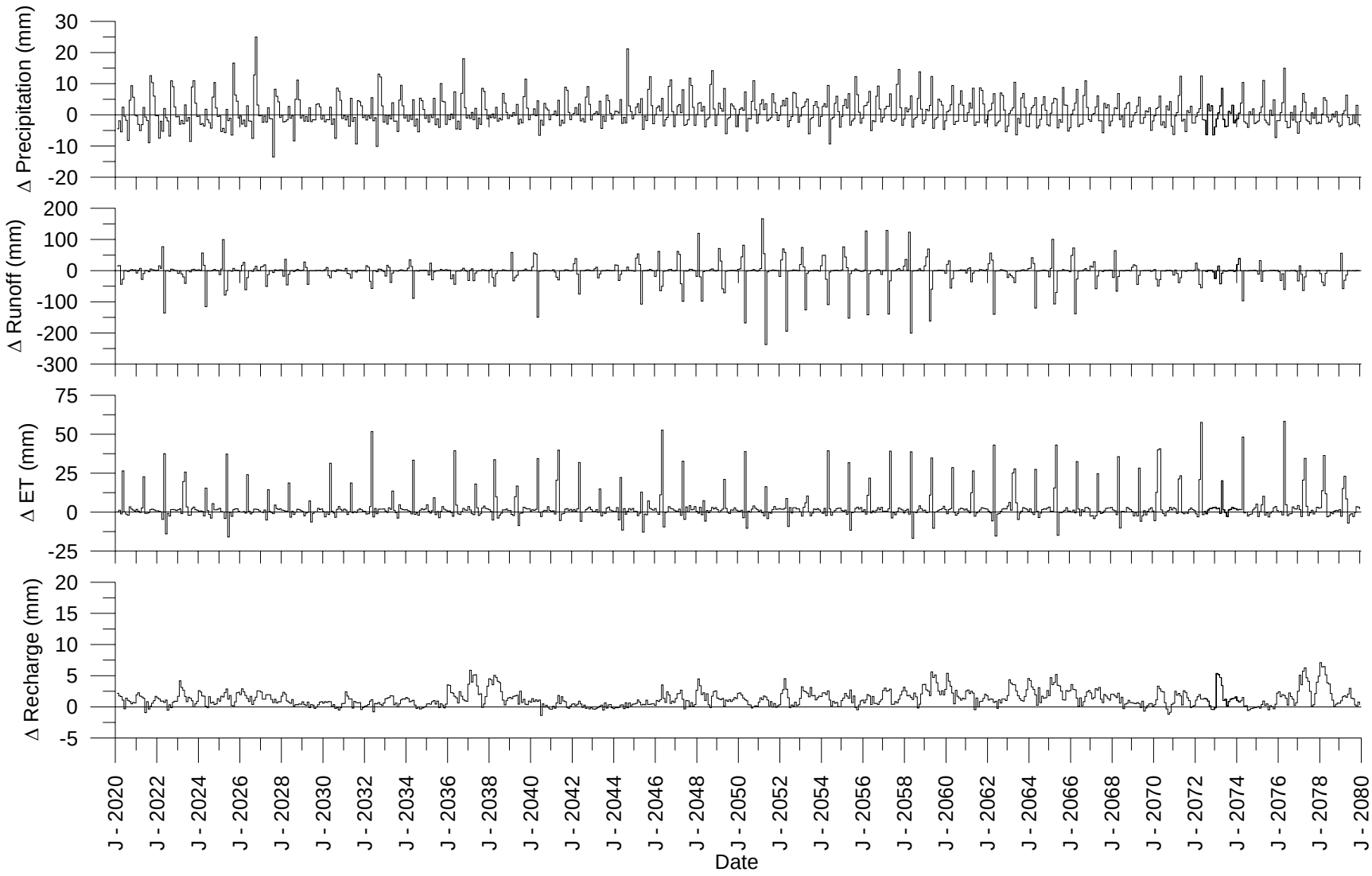

Figure 5.10 Relative impact of B2x scenario for the urban related class

5.3.4 HydroSphere Results

The surface and vadose zone impacts of projected climate change scenarios are applied to the groundwater flow model through the recharge boundary condition. The impacts of climate change scenarios A2x and B2x relative to the reference scenario are presented using hydrographs plotting changes to hydraulic head at select monitoring locations from the observation dataset.

Three locations from the groundwater observation dataset, WM22-93B, OW2-85A, and AC5A-01, shown on Figure 4.14, are selected to illustrate the impacts of climate change to the groundwater table. Observation points WM2-93B and OW2-85A are located in the north and central portions of the Alder Creek Watershed, respectively, and are both situated in the upper overburden; observation point AC5A-01 is located in south central area of the Alder Creek Watershed and situated in the lower overburden aquifer.

The relative change to hydraulic head at these selected locations for climate change scenarios A2x and B2x is shown on Figures 5.11 and 5.12, respectively. Also plotted is the relative change to the spatially averaged recharge boundary condition. The hydrographs for both climate change scenarios appear quite similar but their relative differences can vary as much as approximately 37 cm, though these differences cannot be discerned at the scale of Figures 5.11 and 5.12. The greatest difference in groundwater table elevations between the two scenarios is approximately 54 cm, occurring at WM2-93B.

The impact of climate change is greatest in the upper overburden aquifer and dampened in the lower overburden aquifer. This is generally the case for the entire observation dataset, not just the selection of monitoring locations plotted in Figures 5.11 and 5.12. This finding is in line with the conceptual understanding of the hydrogeologic system as the lower overburden aquifer is buffered by an aquitard, see Table 4.6. The observation dataset is more heavily populated with upper overburden monitoring locations, see Section 4.3.6, and *soft* monitoring locations should be added to the lower overburden aquifer to monitor fluctuations in future simulations to provide more insight to the response of the lower overburden aquifer. For both climate change scenarios, the remainder of the observation dataset shows trends similar to OW2-85A as presented in Figures 5.11 and 5.12, with an overall increase in simulated hydraulic head.

Though the differences in the timing of the precipitation between the A2x and B2x scenarios is quite variable, see Table 5.1, similar trends to changes in groundwater elevations are simulated. This is attributed to changes to the timing of the spring snow melt that promotes infiltration earlier in the annum which is not available to the reference scenario. The simulation results show that climate

change scenarios evaluated will have pronounced affect on the timing of surface and vadose zone hydrological processes and relatively little impact on to groundwater resources for the Alder Creek Watershed. A study of climate change impacts to the surficial unconfined aquifer at Grand Forks, BC presented similar findings; relatively small changes to the water table configuration and general direction of flow from both high and low recharge simulations (Allen et al., 2004).

The GCM simulation results for evaluations of other scenarios are available from CICS (2007) for the CGCM2 model and other GCMs as well. The impacts of alternative climate change scenarios, with greater contrast, can be readily evaluated for the Study Area using the developed methodology and existing model structure. This effort is reserved for future work.

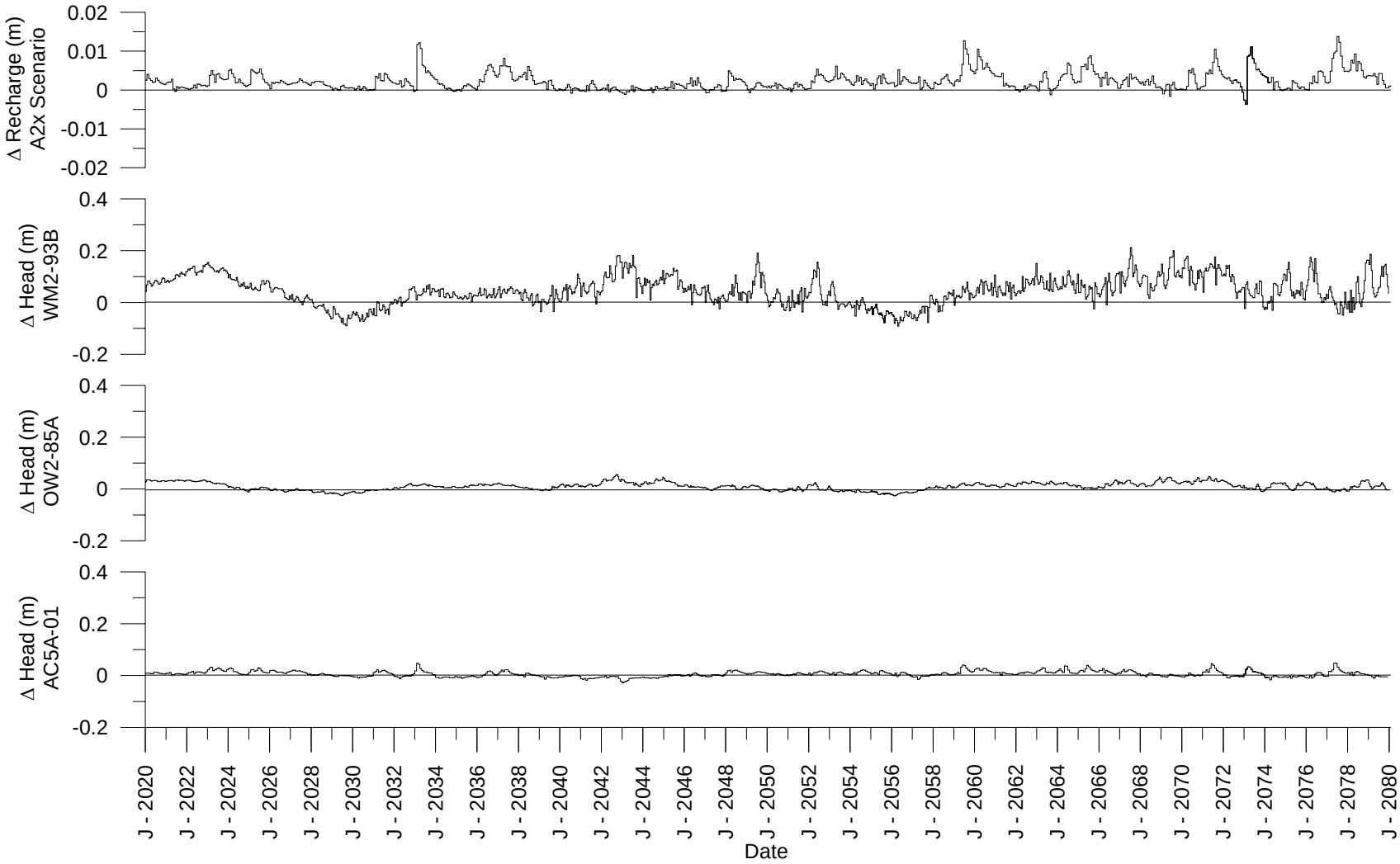

Figure 5.11 Relative impact of A2x scenario for select groundwater monitoring locations

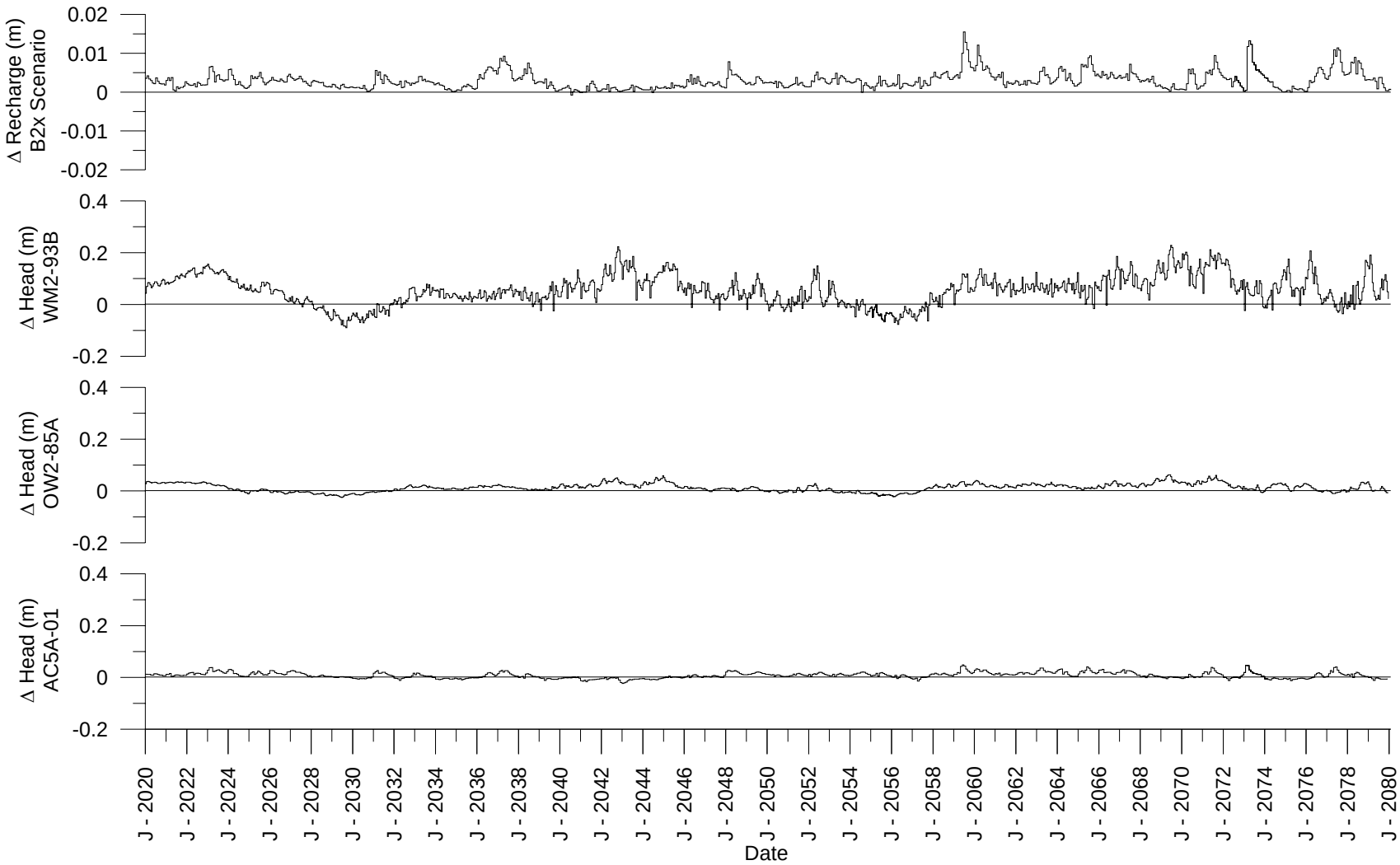

Figure 5.12 Relative impact of B2x scenario for select groundwater monitoring locations

5.4 Model Limitations

In this modeling effort, several limitations have been identified. All HELP3 input parameters other than precipitation, temperature, and solar radiation are held constant over the duration of the simulation. This impacts the simulated response of the recharge delivered to the water table as well as evapotranspiration and surface runoff abstractions. The soil column length is held constant over the duration of the simulation which affects the timing of the recharge being delivered to the water table.

Parameters influencing evapotranspiration include the length of the growing season and the LAI. The duration of the growing season is expected to lengthen with increasing temperatures. Increasing temperatures and concentrations of atmospheric CO_2 will also change the physiological response of plants which are not reflected in the model due to a constant LAI and pre-defined vegetative growing functions. Eckhardt and Ulbrich (1998) shows that the evapotranspiration processes under the influence of climate change are not well understood and that changes to the physiological response of plants can both intensify and lessen evapotranspiration processes. These may be important considerations as based on the results of this case study evapotranspiration accounts for approximately two-thirds of abstractions from precipitation.

The parameters characterizing runoff are static over the duration of the simulation and thus are not able to accommodate changes to LULC practices (e.g., urban development). Given the long-term nature of these simulations, the super-position of these stresses may accentuate or dampen the impacts of climate change (Loaiciga, 2000). Due to the daily time step of HELP3, individual storm events cannot be represented. The increase in frequency and intensity of severe storm events that is expected to accompany climate change cannot be incorporated and consequently the simulated values of runoff may be underestimated. Rounsevell et al. (1999) presents that through changes in climate, primary alterations to precipitation and temperature, the structure of the soil can change leading to changes in land use and agricultural practices. There is much uncertainty in incorporating socio-economic development, through the spatial and temporal changes to LULC and water demand, in relation to climate change (Loaiciga, 2000; Holman, 2006).

The limitations of this study for addressing the potential impacts from climate change primarily relate to the internal coding of the HELP3 program. The author feels that the greatest improvements to this case study would be gained by modifying the source code for HELP3 to incorporate plant physiology and a dynamic specification of input parameters for runoff and evapotranspiration.

The computational requirements, in terms of disk space, memory, and time are an encumbrance to evaluating the impacts of climate change. For each 1990-2080 transient simulation the HELP3 and HydroSphere model inputs and outputs required approximately 168.5 GB and 94.5 GB, respectively. The time required for simulating both the HELP3 and HydroSphere models and to process model files requires approximately 8 days of CPU time (using a dual core with 3.5 Ghz processors with 3 GB of memory). Applying this approach to a larger scale problem, e.g., the Grand River Watershed, which is nearly 7000 km^2 (Jrykama and Sykes, 2007), would be a challenge.

6 Conclusions and Recommendations

This thesis investigates the state of the science of conjunctive surface-subsurface water modeling with the aim of determining a suitable approach for conducting long-term simulations at the watershed scale. A review of the application of numerical techniques employed by fully-integrated models to simulate variably saturated groundwater flows (i.e., the Richards' Equation) and overland flows (i.e., approximations to the Saint Venant Equations) reveals that this approach is computationally intensive and suffers from the effects of scale. Measurement techniques that capture the full variability of the natural environment do not exist thus requiring these approaches to utilize a lumping or zonation approach which degrades their physical basis. Ultimately, the limiting factor of the fully-integrated approach is that it requires a very fine discretization of spatial and temporal domains. This effectively limits this robust numerical approach to the simulation of small catchments for relatively short durations.

As an alternative, a coupled approach is employed in this study. The HELP3 model is used to simulate surface and vadose zone hydrological process and is externally coupled (via the recharge boundary condition) to the HydroSphere model which is used to simulate saturated groundwater flows. Though not as physically robust as the fully-integrated approach, the increase in computational efficiency gained by employing simpler hydrologic models allows for long-term simulations to be conducted at the watershed scale. Furthermore, empirical relationships to approximate flow of water in porous media under freezing temperatures are built into the HELP3 model, allowing this coupled approach to conduct transient year-round and multi-year simulations. As a case study, this coupled approach is applied to conduct long-term transient simulations with the objective of evaluating the hydrologic response of the Alder Creek Watershed under the influence of climate change scenarios.

The evaluation of two contrasting scenarios of future climate (i.e., drier and wetter) produces similar results for both the HELP3 and HydroSphere models. This indicates that changes to the timing of seasonal hydrological processes caused by increasing temperatures have a greater impact than changes to the distribution of precipitation. Specifically, the shift in the spring snow melt to earlier in the year allows for increased infiltration before the onset of evaporation demands. Changes to the groundwater levels and the configuration of the water table are small. Fluctuations to the upper overburden aquifer are on the order of 0.5 m (at the upper end) while the signature of climate change

impacts are barely discernable in the lower overburden aquifer which is attributed to the aquitard separating the aquifers. This case study assessed the potential impacts of projected future climate for two scenarios of the forty that have been constructed. The ensemble of these forty scenarios represents the range of potential future worlds all of which are assumed to be equally likely (IPCC, 2000). It is recommended that additional scenarios of climate change be evaluated as they can be readily incorporated into the developed methodology and existing model structure.

The focus of this case study is aimed at evaluating the isolated impacts of climate change (i.e., all other stresses remain static). As such, this work provides a suitable benchmark for future studies to investigate the potential impacts of concurrent future stress conditions such as the superposition climate change scenarios and regional urban development. Given the long-term nature of climate change, incorporating the effects of urban development into the modeling approach will provide valuable insights to managing the surface water and groundwater resources of the Alder Creek Watershed. Broadening the scope of the modeling effort to incorporate these additional stress conditions is reserved for future research.

With respect to the coupled approach adopted in this study, the greatest limitations stem from the internal structure of the HELP3 code. The inability to assign dynamic runoff and evapotranspiration properties limits the models ability to respectively incorporate feedback from changes to LULC (e.g., urban development) and plant physiology (e.g., adjustment of stomatal conductance and plant growth for increasing CO_2 concentrations). It is recommended that future studies investigate updating the HELP3 code to address these limitations. Updating the HELP3 code may also fortuitously improve the speed of model execution as at the time of its release, HELP3 was designed to run on 80486-based CPUs.

This work presents a methodology capable of carrying out detailed long-term transient simulation of surface water and groundwater interaction. The case study demonstrates the ability of the coupled approach to assess the potential impacts of climate change at the watershed scale.

References

Abbott M.B. 1986a. An Introduction to the European Hydrological System - Systeme Hydrologique Europeen, “SHE”, 1 - History and Philosophy of a Physically-based, Distributed. Journal of Hydrology 87(3): 45-59.

Abbott M.B. 1986b. An Introduction to the European Hydrological System - Systeme Hydrologique Europeen, “SHE”, 2 - Structure of a physically-based, distributed modelling system. Journal of Hydrology 87(3): 61-77.

Abrahams A.D. and A.J. Parsons. 1994. Hydraulics of Interrill Overland Flow on Stone-covered Desert Surfaces. Catena 23(1-2): 111-140.

Abrahams A.D., A.J. Parsons, and J. Wainwright. 1995. Resistance to Overland Flow on Semiarid Grassland and Shrubland Hillslopes, Walnut Gulch, southern Arizona. Journal of Hydrology 156(1-4): 431-446.

Acrement G. J. Jr. and V.R. Schneider. 1989. Guide for Selecting Manning’s Roughness Coefficients for Natural Channels and Flood Plains. Water-Resource Paper 2339. U.S. Geological Survey, Washington, D.C.

Allen D.M., D.C. Makie, and M. Wei. 2004. Groundwater and Climate Change: A Sensitivity Analysis for the Grand Forks Aquifer, Southern British Columbia, Canada. Hydrogeology Journal 12(3): 270-290.

Anderson and Woessner. 1992. Applied Groundwater Modeling - Simulation of Flow and Advective Transport. Academic Press. New York.

AquaResource Inc. 2007. Integrated Water Budget Report - Grand River Watershed, prepared for the Grand River Conservation Authority, Ontario. pp. 200.

Bathurst J.C. and P.E. O'Connell. 1993. Future of Distributed Modelling In The Systeme Hydrologique Europeen In: Terrain Analysis and Distributed Modelling in Hydrology. pp. 213-226.

Bear J., M.S. Beljin, R.R. Ross. 1992. Fundamentals of Ground-Water Modeling. EPA. EPA/540/S-92/005.

Beven K.J. 1993. Prophecy, Reality and Uncertainty in Distributed Hydological Modelling. Advances in Water Resources 16(1): 41-51.

Bouraoui F., G. Vachaud, L.Z.X. Li, H. Le Treut, and T. Chen. 1999. Evaluation of the Impact of Climate Changes on Water Storage and Groundwater Recharge at the Watershed Scale. Climate Dynamics 15(2-3): 153-161.

Bradbury K.R. and M.A. Muldoon. 1989. Hydraulic Conductivity Determinations in Unlithified Glacial and Fluvial Materials. Standard Technical Publication. Vol 1053, American Society for Testing and Materials. pp. 138-151.

Bredehoeft J.D. 2003. From Models to Performance Assessment: The Conceptual Problem. Ground Water 41(5): 571-577.

Brooks R.H. and A.T. Corey. 1964. Hydraulic Properties of Porous Media. Hydrology Paper No. 4, Civil Engineering Department, Colorado State University, Fort Collins, Colorado.

Brouyere S., G. Carabin and A. Dassargues. 2004. Climate Change Impacts on Groundwater Resources: Modelled Deficits in a Chalky Aquifer, Geer Basin, Belgium. Hydrogeology Journal 12(2): 123-134.

Brutsaert W. 2005. Hydrology: An Introduction. Cambridge University Press. Cambridge, United Kingdom.

CH2M-Hill and SS Papadopulos & Ascociates Inc. 2003. Alder Creek Groundwater Study - Final Report, prepared for the Regional Municipality of Waterloo, Ontario. pp. 290.

Chen M., D. Pollard, and E.J. Barron. 2003. Comparison of Future Climate Change over North America Simulated by Two Regional Models. Journal of Geophysical Research 108(D12): 1-19.

Chen Z., S.E. Grasby, K.G. Osadetz. 2004. Relation between Climate Variability and Groundwater Levels in the Upper Carbonate Aquifer, Southern Manitoba, Canada. Journal of Hydrology 290(1-2): 43-62.

Chow V.T. 1959. Open Channel Hydraulics. McGraw-Hill, New York, N.Y.

Canadian Institute for Climate Studies. 2007. www.cics.uvic.ca/scenarios. Last updated Tue Jan 30 09:55:20 2007.

Dorken K. 2003. Automated Data Extraction and Synthesis of Channel Parameters for Watershed Scale Modelling. M.A.Sc. Thesis, Department of Civil Engineering, University of Waterloo, Waterloo, Ontario, Canada.

Downer C.W. and F.L. Ogden. 2004. Appropriate Vertical Discretization of Richards' Equation for Two-Dimensional Watershed-Scale Modelling. Hydrological Processes 18: 1-22.

Duke G.D., S.W. Kienzle, D.L. Johnson, and J.M. Byme. 2003. Improving Overland Flow Routing by Incorporating Ancillary Road Data into Digital Elevation Models. Journal of Spatial Hydrology 3(2): 1-27.

Duke G.D., S.W. Kienzle, D.L. Johnson, and J.M. Byme. 2006. Incorporating Ancillary Data to Refine Anthropogenically Modified Overland Flow Paths. Hydrological Processes 20(8): 1827-1843.

Dunne T. and R.D. Black. 1970. Partial Area Contributions to Storm Runoff in a Small New-England Watershed. Water Resources Research 6(5): 1296-1311.

Dunne T., W. Zhang, and B.F. Aubrey. 1991. Effects of Rainfall, Vegetation, and Microtopography on Infiltration and Runoff. Water Resources Research 27: 2271-2286.

Dunne T. 1970. An Experimental Investigation of Runoff Production in Permeable Soils. Water Resources Research 6(2): 478-490.

Eckhardt K. and U. Ulbrich. 2003. Potential Impacts of Climate Change on Groundwater Recharge and Streamflow in a Central European Low Mountain Range. Journal of Hydrology 284(1-4): 244-252.

El-Kadi A.I. and G. Ling. 1993. The Courant and Peclet Number Criteria for the Numerical Solution of the Richards Equation. Water Resources Research. 29: 3485-3494

Emmett W.W. 1970. The Hydraulics of Overland Flow on Hillslopes. United States Geological Survey Professional Paper 662-A.

Fairbanks J., S. Panday, and, P.S. Huyakorn. 2001. Comparisons of Linked and Fully Coupled Approaches to Simulating Conjunctive Surface/Subsurface Flow and their Interactions. In: Seo,

Poeter, Zheng, Poeter, editors. MODFLOW 2001 and Other Modeling Odysseys–Conference Proceedings, Golden, CO. p. 356-61.

Fathi-Moghadam M. and N. Kouwen. 1997. Nonrigid, Nonsubmerged, Vegetative Roughness on Floodplains. Journal of Hydraulic Engineering 123(1): 51-57.

Filon Y. 2000. Climate Change: Implications for Canadian Water Resources and Hydropower Production. Canadian Water Resources Journal 25(3): 255-269.

Flato G.M., G.J. Boer. 2001. Warming Asymmetry in Climate Change Simulations. Geophysical Research Letters 28(1): 195-198.

Fleenor W.E. and I.P. King. 1995. Identifying Limitations on the use of the HELP Model. In: Dunn R.J. and U.P. Singh. (eds) Landfill Closures. Environmental Protection and Land Recovery. ASCE, Geotechnical Special Publication. 53: 121-138.

Freeze R.A. 1971b. Influence of the Unsaturated Flow Domain on Seepage through Earth Dams. Water Resources Research 7(4): 929-941.

Freeze, R.A. 1972a. Role of Subsurface Flow in Generating Surface Runoff: 1. Base Flow Contributions to Channel Flow. Water Resources Research 8(5): 609-623.

Freeze, R.A. 1972b. Role of Subsurface Flow in Generating Surface Runoff: 2. Upstream Source Areas. Water Resources Research 8(5): 1272-1283.

Freeze R.A. and J.A. Cherry. 1979. Groundwater. Prentice-Hall Inc., Englewood Cliffs, New Jersey, USA.

Freeze R.A. and R.L. Harlan. 1969. Blueprint for a Physically-Based Digitally-Simulated Hydrologic Response Model. Journal of Hydrology 9(3): 237-258.

Freeze R.A. 1971a. Three-dimensional, Transient, Saturated-Unsaturated Flow in a Groundwater Basin. Water Resources Research 7(2): 347-366.

Gellens D. and E. Roulin. 1998. Streamflow Response of Belgian Catchments to IPCC Climate Change Scenarios. Journal of Hydrology 210(1-4): 242-258.

Gillham R.W. and R.N. Farvolden. 1974. Sensitivity Analysis of Input Parameters in Numerical Modeling of Steady-State Regional Groundwater Flow. Water Resources Research 10: 529-538.

Gillham R.W. 1984. The Capillary Fringe and its Effects on the Water-table Response. Journal of Hydology 67(1-4): 307-324.

Gogolev M.I. 2002. Assessing Groundwater Recharge with Two Unsaturated Zone Modeling Technologies. Environmental Geology 42(2-3): 248-258.

Gottardi G. and M. Venutelli. 1993. A Control-Volume Finite-Element Model for Two-Dimensional Overland Flow. Advances in Water Resources 16(5): 277-284.

Hart D.J., K.R. Bradbury, and D.T. Feinstein. 2006. The Vertical Hydraulic Conductivity of an Aquitard at Two Spatial Scales. Ground Water 44(2): 201-211.

Harter T. and J.W. Hopkins. 2004. Role of Vadose-Zone Flow Processes in Regional-Scale Hydrology: Review, Opportunities and Challenges. IN: Unsaturated Zone Modeling: Progress, Challenges, and Applications. Eds. R.A. Feddes, G.H. De Rooij, and J.C. van Dam.

Holman I.P. 2006. Climate Change Impacts on Groundwater Recharge-Uncertainty, Shortcomings, and the Way Forward? Hydrogeology Journal 14: 637-647.

Horton R.E. 1933. The Role of Infiltration in the Hydrologic Cycle. EOS Trans. AGU 14: 446-460.

IPCC (Intergovernmental Panel on Climate Change). 1995. Working Group I 1995 Summary for Policymakes. Report prepared by the Intergovernmental Panel on Climate Change Working Group I, World Meteorlogical Organization, United Nations Environment Program, Geneva.

IPCC (Intergovernmental Panel on Climate Change). 2000. In: Nakicenovic, N., Swart, R. (Eds.), Special Report on Emissions Scenarios. Cambridge University Press, Cambridge, United Kingdom.

IPCC (Intergovernmental Panel on Climate Change). 2001. In: McCarthy, J.J., Canziani, O.F., Leary, N.A., Dokken, D.J., White, K.S. (Eds.), Climate Change 2001: Impacts, Adaptation, and Vulnerability. Cambridge University Press, Cambridge, United Kingdom.

Jyrkama M.I.1999. Modeling of Non-Equilibrium Dissolution and Multiphase Contaminant Transport in Freezing Porous Media. M.A.Sc. Thesis, Department of Civil Engineering, University of Waterloo, Waterloo, Ontario, Canada.

Jyrkama M.I. 2003. A Methodology for Estimating Groundwater Recharge. PhD Thesis, Department of Civil Engineering, University of Waterloo, Waterloo, Ontario, Canada.

Jyrkama M.I., J.F. Sykes, and Normani S.D. 2002. Recharge Estimation for Transient Ground Water Modeling. Ground Water 40(6): 638-648.

Jyrkama M.I. and J.F. Sykes. 2006. Sensitivity and Uncertainty Analysis of the Recharge Boundary Condition. Water Resources Research 42(1): W01404.

Jyrkama M.I. and J.F. Sykes. 2007. The Impact of Climate Change on Spatially Varying Groundwater Recharge in the Grand River Watershed (Ontario). Journal of Hydrology 338: 237-250.

Klemes V. 1986. Dilettantism in Hydrology: Transition or Destiny? Water Resources Research 22(9S): 177S-188S.

Kristensen K.J. and S.E. Jensen. 1975. A Model for Estimating Actual Evapotranspiration from Potential Evapotranspiration. Nordic Hydrology 6: 170-188.

Lappala E.G., Healy R.W., Weeks E.P. 1993. Documentation of Computer Program VS2D to Solve the Equations of Fluid Flow in Variably Saturated Porous Media. Denver, Colorado, Water-Resources Inv. Rep. 83-4099.

Lawerence D.S.L. 997. Macroscale Surface Roughness and Frictional Resistance in Overland Flow. Earth Surface Processes and Landforms 22(4): 365-382.

Leopold L.B. and J.P. Miller. 1956. Ephemeral Streams - Hydraulic Factors and Their Relation to the Drainage Net. U.S. Geological Survey Professional Paper 282-A. pp. 45.

Lerner, D.N. 2002. Identifying and quantifying urban recharge - a review. Hydrogeology Journal 10(1): 143-152.

Lerner, D.N. 2002. Identifying and Quantifying Urban Recharge - A Review. Hydrogeology Journal 10(1): 143-152.

Loaiciga, H.A., J.B. Valdes, R. Vogel, J. Garvey, and H. Schwarz. 1996. Global Warming and the Hydrologic Cycle. Journal of Hydrology 174(1-2): 83-127.

Loaiciga, H.A., D.R. Maidment, and J.B. Valdes. 2000. Climate Change Impacts in a Regional Karst Aquifer, Texas, USA.. Journal of Hydrology 227(1-4): 173-194

Loaiciga H.A. 2003. Climate Change and Groundwater. Annals of the Association of American Geographers 93(1): 30-41.

Lofgren B.M., F.H. Quinn, A.H. Clites, R.A. Assel, A.J. Eberhardt, and C.L. Luukkonen. 2002. Evaluation of Potential Impacts on Great Lakes Water Resources Based on Climate Scenarios of Two GCMs. Journal of Great Lakes Research 28(4): 537-554.

Lorenz E.N. 1963. Deterministic Nonperiodic Flow. Journal of Atmospheric Sciences 20: 130-141.

Martz L.W. and J. Garbrecht. 1992. Numerical Definition of Drainage Network and Subcatchment Areas from Digital Elevation Models. Computers and Geosciences 18(6): 747-761.

McDonald, M.G. and A.W. Harbaugh. 1988. A Modular Three-Dimensional Finite-Difference Ground-Water Flow Model. USGS Techniques of Water Resources Investigations Book 6, Reston, Virginia, US.

McDonald, M.D. and A.W. Harbaugh. 1996. A Modular Three-Dimensional Finite Difference Groundwater Flow Model. United States Geological Survey Open-File Report 83-875. pp 258.

Mualem Y. 1976. A New Model for Predicting the Hydraulic Conductivity of Unsaturated Porous Media. Water Resources Research 12: 513-522.

Neuman S.P. and P.J. Wierenga. 2003. A Comprehensive Strategy of Hydrogeologic Modeling and Uncertainty Analysis for Nuclear Facilities and Sites. NUREG/CR-6805. U.S. Nuclear Regularoty Commision, Washingtion D.C.

Natural Resources Conservation Service. 1986. Urban Hydrology for Small Watersheds. Technical Report 55, United States Department of Agriculture.

Natural Resources Conservation Service. 1986. Urban Hydrology for Small Watersheds. Technical Report 55, United States Department of Agriculture.

O'Callaghan J.F. and D.M. Mark. 1984. The Extraction of Drainage Networks from Digital Elevation Data. Computer Vision, Graphics and Image Processing 28: 328-344.

Ogend F.L., J. Garbrecht, P.A. DeBarry, and L.E. Johnson. 2001. GIS and Distributed Watershed Models. II: Modules, Interfaces, and Models. Journal of Hydrologic Engineering 6(6): 515-523.

Oreskes N. K. Shrader-Frechette, and K. Belitz. 1994. Verification, Validation, and Confirmation of Numerical Models in Earth Sciences. Science 263(5147): 641-646.

Panday S. and P.Huyakorn. 2004. A Fully Coupled Physically-Based Spatially-Distributed Model for Evaluating Surface/Subsurface Flow, J. Advances in Water Resources 27(4): 361-382.

Paniconi C., A.A. Aldama, and E.F. Wood. 1991. Numerical Evaluation of Iterative and Noniterative Methods for the Solution of the Nonlinear Richards Equation. Water Resources Research 27(6): 1147-1163.

Paniconi C. and M. Putti. 1994. A Comparison of Picard and Newton Iteration in the Numerical Solution of Multidimensional Variably Saturated Flow Problems. Water Resources Research 30(12): 3357-3374.

Parry M. 2002. Scenarios for climate impact and adaptation assessment. Global Environmental Change 12: 149-153.

Patriarche D., M.C. Castro, and P. Goovaerts. 2005. Estimating Regional Hydraulic Conductivity Fields - A Comparative Study of Geostatistical Methods. Mathematical Geology 37(6): 587-613.

Presant E.W. and R.E. Wicklund. 1971. The Soils of Waterloo County. Report No. 44 of the Ontario Soil Survey. Research Branch, Canada Department of Agriculture, Department of Soil Science, University of Guelph and the Ontario Department of Agriculture and Food. Guelph, Ontario.

Rauws G. 1988. Laboratory Experiments on Resistance to Overland Flow due to Composite Roughness. Journal of Hydrology 103(1-2): 37-52.

Richardson, C. W., and D.A. Wright. 1984. WGEN: A model for generating daily weather variables. ARS-8, Agricultural Research Service, USDA. 83 pp.

Regional Municipality of Waterloo, Ontario. 2007. ww.region.waterloo.ca

Rolston D.E. 2007. Historical Development of Soil-Water Physics and Solute Transport in Porous Media. Water Science & Technology 7(1): 59-66.

Rounsevell M.D.A., S.P. Evans, and P. Bullock. 1999. Climate Change and Agricultural Soils: Impacts and Adaptation. Climate Change 43(4): 683-709.

Rubin J. 1966. Theory of Rainfall Uptake by Soils Initially Drier than their Field Capactiy and its Applications. Water Resources Research 2(4): 739-749.

Schaffranek, R.W., R.A. Baltzer, and D.E. Goldberg. 1981. A Model for Simulation of Flow in Singular and Interconnected Channels. Techniques of Water-Resources Investigations of the USGS. Book 7(Chapter C3). pp. 110.

Scheraga J.D. and J. Furlow. 2002. Preface to the Potential Impacts of Climate Change in the Great Lakes Region. Journal of Great Lakes Research 28(4): 493-495.

Schroeder P.R., N.M. Aziz, C.M Lloyd, and P.A. Zappi. 1994a. The Hydrologic Evaluation of Landfill Performance (HELP) Model: User's Guide for Version 3. EPA/600/R-94/168a, U.S. Environmental Protection Agency Office of Research and Development, Washington.

Schroeder P.R., T.S. Dozier, P.A. Zappi, B.M. McEnroe, J.W. Sjostrom, and R.L. Peyton. 1994b. The Hydrologic Evaluation of Landfill Performance (HELP) Model: Engineering Documentation for Version 3. EPA/600/R-94/168b, U.S. Environmental Protection Agency Office of Research and Development, Washington.

Schroeter H.O., D.K. Boyd, and H.R. Whitely. 2000. GAWSER: A versatile tool for water management planing. Proceeding of the Ontario Water Conference 2000, April 26-27, 2000, Richmond Hill, Ontario.

Scibek J. and D.M. Allen. 2006. Modeled Impacts of Predicted Climate Change on Recharge and Groundwater Levels. Water Resources Research 42(11): W11405.

Scibek J., D.M. Allen, A.J. Cannon, and P.H Whitfield. 2007. Groundwater-Surface Water Interaction under Scenarios of Climate Change using a High-Resolution Transient Groundwater Model. Journal of Hydrology 333(2-4): 165-181.

Sibul U., D. Walmsley, and R. Szudy. 1980. Ground water resources in the Grand River Basin; Technical Report 10. Ontario Ministry of the Environment.

Singer S.N., C.K. Cheng, and M.G. Scafe. 1997. The Hydrogeology of Southern Ontario. Volume 1. Hydrogeology of Ontario Series (Report 1). Ministry of Environment and Energy. Toronto, Ontario.

Singh V.P. 1997. Effect of Spatial and Temporal Variability in Rainfall and Watershed Characteristics on Stream Flow Hydrograph. Hydrological Processes 11(12): 1169-1669.

Singh V.P. 2002. Is Hydrology Kinematic. Hydrological Processes 16(3): 667-716.

Singh V.P. 2005. Effects of Storm Direction and Duration on Infiltrating Planar Flow with Partial Coverage. Hydrological Processes 19(4): 969-992.

Sneyers R. 1997. Climate Chaotic Instability: Statistical Determination and Theoretical Background. Environmetrics 8: 517-532.

Sousounis P.J. and E.K. Grover. 2002. Potential Future Weather Patterns over the Great Lakes Region. Journal of Great Lakes Research 28(4): 496-520.

Sudicky E.A. 1986. A Natural Gradient Experiment on Solute Transport in a Sand Aquifer: Spatial Variability of Hydraulic Conductivity and its Role in the Dispersion Process. Water Resources Research 22(13): 2096-2082.

Shewchuk J.R. Triangle: Engineering a 2D Quality Mesh Generator and Delaunay Triangulator, in ``Applied Computational Geometry: Towards Geometric Engineering" (Ming C. Lin and Dinesh Manocha, editors), volume 1148 of Lecture Notes in Computer Science, pages 203-222, Springer-Verlag, Berlin, May 1996. (From the First ACM Workshop on Applied Computational Geometry.)

Sykes J.F. 1985. Sensitivity Analysis for Steady State Groundwater Flow using Adjoint Operators. Water Resources Research 21(3): 359-371.

Therrien, R. and E.A. Sudicky. 1996. Three-dimensional analysis of variably-saturated flow and solute transport in discretely-fractured porous media. Journal of Contaminant Hydrology 23(1-2): 1-44.

Therrien R., R.G. McLaren, E.A. Sudicky, and S.M. Panday. 2005. HydroGeoSphere: A Three-dimensional Numerical Model Describing Fully-integrated Subsurface and Surface Flow and Solute Transport, Groundwater Simulations Group, Waterloo, Ontario.

Toth J.A. 1962. A theory of groundwater motion in small drainage basins in central Alberta, Canada. Journal of Geophysical Research 67(11): 4375–4387.

Tsonis A. 1991. Sensitivity of the Global Climate System to Initial Conditions. EOS, Trans. Am. Geophys. Union 27: 313-328.

van Genuchten M. Th. 1980. A Closed-Form Equation For Predicting the Hydraulic Conductivity of Unsaturated Soils. Soil Science Society of America Journal 44(5): 892-898.

VanderKwaak J.E. and K. Loague. 2001. Hydrologic Response Simulations for the R-5 Catchment with a Comprehensive Physics-Based Model. Water Resources Research 37(4): 999-1013.

Vieira J.H.D. 1983. Conditions Governing the use of Approximations for the Saint Venant Equations for Shallow Surface Flow. Journal of Hydrology 60(1-4): 43-58.

Vieux B.E. 1993. Geographic Information Systems and Non-Point Source Water Quality and Quantity Modelling In: Terrain Analysis and Distributed Modelling in Hydrology. Kluwer Academic Publishing. Dordrecht, The Netherlands.

Walker, G.R. L. Zhang, T.W. Ellis, T.J. Hatton, C. Pertheram. 2002. Estimating impacts of changed land use on recharge - review of modelling and other approaches appropriate for management of dryland salinity. Hydrogeology Journal 10(1): 68-90.

WASY, Institute for Water Resources Planning and Systems Research Ltd. 2005. FEFLOW 5.2: Finite Element Subsurface Flow & Transport Simulation System. Reference Manual, User's Manual and White Papers. Berlin, Germany.

Waterloo Hydrogeologic Inc. 1997. Visual MODFLOW, version 2.6, Waterloo, Ont., Canada.

Waterloo Hydrogeologic Inc. 2000. WHI UnSat Suite user's manual: 1–D Unsaturated Zone Groundwater Flow and Contaminant Transport Modeling using VLEACH, PESTAN, VS2DT, and HELP, Waterloo, Ontario.

Waterloo Hydrogeologic Inc. 2002. Visual MODFLOW: The Proven Standard for 3-D Groundwater and Contaminant transport Modelling using MODFLOW, MODPATH and MT3D. Waterloo, Ontario.

Waterloo Hydrogeologic Inc. 2004. VisualMODFLOW version 3.1.84 Software and Documentation, Waterloo, Ontario.

Wicklund R.E. and N.R. Richards. 1961. The Soil Survey of Oxford County. Report No. 28 of the Ontario Soil Survey. Research Branch, Canada Department of Agriculture and the Ontario Agriculture College. Guelph, Ontario.

Winter T.C., J.W. Harvey, O.L. Franke, and W.M. Alley. 1998. Ground Water and Surface Water, a Single Resource. USGS Circular 1139. Denver, CO.

Winter T.C., D.O. Rosenberry, and J.W. LaBaugh. 2003. Where Does the Ground Water in Small Watersheds Come From. Ground Water 41(7): 989-1000.

Wood E.F., M. Sivapalan, K.J. Beven, and L. Band. 1988. Effects of Spatial Variability and Scale with Implications to Hydrologic Modeling. Journal of Hydrology 102(1-4): 29-47.

Woolhiser D.A. and Liggett J.A. 1967. Unsteady One-Dimensional Flow Over a Plane – the Rising Hydrograph. Water Resources Research 3(3): 753-771.

Woolhiser D. A., R.E. Smith, and D.C. Goodrich. 1990. KINEROS, A Kinematic Runoff and Erosion Model: Documentation and User Manual. ARS-77. US Department ofAgriculture, Agricultural Research Service. pp. 130.

Woyshner M.R. and E.K. Yanful. 1995. Modelling and Field Measurements of Water Percolation through an Experimental Soil Cover on Mine Tailings. Canadian Geotechnical Journal 32(4): 601-609.

Zhang X., L.A. Vincent, W.D. Hogg, and A. Niitsoo. 2000. Temperature and Precipitation Trends in Canada During the 20th Century. Atmosphere-Ocean 38(3): 395-429.

Zimmerman D.A., G. de Marsily, C.A. Gotway, M.G. Marietta, C.L. Axness, R.L. Beauheim, R.L. Bras, J. Carrera, G. Daga, P.B. Davies, D.P. Gallegos, A. Galli, J. Gomez-Hernandez, P. Grindrod, A.L. Gutjahr, P.K. Kitanidis, A.M. Lavenue, D. McLaughlin, S.P. Neuman, B.S. RamaRao, C. Ravenne, and Y. Rubin. 1998. A Comparison of Seven Geostatistically Based Increase Approaches to Estimate Tranamissivities for Modeling Advective Transport by Groundwater Flow. Water Resources Research 34(6): 1373-1413.